UNIVERSITÉ CÔTE D'AZUR

ÉCOLE DOCTORALE
SCIENCES ET TECHNOLOGIES DE L'INFORMATION ET DE LA COMMUNICATION

# THÈSE DE DOCTORAT

# Analyse Spectrale de Graphes Géométriques Aléatoires


**Mounia HAMIDOUCHE**

EURECOM


**Présentée en vue de l'obtention du grade de docteur en automatique, traitement du signal et des images d'Université Côte d'Azur**

**Dirigée par** : Laura Cottatellucci et Konstantin Avrachenkov

**Soutenue le**: 29/05/2020

**Devant le jury, composé de** :

| | |
|---|---|
| Laura Cottatellucci | Directeur |
| *Professeur, FAU, Allemagne* | |
| Konstantin Avrachenkov | Directeur |
| *Directeur de recherche (Inria), Sophia Antipolis* | |
| Pierre Borgnat | Rapporteur |
| *Directeur de recherche (CNRS), ENS de Lyon* | |
| Sergey Skipetrov | Rapporteur |
| *Directeur de recherche (CNRS), Grenoble* | |
| Hocine Cherifi | Examinateur |
| *Professeur, Université de Boulogne* | |
| Dirk Slock | Examinateur |
| *Professeur, Eurecom, Sophia Antipolis* | |

EURECOM
Sophia Antipolis

# Abstract (English)

In this thesis we study random geometric graphs (RGGs) using tools from random matrix theory and probability theory to tackle key problems in complex networks. An RGG is constructed by uniformly distributing $n$ nodes on the $d$-dimensional torus $\mathbb{T}^d \equiv [0,1]^d$ and connecting two nodes if their $\ell_p$-distance, with $p \in [1,\infty]$ is at most $r_n$. Three relevant scaling regimes for the RGG are of special interest. One of these is the connectivity regime, in which the average vertex degree $a_n$ grows logarithmically with $n$ or faster, i.e., $a_n = \Omega(\log(n))$. The second scaling regime is the dense regime, in which $a_n \equiv \Theta(n)$. The third scaling regime is the thermodynamic regime, in which the average vertex degree is a constant.

First, when $d$ is fixed and $n \to \infty$, we study the spectrum of the normalized Laplacian matrix and its regularized version for RGGs in both the connectivity and thermodynamic regime. We propose an approximation for the RGG regularized normalized Laplacian matrix based on the deterministic geometric graph (DGG) with nodes in a grid. Then, we provide an upper bound for the probability that the Hilbert-Schmidt norm of the difference between the RGG and the deterministic geometric graph (DGG) normalized Laplacian matrices is greater than a certain threshold in both the connectivity and thermodynamic regime. In particular, in the connectivity regime, we prove that the normalized Laplacian matrices of the RGG and the DGG are asymptotically equivalent with high probability. Then, when $n \to \infty$, we show that the limiting spectral distributions (LSDs) of the normalized Laplacian matrices of RGGs and DGGs converge in probability to the Dirac distribution at one in the full range of the connectivity regime. In the thermodynamic regime, we show that the LSD of the RGG regularized normalized Laplacian matrix can be approximated by the one in the DGG and we provide an upper bound for the approximation error. Therefore, we can use the deterministic structure of the DGG to provide an analytical expression for the eigenvalues of the RGG in both the connectivity and thermodynamic regime.

Next, we study the spectrum of the adjacency matrix of an RGG in the connectivity regime. Under some conditions on the average vertex degree $a_n$, we show that the Hilbert-Schmidt norm of the difference between two sequences of adjacency matrices of RGGs and DGGs converges in probability to zero as $n \to \infty$. Then, using this result, we show that the Levy distance between the eigenvalue distributions of the DGG and RGG adjacency matrices vanishes with high probability as $n \to \infty$. Then, for $n$ finite, we use the structure of the DGG to approximate the eigenvalues of the adjacency matrix of the RGG.

Finally, we tackle the problem of determining the spectral dimension (SD) $d_s$, that characterizes the return time distribution of a random walk (RW) on RGGs. First, we show that the SD depends on the eigenvalue density (ED) of the RGG normalized Laplacian in the neighborhood of the minimum eigenvalues. We show that the smallest non zero eigenvalue converges to zero in the large graph limit. Then, based on the analytical expression of the normalized Laplacian eigenvalues around zero, we show that the ED in a neighborhood of the minimum value follows a power-law tail. Therefore, us-

ing these results, we approximate the SD of RGGs by the Euclidean dimension $d$ in the thermodynamic regime.

**Keywords**: Random Geometric Graph, Spectral Graph Theory, Random Matrix Theory, Spectral Dimension.

# Abstract (Français)

Nous étudions le graphe géométrique aléatoire (GGA) afin d'aborder des problèmes clés dans les réseaux complexes. Un GAA est construit en distribuant uniformément n nœuds sur un tore de dimension d et en connectant deux nœuds si leur distance ne dépasse pas un seuil. Trois régimes pour GGA présentent un intérêt particulier. Le régime de connectivité dans lequel le degré moyen d'un nœud $a_n$ croit de manière logarithmique avec n ou plus vite. Le régime dense dans lequel $a_n$ est linéaire avec n. Le régime thermodynamique dans lequel $a_n$ est une constante.

Premièrement, on étudie le spectre du Laplacien normalisé (LN) et régularisé du GGA dans les trois régimes. Lorsque d est fixe et n tend vers l'infini, on prouve que la distribution spectrale limite (DSL) du LN converge vers la distribution de Dirac concentrée en 1 dans le régime de connectivité. Dans le régime thermodynamique, on propose une approximation pour DSL du LN régularisé et on fournit une borne d'erreur sur l'approximation. On montre que DSL du LN régularisé d'un GGA est approximée par DSL d'un graphe géométrique déterministe (GGD).

Ensuite, on étudie la DSL de la matrice d'adjacence d'un GGA dans le régime de connectivité. Sous des conditions sur $a_n$, on montre que DSL de la matrice d'adjacence du GGD est une bonne approximation du GGA pour n large.

Finalement, on détermine la dimension spectrale (DS) d'un GGA qui caractérise la distribution du temps de retour d'une marche aléatoire sur le GGA. On montre que DS dépend de la densité spectral de LN au voisinage des valeurs propres minimales. On prouve que la densité spectral au voisinage de la valeur minimale suit une loi de puissance et que DS du GGA est approximé par d dans le régime thermodynamique.

**Keywords**: Graphe Géométrique Aléatoire, Théorie Spectrale des Graphes, Théorie des Matrices Aléatoires, Dimension Spectrale.

# Acknowledgments

I would like to express my sincere appreciation and gratitude to my supervisors Laura Cottatellucci and Konstantin Avrachenkov for their excellent guidance, encouragement, and their availability. I thank them for all their useful suggestions, advices, insightful comments, and useful discussions throughout this journey.

Moreover, I sincerely thank Dr. Borgnat Pierre, Dr. Skipetrov Sergey, Prof. Cherifi Hocine and Prof. Slock Dirk for accepting to be members of my defense jury.

During my Ph. D, I had the opportunity to go for an internship at Friedrich-Alexander University (FAU) in Erlangen-Nuremberg which really was an amazing experience. I had the opportunity to meet amazing people with whom I had many group discussions, which helped me to deepen my knowledge on various topics, and also helped me get acclimatized to life in a new environment. I would like to thank Prof. Robert Schober for hosting me in his lab at FAU.

To all my colleagues and friends that I have met during this whole path, it was a great honor for me to have spent amazing moments with them!

Finally, my heartfelt thanks go to my family. I thank my parents for their everlasting support. A very special thank-you goes to Kenza, for her help and unfailing support in bad times. This thesis is dedicated to them.

# Contents

# List of Figures

# Acronyms

**DFT** discrete Fourier transform.

**DGG** deterministic geometric graph.

**ED** eigenvalue density.

**ER** Erdös-Rényi.

**ERM** Euclidean random matrices.

**ESD** empirical spectral distribution.

**LSD** limiting spectral distribution.

**RGG** random geometric graph.

**RGT** random graph theory.

**RMT** random matrix theory.

**RW** random walk.

**SD** spectral dimension.

**SF** scale-free.

**SGT** spectral graph theory.

**SW** small-world.

# Notations

| | |
|---|---|
| $x$ | Scalar. |
| $\mathbf{x}$ | Column vector. |
| $\mathbf{X}$ | Matrix. |
| $\mathbf{X}^T$ | Transpose of matrix $\mathbf{X}$. |
| $X_{ij}$ | Entry $(i, j)$ of matrix $\mathbf{X}$. |
| $x_i$ | Entry $i$ of vector $\mathbf{x}$. |
| $\mathbb{R}$ | Space of real numbers. |
| $\mathbb{Q}$ | Space of rational numbers. |
| $\mathbb{N}$ | Space of integer numbers. |
| $d$ | Space dimension. |
| $\|.\|_p$ | $\ell_p$-metric on $\mathbb{R}^d$, $p \in [1, \infty]$. |
| $\mathcal{X}_n$ | Set of $n$ vertices of the graph. |
| $\mathbf{1}_A(x)$ | Indicator function of the set $A$, $1_A(x) = 1$ if $x \in A$ and $1_A(x) = 0$ if $x \notin A$. |
| $\delta(x)$ | Dirac delta function. |
| $\delta_{ij}$ | Kronecker's delta, $\delta_{ii} = 1$ and $\delta_{ij} = 0$ if $i \neq j$. |
| $\mathbb{E}[x]$ | Expectation of the random variable $x$. |
| $\mathrm{Var}(x)$ | Variance of the random variable $x$. |
| $a_n$ | Average vertex degree in a graph of $n$ vertices. |
| $r_n$ | Distance threshold. |
| $\mathbf{L}$ | Combinatorial Laplacian matrix. |
| $\boldsymbol{\mathcal{L}}$ | Normalized Laplacian matrix. |
| $\boldsymbol{\mathcal{L}}^{\mathrm{RW}}$ | Random walk normalized Laplacian matrix. |

| | |
|---|---|
| $\hat{\boldsymbol{\mathcal{L}}}$ | Regularized normalized Laplacian matrix. |
| $\mathbf{P}$ | Transition matrix of the random walk in a graph. |
| $\mathbf{I}_n$ | Identity matrix of size $n \times n$. |
| $d_s$ | Spectral dimension, describing the scaling of the Laplacian spectral density. |
| $P_0(t)$ | Return probability at the origin at time $t$. |
| $\mathbb{T}^d$ | $d$-dimensional unit Torus. |
| $\|.\|$ | Absolute value. |

# Chapter 1

# Introduction

## 1.1 Context

The last decade has witnessed an explosion of the amount of data that are generated and processed on a daily basis. In this era of big data, there is a spectacular increase in the size of networks, such as the Internet, social networks like Facebook™ and Twitter™, information and biological networks [1]. The analysis of such networks is very complex, therefore they are commonly referred to as complex networks [2].

Complex Networks are often inherently difficult to understand due to their large sizes, structural complexity, their evolution over time and their connection diversity[1] [3]. A remedy to this problem is to model complex networks using *graphs*, which translate objects into vertices and relations into edges connecting the vertices. For example, neural engineers represent the connectivity of neurons in the human brain using graphs, whereas, electrical engineers use graphs to understand large and complex systems, such as the Internet. Software engineers at Facebook™ use graphs to enable us to visualize social relationships, whereas, bio-engineers study how an infectious disease, like the flu, might spread over a social network. Understanding the mathematics behind graph theory can help bio-medical engineers and scientists to develop better cancer treatments, and electrical engineers to design faster and more reliable communication networks among electronic devices. Additionnaly, considering the large amount of variability in the connections between vertices, complex networks can be modelled using *random graphs*. Random graphs are probabilistic models where links exist between pairs of vertices according to some probabilistic rule [4].

The theory of random graphs originated in a series of papers [5], [6], [7] published in the period 1959-1968 by Paul Erdös and Alfred Rényi. Over the sixty years that have passed since then, *random graph theory (RGT)* which is an interdisciplinary field between graph theory and probability theory, has developed into an independent and fast growing branch of discrete mathematics. The interest in this field has been rapidly growing in recent years

[1]The links between vertices could have different weights, directions and signs.

driven by many applications both in theoretical and practical aspects. A very simple yet very useful random graph is the Erdös-Rényi (ER) random graph, developed by Erdös and Rényi [5], [6] and Gilbert [8] that consists of all graphs that arise by taking $n$ vertices, and placing independently and with probability $p$ an edge between any pair of distinct vertices. The edge probability can be fixed, or, more generally can be a function of $n$. ER graphs are the most thoroughly studied variety of random graphs along with many of their different variants due to its numerous applications in different real-world problems.

Until the late 1990s, most of the studies concerned either completely random or completely deterministic graphs even though most real-world networks contain features captured by neither of these two models. Around this time, computing power increased and empirical studies became possible, drawing the attention of researchers on introducing other models that capture unique features of real-world networks. Models that are neither completly random nor regular, such as the Barabasi and Albert scale-free (SF) model [9], [10], the small-world (SW) network by Watts and Strogatz [11] were introduced to model real-world networks. In particular, the ER model is inadequate to describe networks whose interactions between vertices depends on their proximity as the ER graph structure disregards uncountable information about the goegraphical position of the vertices. In order to model these features, Gilbert in [12] introduced another random graph called random geometric graph (RGG) whose vertices have some random positions in a metric space and edges are determined by the pairwise distance between vertices. RGGs are very useful to model problems in which the geographical distance is a critical factor. For example, RGGs have been applied to wireless communication networks [13], [14], sensor networks [15], and to study the dynamics of a viral spreading processes in large-scale complex networks [16], [17].

Several different matrices can be associated with a given graph, e.g., adjacency matrix, Laplacian matrix, normalized Laplacian matrix. Matrices associated to random graphs are also random and their study belongs to *random matrix theory (RMT)* domain. In Chapter 2, we will briefly give the definitions and some of the main properties of different graph models and describe their associate matrices. In particular, a special attention will be given to RGGs, the random graph under study in this thesis.

Understanding the mathematics behind graph theory and equivalently their associate random matrices challenges our capacities of understanding. The study of eigenvalues and eigenvectors of these random matrices, known as *spectral graph analysis* plays a central role in information aggregation and our understanding of random graphs. Spectral graph analysis is the study of the spectra, i.e., the eigenvalues and eigenvectors of graph matrices and their relationship to important graph properties. The set of graph eigenvalues is called the *spectrum* of the graph. The goal of many problems in the field of graph theory concerns the characterization of properties or structures of a graph from its spectrum, such as connectivity, bipartitedness[2], graph diameter[3]. In addition, the evolution of various

[2]Bipartite graph is a graph whose vertices can be divided into two disjoint and independent sets $U$ and $V$ such that every edge connects a vertex in $U$ to one in $V$.

[3]Diameter $\gamma$ is an index measuring the topological length or extent of a graph by counting the number of edges in the shortest path between the most distant vertices, i.e., $\gamma = \max_{ij}\{s(i,j)\}$, where $s(i,j)$ is

random processes defined on the graph are closely related to the eigenvalues of a suitable graph matrix [18], [19]. Over the past thirty years, many interesting discoveries have been made regarding the relationship between various graph properties and the spectrum of the associate matrices. In this thesis, we investigate the spectrum of RGGs in different scaling regimes. In Chapter 3, we introduce some fundamental results from RMT and RGT. In particular, we review spectral properties of various random matrices. In Chapters 4 and 5, we investigate the spectra and spectral properties of RGGs, such as the RGG normalized Laplacian matrix eigenvalues, its spectral gap, the eigenvalue distribution of RGGs, the RGG adjacency matrix eigenvalues.

Recently, there is a growing interest in characterizing network structures using geometrical and topological tools [20], [21]. On the one hand, an increasing number of works aim at unveiling the hidden geometry of networks using statistical mechanics [22], [23], discrete geometry [24], and machine learning [25], [26]. On the other hand, topological data analysis is tailored to capture the structure of a large variety of network data. Diffusion on these random geometric structures has received considerable attention in recent years. The motivation comes from a wide range of different areas of physics such as percolation theory, where the percolation clusters provide fluctuating geometries, the physics of random media, where the effect of impurities is often modeled by random geometry [27], and finally quantum gravity, where space-time itself is treated as a fluctuating manifold [28]. In particular, the long time characteristics of diffusion have been studied for the purpose of providing quantitative information on the mean large scale behavior of the geometric object in question. The *spectral dimension (SD)* is one of the simplest quantities which provides such information. In Chapter 6, we investigate the SD of RGGs.

We conclude this chapter by describing in detail the major contributions and the structure of this thesis.

## 1.2 Thesis Organization and Contributions

### 1.2.1 Chapter 2

In this chapter, we introduce some basic concepts related to the representation and analysis of complex networks using graph theory. We describe different types of graphs that can be used to represent complex networks and describe the corresponding matrices and their properties. Finally, we state results from probability theory such as concentration inequalities useful for the analyses in the following chapters.

the number of edges in the shortest path from vertex $i$ to vertex $j$.

### 1.2.2 Chapter 3

In this chapter, we provide a survey of fundamental results on RMT, RGT and probability theory. In particular, we review spectral properties of different random matrices such as adjacency matrix, combinatorial and normalized Laplacian matrices corresponding to different random graphs, in addition to Euclidean random matrices. We compare the existing results on the spectrum of the different random matrices with the spectrum of RGGs. In addition, we give a brief background on the SD, an important characteristic of diffusion behavior over graphs.

### 1.2.3 Chapter 4

In this chapter, we study the spectrum of the normalized Laplacian and its regularized version for RGGs in different scaling regimes. We consider $n$ vertices distributed uniformly and independently on the $d$-dimensional torus $\mathbb{T}^d \equiv [0,1]^d$ and form an RGG by connecting two vertices when their $\ell_p$-distance, $1 \leq p \leq \infty$, does not exceed a certain threshold $r_n$. Two scaling regimes for $r_n$ are of special interest. One of these is the connectivity regime, in which the average vertex degree grows logarithmically in $n$ or faster. The second scaling regime is the thermodynamic regime, in which the average vertex degree is a constant. First, we provide an upper bound for the probability that the Hilbert-Schmidt norm of the difference between the RGG and the deterministic geometric graph (DGG) with nodes in a grid normalized Laplacian matrices is greater than a certain threshold, in both the connectivity and thermodynamic regime. In particular, in the connectivity regime, when $d$ is fixed and $n \to \infty$, we show that the RGG and DGG normalized Laplacian matrices are asymptotically equivalent with high probability. We show that the LSDs of the normalized Lapalcian matrices of RGGs and DGGs converge in probability to the same limit as $n \to \infty$. Therefore, we use the regular structure of the DGG to show that the limiting spectral distribution (LSD) of the normalized Laplacian matrix of RGGs converges to the Dirac distribution at one in the full range of the connectivity regime as $n \to \infty$. In the thermodynamic regime, we approximate the eigenvalues of the regularized normalized Laplacian matrix of the RGG by the eigenvalues of the DGG regularized normalized Laplacian, with an error bound that depends upon the average vertex degree.

#### Related Publications

1) **M. Hamidouche**, L. Cottatellucci, and K. Avrachenkov, "On the Normalized Laplacian Spectra of Random Geometric Graphs" *Submitted to Journal of theoretical probability.*

2) **M. Hamidouche**, L. Cottatellucci, and K. Avrachenkov, "Spectral Bounds of the Regularized Normalized Laplacian for Random Geometric Graphs." *4th Graph Signal Processing Workshop*, Jun. 2019, Minneapolis, USA.

### 1.2.4 Chapter 5

In this chapter, we analyze the spectrum of the adjacency matrix of random geometric graphs in the connectivity regime. Similarly to Chapter 4, the RGG is constructed by uniformly distributing $n$ vertices on the $d$-dimensional torus $\mathbb{T}^d \equiv [0,1]^d$ and connecting two vertices if their $\ell_p$-distance, with $p \in [1,\infty]$ is at most $r_n$. In the connectivity regime and under some conditions on the average vertex degree $a_n$, we show that the Hilbert-Schmidt norm of the difference between two sequences of adjacency matrices of RGGs and DGGs converges to zero in probability as $n \to \infty$. We show that the strong norms of adjacency matrices of DGGs and RGGs are not uniformly bounded asymptotically and then the convergence of the Hilbert-Schmidt norm is not sufficient to prove the asymptotic equivalence of the sequences of adjacency matrices of DGGs and RGGs. However, for adjacency matrices, we consider a weaker form of convergence in probability in terms of the Levy distance between the eigenvalue distributions of the adjacency matrices of DGGs and RGGs. Therefore, we show that the Levy distance between the eigenvalue distributions of the DGG and RGG adjacency matrices vanishes with high probability as $n \to \infty$. Then, we use the structure of the DGG to approximate the eigenvalues of the adjacency matrix of the RGG.

#### Related Publications

3) **M. Hamidouche**, L. Cottatellucci, and K. Avrachenkov, "Spectral Analysis of the Adjacency Matrix of Random Geometric Graphs." *57th Annual Allerton Conference on Communication, Control, and Computing*, Sep. 2019, Illinois, USA.

### 1.2.5 Chapter 6

In this chapter, we study the spectral dimension (SD) $d_s$ of RGGs in the thermodynamic regime. The spectral dimension characterizes the return time distribution of a random walk on the graph. The SD depends on the eigenvalue density (ED) of the graph normalized Laplacian in the neighborhood of the minimum eigenvalues. In fact, the behavior of the ED in such a neighborhood is what characterizes the random walk. First, we use the analytical approximation of the eigenvalues of the regularized normalized Laplacian matrix of RGGs in the thermodynamic regime from Chapter 4 to show that the smallest non zero eigenvalue converges to zero in the large graph limit. Based on the analytical expression of the RGG eigenvalues, we show that the eigenvalue distribution in a neighborhood of the minimum value follows a power-law tail. Using this result, we find that the SD of RGGs is approximated by the Euclidean dimension $d$ in the thermodynamic regime.

**Related Publications**

4) K. Avrachenkov, L. Cottatellucci and **M. Hamidouche**, "Eigenvalues and Spectral Dimension of Random Geometric Graphs" *8th International Conference on Complex Networks and their Applications*, Dec. 2019, Lisbon, Portugal.

# Chapter 2

# Mathematical Background

## 2.1 Introduction

In this chapter, we introduce theoretical concepts necessary to derive the results in the subsequent chapters. As stated in Chapter 1, numerous scientific fields deal with data that can be represented by graphs, and due to the random structure observed in real-world networks, random graphs result to be a very useful technique to model complex networks. Then, random graphs can be represented by random matrices in which rows and columns are indexed by the vertices.

In Section 2.2, we briefly describe some relevant random graph models and introduce different matrix representations for them. In 2.3, we present fundamental concepts from RMT and discuss some introductory results. Finally, in 2.3.3 and 2.3.4, we introduce relevant results from probability theory. In particular, we state fundamental concentration inequalities and the asymptotic behavior of matrices.

## 2.2 Random Graph Theory (RGT)

In the 1950s, Erdös and Rényi laid the foundations for the creation of the RGT. Since then, random graphs have become fundamental for the analysis of many complex networks. In graph theory, a graph consists of a set of points along with a certain linking structure. These points are called *vertices* or *nodes*. Two vertices are *adjacent* or *neighbours* if they are connected by a link. The connections are described as pairs of vertices and are called *edges*. Any edge connecting a vertex to itself is a *loop*. A graph with no loops is called a simple graph.

We use the notation $\mathcal{X}_n$ to denote the set of $n$ vertices of a graph. The collection of all edges is denoted by the set $E$. The pair consisting of vertex set $\mathcal{X}_n$ and the edge set $E$ forms a graph $G = (\mathcal{X}_n, E)$. A graph is undirected if its edges do not have an orientation. It is a directed graph if the edges have an associated direction. Mathematically, a graph is defined

by an ordered pair $G = (\mathcal{X}_n, E)$, consisting of a countable vertex set $\mathcal{X}_n = \{x_1, ...x_n\}$, where $n = |\mathcal{X}_n|$ denotes the number of vertices in the graph. The edge set is then the list of pairs $E = \{(x_i, x_j); x_i, x_j \in \mathcal{X}_n\}$ where $m = |E|$ is the total number of edges in the graph. The *size* of a graph is defined by the number of its edges. The number of vertices in $\mathcal{X}_n$ is called the *order* of the graph $G = (\mathcal{X}_n, E)$. In the following, graphs are undirected and finite and the connections between vertices are represented in the form of an $n \times n$ matrix. Rows and columns of the matrices correspond to vertices in $\mathcal{X}_n$. The element in the matrix reveals the corresponding relation between $x_i \in \mathcal{X}_n$ and $x_j \in \mathcal{X}_n$. Subsequently, $x_i$ is referred to as vertex $i$.

In this thesis, we focus on simple undirected graphs and we assume that there is always at most one edge between each pair of vertices. In the following, we define some fundamental properties related to graphs.

**Definition 1** (Connected Graph)**.** *An undirected graph is connected in the sense of a topological space when there is a path from any vertex to any other vertex in the graph. A graph that is not connected is said to be disconnected.*

**Definition 2** (Subgraph)**.** *A subgraph of a graph $G$ is another graph formed from a subset of the vertices and edges of $G$. The vertex subset must include all endpoints of the edge subset, but may also include additional vertices.*

**Definition 3** (Supergraph)**.** *A supergraph is a graph formed by adding vertices, edges, or both to a given graph. If $H$ is a subgraph of $G$, then $G$ is a supergraph of $H$.*

**Definition 4** (Connected Component)**.** *Connected component of an undirected graph is a subgraph in which any two vertices are connected to each other by paths, and which is connected to no additional vertices in the supergraph.*

**Definition 5** (Giant Component)**.** *A giant component is a connected component of a given graph $G$ that contains a finite fraction of the entire graph's vertices.*

**Definition 6** (Vertex Degree)**.** *The degree of a vertex in a graph is the number of edges incident to it. The degree of a vertex $x_i$ is denoted by $d_i$. In a regular graph, every vertex has the same degree.*

**Definition 7** (Chromatic Number)**.** *The chromatic number of a graph is the smallest number of colours with which one can colour the vertices in such a way that no two adjacent vertices have the same colour.*

**Definition 8** (Clique and Clique Number)**.** *A clique of a graph is a subset of its vertices such that every two vertices of the subset are connected by an edge. A maximum clique is a clique with the maximum number of vertices in a given graph $G$. The clique number of a graph $G$ is the number of vertices in a maximum clique of this graph.*

**Definition 9** (Walk)**.** *A walk on a graph refers to a finite or infinite sequence of edges which joins a sequence of vertices.*

**Definition 10** (Random Walk)**.** *A simple random walk (RW) process on a graph is a discrete time stochastic process that has as initial value an initial vertex $i_0$ from the set of vertices $\mathcal{X}_n$ under some distribution at time $t = 0$. At $t = 1$, the process unfolds taking as value one of the neighbors of this initial vertex $i_0$ chosen uniformly at random, i.e., with probability $d_{i_0}^{-1}$. At $t = 2$, the process unfolds taking as value a random neighbor of this new vertex, and so on.*

RW is a fundamental topic in discussions of Markov processes[1]. Their mathematical study has been extensive. Several properties, including dispersal distributions, first-passage or hitting times[2], encounter rates, recurrence or transience, have been introduced to quantify their behavior.

**Definition 11** (Recurrence and Transience)**.** *We say that a random walk is recurrent if it visits its starting position infinitely often with probability one and transient if it visits its starting position finitely often with probability one.*

Let the variable $S_n$ mark the position of the walk at time $n$ and $Z$ be the number of visits of $S_n$ to its starting point $S_0$, i.e.,

$$Z = \sum_{n \geq 0} \mathbf{1}_{\{S_n = S_0\}}.$$

Thus, recurrence means $\mathbb{P}(Z = \infty) = 1$ while transience means $\mathbb{P}(Z < \infty) = 1$.

### Convergence of Random Variables

The convergence of sequences of random variables to some limit random variable is an important concept in probability theory, and its applications to statistics and stochastic processes. In probability theory, there exist several different notions of convergence of random variables. In the following, we recall some of them.

**Definition 12** (Almost Sure Convergence )**.** *Let $\{x_n\}$ be a sequence of random variables defined on a sample space $\Omega$. We say that $\{x_n\}$ converges to $x$ almost surely, if there is a measurable set $A \subseteq \Omega$ such that*

- $\lim_{n\to\infty}\{x_n(w)\} = x(w)$, *for all* $w \in A$,
- $\mathbb{P}(A) = 1$.

[1] A Markov chain is a stochastic model describing a sequence of possible events in which the probability of each event depends only on the state attained in the previous event. In continuous-time, it is known as a Markov process.

[2] A hitting time is the first time at which a given process "hits" a given subset of the state space. Return time is also example of hitting times.

**Definition 13** (Convergence in Distribution ). *Let $x$ and $x_n$, $n \in \mathbb{N}$, be random variables with cumulative distribution functions $F$ and $F_n$, respectively. The sequence $\{x_n\}$ converges to $x$ in distribution if*

$$\lim_{n\to\infty} F_n(y) = F(y),$$

*for every $y \in \mathbb{R}$ at which $F$ is continuous.*

**Definition 14** (Convergence in Probability ). *Let $x$ and $x_n$, $n \in \mathbb{N}$ be random variables. The sequence $\{x_n\}$ converges to $x$ in probability if for all $\epsilon > 0$*

$$\lim_{n\to\infty} \mathbb{P}(|x_n - x| \geq \epsilon) = 0.$$

### Asymptotics

In the following, we introduce standard notations to describe the asymptotic behavior of the relative order of magnitude of two sequences of numbers $a_n$ and $b_n$, depending on a parameter $n \to \infty$. For simplicity, we assume $b_n > 0$ for all sufficiently large $n$.

- $a_n = \mathcal{O}(b_n)$ as $n \to \infty$ if there exists a constant $C$ and $n_0$ such that $|a_n| \leq Cb_n$ for $n \geq n_0$, i.e., if the sequence $|a_n|/b_n$ is bounded, except possibly for some small values of $n$ for which the ratio may be undefined.
- $a_n = \Omega(b_n)$ as $n \to \infty$ if there exists a constant $c > 0$ and $n_0$ such that $a_n \geq cb_n$ for $n \geq n_0$. If $a_n \geq 0$, this notation is equivalent to $b_n = \mathcal{O}(a_n)$.
- $a_n = \Theta(b_n)$ as $n \to \infty$ if there exists constants $C, c > 0$ and $n_0$ such that $cb_n \leq a_n \leq Cb_n$ for $n \geq n_0$, i.e., if $a_n = \mathcal{O}(b_n)$ and $a_n = \Omega(b_n)$. This asymptotic behavior is sometimes expressed by saying that $a_n$ and $b_n$ are of the same order of magnitude.
- $a_n = o(b_n)$ as $n \to \infty$ if $a_n/b_n \to 0$, i.e., $\forall \epsilon > 0$, $\exists\ n_0$ such that $|a_n| \leq \epsilon |b_n|$ for $n \geq n_0$.
- $a_n = w(b_n)$ as $n \to \infty$ if $a_n/b_n \to \infty$, i.e., $\forall k > 0$, $\exists\ n_0$ such that $|a_n| \geq k|b_n|$ for $n > n_0$.
- $a_n \ll b_n$ or $b_n \gg a_n$ if $a_n \geq 0$ and $a_n = o(b_n)$.

### Normed Vector Spaces

In order to define the distance between two vectors or two matrices and the convergence of sequences of vectors or matrices to asymptotic values, we can use the notion of a *norm*.

**Definition 15** (Norm). *Let $\mathbb{E}$ be a vector space over a field $\mathbb{K}$. The filed $\mathbb{K}$ is either the field $\mathbb{R}$ of reals, or the field of complex numbers $\mathbb{C}$. A norm on $\mathbb{E}$ is a function $\|.\| : \mathbb{E} \to \mathbb{R}^+$ with the following properties: for all $\lambda \in \mathbb{K}$ and all $\mathbf{x}, \mathbf{y} \in \mathbb{E}$, we have*

- *Positivity:* $\|\mathbf{x}\| \geq 0$, *and* $\|\mathbf{x}\| = 0$ *if and only if* $\mathbf{x} = 0$.
- *Scaling: For* $\lambda \geq 0$, $\|\lambda\mathbf{x}\| = |\lambda|\|\mathbf{x}\|$.
- *Triangle inequality:* $\|\mathbf{x} + \mathbf{y}\| \leq \|\mathbf{x}\| + \|\mathbf{y}\|$.

Let $\mathbb{E} = \mathbb{R}^d$ (or $\mathbb{E} = \mathbb{C}^d$). Let $p \geq 1$ be a real number. For any $\mathbf{x} \in \mathbb{E}$, we have the standard $p$-norm defined as

$$\|\mathbf{x}\|_p = \begin{cases} \left(\sum_{k=1}^{d} |x_k|^p\right)^{1/p} & \text{for } \; p \in [1, \infty), \\ \max\{|x_k|, \; 1 \leq k \leq d\} & \text{for } \; p = \infty. \end{cases}$$

The case $p = 2$ corresponds to the standard Euclidean norm.

A vector space $\mathbb{E}$ together with a norm $\|.\|$ is called *normed vector space*. To study the asymptotic equivalence of matrices, a metric on the space of linear space of matrices is required. A matrix norm is a norm on the vector space $\mathbb{E}$ of all matrices of size $n \times m$. Let $\mathbb{R}^{n\times m}$ be a vector space. Thus, the matrix norm is a function $\|.\| : \mathbb{R}^{n\times m} \to \mathbb{R}^+$ that must satisfy the properties described above.

Two matrix norms are of particular interest called the **strong** or **operator** norm and the **Hilbert-Schmidt** or **weak** norm. Let $\mathbb{V}$ and $\mathbb{W}$ be two normed vector spaces. The operator norm of a linear operator $T : \mathbb{V} \to \mathbb{W}$ is the largest value by which $T$ stretches an element of $\mathbb{V}$, i.e.,

$$\|T\| = \sup_{\|v\|=1} \|T(v)\|.$$

Let $\lambda_k \geq 0$ be the eigenvalues of the Hermitian nonnegative definite matrix $\mathbf{A}^T\mathbf{A}$. When $T$ is given by a matrix, i.e., $T(v) = \mathbf{A}v$. Then, $\|T\|$ is the square root of the largest eigenvalue of the symmetric matrix $\mathbf{A}^T\mathbf{A}$, i.e.,

$$\|\mathbf{A}\|^2 = \max_k \lambda_k.$$

The Hilbert-Schmidt norm of the $n \times n$ matrix $\mathbf{A}$ is defined by

$$\begin{aligned} \|\mathbf{A}\|_{\text{HS}} &= \left(\frac{1}{n}\sum_{k=0}^{n-1}\sum_{j=0}^{n-1} |A_{k,j}|^2\right)^{1/2} \\ &= \left[\frac{1}{n}\text{Trace}(\mathbf{A}^T\mathbf{A})\right]^{1/2} = \left(\frac{1}{n}\sum_{k=0}^{n-1} \lambda_k\right)^{1/2}. \end{aligned}$$

The Hilbert-Schmidt norm is the weaker of the two norms since

$$\|\mathbf{A}\|^2 = \max_k \lambda_k \geq \frac{1}{n}\sum_{k=0}^{n-1} \lambda_k = \|\mathbf{A}\|_{\mathrm{HS}}^2.$$

Various graphs are often used to model complex topologies found in real-world networks. In the following subsection, we briefly overview relevant random graphs used to model complex networks and present some of their properties.

### 2.2.1 Types of Graphs

Several graph models have been proposed for analytical studies such as ER random graph [5], Barabasi-Albert SF network model [9], Watts-Strogatz SW network model [11] and RGG [12], [29]. In the following, we describe different properties of these random graphs.

#### Erdös-Rényi Random Graph

The study of random graphs began in its own right with the seminal paper of Erdös and Rényi random graph and dates back to 1947 [5]. In the mathematical field of graph theory, Erdös-Rényi model refers to either of two closely related models for generating random graphs, namely *uniform model* and *binomial model*. They are named after the mathematicians Paul Erdös and Alfréd Rényi, who first introduced the model in 1959 called uniform model [5]. It is considered by some as the first conscious application of the probabilistic method for complex networks. While Edgar Gilbert introduced the binomial model [8] contemporaneously and independently of Erdös and Rényi.

**Definition 16** (Uniform Random Graph)**.** *Given an integer* $m$, $0 \leq m \leq \binom{n}{k}$, *the uniform random graph, denoted by* $G_u(n,m)$ *is defined on the space of events* $\Omega$, *consisting of all graphs on vertex set* $\mathcal{X}_n = \{x_1, ..., x_n\}$ *and exactly* $m$ *edges, with uniform probability on* $\Omega$, *i.e.,*

$$\mathbb{P}(G_u) = \binom{\binom{n}{2}}{m}^{-1}, \quad G_u \in \Omega.$$

Equivalently, uniform random graphs are obtained from an empty graph on the vertex set $\mathcal{X}_n$ by inserting $m$ edges, in such a way that all possible $\binom{\binom{n}{2}}{m}^{-1}$ are equally likely. In the following, we describe the binomial random graph.

**Definition 17** (Binomial Random Graph)**.** *Fix* $0 \leq p \leq 1$. *The binomial random graph denoted by* $G_b(n,p)$ *is defined on the space of event* $\Omega$ *consisting of the set of all graphs on the vertex set* $\mathcal{X}_n$ *and* $0 \leq m \leq \binom{n}{2}$ *edges and follows the probability given by*

$$\mathbb{P}(G_b) = p^m(1-p)^{\binom{n}{2}-m}, \quad G_b \in \Omega.$$

Equivalently, a binomial random graph $G_b(n,p)$ is obtained from an empty graph with vertex set $\mathcal{X}_n$ by performing $\binom{n}{2}$ Bernoulli experiments to generate edges independently with probability $p$.

**Lemma 1** (Relationship between $G_u(n,m)$ and $G_b(n,p)$, [30])**.** *A binomial random graph $G_b(n,p)$ with $m$ edges, is equally likely to be one of the $\binom{\binom{n}{2}}{m}$ graph realizations with $m$ edges of a uniform random graph $G_u(n,m)$.*

The main difference between the uniform and binomial model is that in the uniform model $G_u(n,m)$ we choose its number of edges, while in the case of the binomial model $G_b(n,p)$, the number of edges is the Binomial random variable with parameters $\binom{n}{2}$ and $p$.

The expected number of edges in $G_b(n,p)$ is $\binom{n}{2}p$. For large $n$, the random graphs $G_b(n,p)$ and $G_u(n,m)$ should behave in a similar way when the number of edges $m$ in a uniform random graph $G_u(n,m)$ equals or is approximately close to the expected number of edges in a binomial random graph $G_b(n,p)$ [30], i.e., when

$$m = \binom{n}{2}p \approx \frac{n^2 p}{2},$$

or equivalently, when the edge probability in a binomial random graph $G_b(n,p)$ is

$$p \approx \frac{2m}{n^2}.$$

Many results are available in random graph literature describing the behavior of binomial random graphs $G_b(n,p)$ for different values of $p$ when $n$ grows [6]. An important studied aspect for $G_b(n,p)$ is the presence of connected components and the evolution of their sizes with respect to the increasing number of vertices $n$ in the graph. In particular, results on the connectivity threshold and the appearance of the giant component in ER random graph are mentioned in the following theorems.

**Theorem 2** (Connectivity Threshold of ER Graph, [6])**.** *Let $G_b(n,p)$ be a binomial random graph. For all $\epsilon > 0$, the probability that the graph is connected for $n \to \infty$ is given by*

$$\mathbb{P}(G_b \text{ is connected}) \to \begin{cases} 1, & \text{if} \quad p > \frac{(1-\epsilon)\log(n)}{n}, \\ 0, & \text{if} \quad p < \frac{(1-\epsilon)\log(n)}{n}. \end{cases}$$

In the following, we provide general results on the existence of a giant component in ER random graphs.

**Theorem 3** (Existence of a Giant Component in ER Graphs, [6])**.** *Let $G_b(n,p)$ be a binomial random ER graph and fix $np = c$, where $c > 0$ is a constant*

- *If $c < 1$, then almost surely the largest connected component of $G_b(n,p)$ has at most $\frac{3\log(n)}{(1-c)^2}$ vertices.*

- *If $c > 1$, then $G_b(n,p)$ contains a giant component of $\Theta(n)$ vertices. Furthermore, almost surely the size of the second largest component of $G_b(n,p)$ is at most $\frac{16c\log(n)}{(1-c)^2}$.*

- *If c=1, then $G_b(n,p)$ almost surely has the largest component of size of order $n^{2/3}$.*

Theorem 2 states that $p = \frac{\log(n)}{n}$ is a sharp threshold for the connectivity of $G_b(n,p)$ and Theorem 3 shows that $p = \frac{1}{n}$ is a sharp threshold for the existence of a giant component in $G_b(n,p)$.

Models based on ER random graphs are often not capable to capture properties that appear in real-world complex networks as pointed out in [3] and [9]. First, as shown by Watts and Strogatz in [11], in some real-world networks, nodes are prone to group in clusters, i.e., vertices having a common neighbor have a higher probability to be connected. Whereas, in Erdös and Rényi's graphs, all pairs of vertices have equal probability to be connected and cannot model this particularity often referred to as clustering. Watts and Strogatz measured clustering by defining a *clustering coefficient*, which is the average probability that two neighbors of a given vertex are also neighbors of one another. In many real-world networks the clustering coefficient is found to have a high value. In contrast, the clustering coefficient in Erdös-Rényi graphs is equal to $p$. A second aspect in which random graphs differ from real-world networks is in their degree distributions. The probability $p_k$ that a vertex in Erdös-Rényi random graph has exactly degree $k$ is given by the binomial distribution

$$p_k = \binom{n-1}{k} p^k (1-p)^{n-1-k}.$$

In the limit where $n \gg kz$, the probability $p_k$ is given by Poisson distribution with parameter $z > 0$

$$p_k = \frac{z^k e^{-z}}{k!}.$$

Comparisons between the degree distribution of Erdös-Rényi graphs and examples from real-world networks in [31] show that in most cases the degree distribution of the real-world network is very diferent from the Poisson distribution. Many real-world complex networks, including Internet and World-Wide Web graphs, appear to have power-law degree distributions [32], which implies that a small but non-negligible fraction of their vertices have a very large degree.

### Small-World (SW) Graph

Most of real-world networks, especially social networks, do not have an homogeneous distribution of degrees in contrast to regular or random networks. To overcome this limitation, Watts and Strogatz [11] propose a model where the connections between vertices in a regular graph are rewired with a certain probability. The resulting graphs have a vertex degree distribution between regular and random graphs and are referred to as SW graphs. SW graphs model very well many social networks in terms of clustering coefficient since they have a higher clustering coefficient and almost the same average path as the actual social networks with the same number of vertices and edges. SW graphs usually have a high modularity. A topologically modular network can be broken down into component modules, each of which comprises a number of nodes that are densely intra-connected to each other but sparsely inter-connected to nodes in other modules.

### Scale-Free (SF) Network

SF networks are a type of network characterized by the presence of few vertices that are highly connected to other vertices in the network, called hubs. The presence of hubs will determine a long tail in the vertex degree distribution because of the presence of vertices with a much higher degree than most other vertices. A scale-free network is characterized as a power-law vertex degree distribution. For an undirected network, the vertex degree distribution is given by

$$P_{\text{deg}}(k) \propto k^{-\gamma},$$

where $\gamma$ is an exponent. This form of $P_{\text{deg}}(k)$ decays slowly as the vertex degree $k$ increases, increasing the likelihood of finding a vertex with a very large degree.

### Random Geometric Graph (RGG)

An RGG consists of a set of vertices distributed randomly over some metric space, with two vertices joined by an edge if the distance between pairs of vertices does not exceed a certain threshold. This construction presents a natural alternative to the classical ER random graph model, in which the presence of each edge is an independent event.

RGGs were first proposed by Gilbert in [12] to model communications among radio stations. Since then, RGGs have been a very relevant and well studied model for large communication networks. Prominent examples in telecommunications are sensor networks [15], where sensors are represented by the vertices of the RGG and the wireless connectivity between sensors is represented by the RGG edges, and wireless ad-hoc network [33]. The model has been also applied to analyze spreading processes in large-scale complex networks [16], [17]. An additional very important motivation for the study of RGGs is their applications to statistics and learning. Clustering techniques such as the nearest-neighbor technique in statistics and machine learning are based on the spatial structure of RGGs [34].

RGGs have also been extensively studied from a mathematical point of view. Various interesting properties of RGGs have been discovered since their introduction, and the monograph [29] by Penrose is a fundamental reference. Very relevant results exist in [29] regarding their connectivity, chromatic number, clique number and other structural properties. They are well studied theoretically, although not at the same extent of ER graphs. A mathematical definition for an RGG is given as follows.

**Definition 18.** *Let $\|.\|_p$ be the $\ell_p$-metric on $\mathbb{R}^d$ and $r$ be a positive parameter. Let $f$ be a specified probability density function on $\mathbb{R}^d$ and let $\mathcal{X}_n = \{\mathbf{x}_1, ..., \mathbf{x}_n\}$ be a set of independent and identically distributed $d$-dimensional random variables with density $f$. The RGG is the undirected graph denoted by $G(\mathcal{X}_n, r)$ with vertex set $\mathcal{X}_n$ and undirected edge connecting $\mathbf{x}_i$ and $\mathbf{x}_j$, for any $i, j \in \{1, ..., n\}$, if $\|\mathbf{x}_i - \mathbf{x}_j\|_p \leq r$.*

The $\ell_p-$**metric** on $\mathbb{R}^d$ is defined as

$$\|\mathbf{x} - \mathbf{y}\|_p = \begin{cases} \left(\sum_{k=1}^{d} |x_k - y_k|^p\right)^{1/p} & \text{for } \ p \in [1, \infty), \\ \max_k\{|x_k - y_k|,\ 1 \leq k \leq d\} & \text{for } \ p = \infty, \end{cases}$$

where the case $p = 2$ gives the standard Euclidean metric on $\mathbb{R}^d$. When $p = \infty$, the maximum distance between two vertices is called the Chebyshev distance.

The above definition of an RGG is very general. In this thesis, we use a more specific definition. In Chapter 4, we assume that the vertices of the RGG denoted by $G(\mathcal{X}_n, r_n)$ are independently and *uniformly* distributed in a unit torus and the radius threshold $r$ is given as a function of $n$, i.e., $r_n$. We will give the detailed definition in Chapter 4.

Let $\theta^{(d)}$ denote the volume of the $d$-dimensional unit hypersphere in $\mathbb{R}^d$. When the vertices are uniformly distributed, the average vertex degree $a_n$ in $G(\mathcal{X}_n, r_n)$ is given by

$$a_n = \theta^{(d)} n r_n^d.$$

Similiraly as with ER graphs, RGGs exhibit thresholds for some properties in terms of the radius $r_n$ or, equivalently, the average vertex degree $a_n$, such as the connectivity threshold. The connectivity threshold of RGGs has a long history. In the late 1990s, Penrose [35], [36], Gupta and Kumar [37], Appel and Russo [38] investigated connectivity properties of RGGs in which vertices are independently and uniformly distributed in a 2-dimensional cube, i.e., $[0, 1]^2$ and edges are determined by the Euclidean distance. An accurate estimation for the smaller value of $r_n$ at which the RGG becomes connected with high probability is derived.

In the following, we recall the fundamental results about connectivity of RGGs. The detailed proofs of the following two results on the connectivity of RGGs can be found in [29], [36], [37], [38]. A necessary condition for connectivity in RGGs is the absence of isolated vertices in the graph. This condition is also sufficient with high probability when $n \to \infty$. Therefore, the following lemma provides a result on the number of isolated vertices in RGGs.

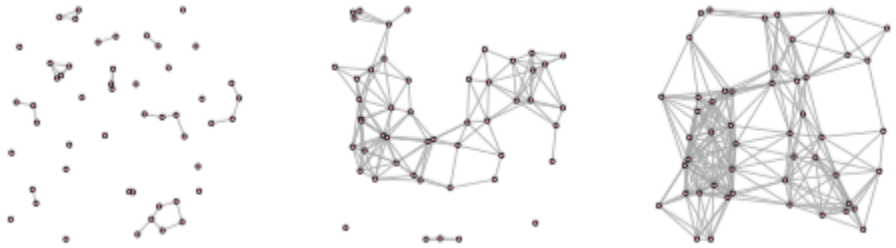

Figure 2.1: From left to right: independent realizations of three RGGs with $n = 50$ and radius 0.1, 0.2, 0.3, respectively.

**Lemma 4** (Number of Isolated Vertices in RGGs)**.** *Consider an RGG $G(\mathcal{X}_n, r_n)$ based on the Euclidean distance, with n vertices independently and uniformly distributed in $[0,1]^2$. Let $K$ be a random variable counting the number of isolated vertices in $G(\mathcal{X}_n, r_n)$. Then, by multiplying the probability that one vertex is isolated by the total number of vertices, we obtain*

$$\mathbb{E}[K] = n(1-\pi r_n^2)^{n-1} = ne^{-\pi r_n^2 n} - \mathcal{O}(r_n^4 n).$$

Notice that $\mathbb{E}[K]$ depends on $\mu = ne^{-\pi r_n^2 n}$. Then, the asymptotic behavior of $\mu$ characterizes the connectivity of $G(\mathcal{X}_n, r_n)$.

**Theorem 5** (Connectivity of RGGs, [37], [36])**.** *Let $\mu = ne^{-\pi r_n^2 n}$.*

- *If $\mu \to 0$ then almost surely $G(\mathcal{X}_n, r_n)$ is connected.*
- *If $\mu = \Theta(1)$ then almost surely $G(\mathcal{X}_n, r_n)$ has a component of size $\Theta(n)$ and $K$ follows a Poisson distribution with parameter $\mu$.*
- *If $\mu \to \infty$ then $G(\mathcal{X}_n, r_n)$ is almost surely disconnected.*

From the definition of $\mu$ we deduce that when $\mu = \Theta(1)$ then $r_n = \sqrt{\frac{\log(n)-\log(\mu)}{\pi n}}$ holds. Therefore, we conclude that the property of connectivity of $G(\mathcal{X}_n, r_n)$ exhibits a sharp threshold at

$$r_n = \sqrt{\frac{\log(n)-\log(\mu)}{\pi n}}. \tag{2.1}$$

This result has been generalized to RGGs in which vertices are uniformly and independently distributed in the hypercube $[0,1]^d$, with $d \geq 2$ under any $\ell_p$-distance, $1 \leq p \leq \infty$ [29],[35], [39]. The connectivity threshold in this case is given by

$$r_c = \left( \frac{\log(n)}{n\alpha_p} \right)^{1/d},$$

for constant $\alpha_p > 0$.

Denote by $\mathcal{C}$ and $\mathcal{D}$ the events that $G(\mathcal{X}_n, r_n)$ is connected and disconnected, respectively. The probability that $G(\mathcal{X}_n, r_n)$ is connected or disconnected is provided by the following corollary.

**Corollary 1.** *Assume that* $\mu = \Theta(1)$. *Then*

$$\mathbb{P}[\mathcal{C}] \sim \mathbb{P}[K = 0] \sim e^{-\mu}.$$

$$\mathbb{P}[\mathcal{D}] \sim \mathbb{P}[K > 0] \sim 1 - e^{-\mu}.$$

Hence, we can distinguish different scaling regimes for $r_n$ or equivalently for $a_n$ in RGGs. The first one is the connectivity regime, in which the average vertex degree $a_n$ grows logarithmically in $n$ or faster, i.e., $\Omega(\log(n))$. The second scaling regime is the dense regime, in which $a_n \equiv \Theta(n)$. An additional relevant scaling regime is the thermodynamic regime, in which the average vertex degree is a constant $\gamma$, i.e., $a_n \equiv \gamma$. In this case the graph is disconnected. As we shall see, if the constant $\gamma$ in the thermodynamic regime is above a certain critical value, likely there is a giant component of $G(\mathcal{X}_n, r_n)$ containing a strictly positive fraction of the vertices. This phenomenon is known as percolation. Exact values for $\gamma$ at which the giant component appears in $G(\mathcal{X}_n, r_n)$ are not known. For $d = 2$, with the Euclidean distance, simulation studies in [29] indicate that the giant component occurs at $\lambda = 1.44$, while rigorous bounds $0.696 < \lambda < 3.372$ are given in [40].

The above characterization of the structure of RGGs provides insights on the spectra observed in the different regimes that are analyzed in the next chapters. Realizations of three RGGs with $n = 50$ vertices uniformly distributed in a unit cube $[0, 1]^2$ with three different radius values is shown in Figure 2.1.

### 2.2.2 Preliminary Notation and Matrix Graph Representation

Graphs can be described by a number of matrices. The most intuitive matrix representation of a graph summarizes the adjacencies of the vertices. For a graph with $n$ vertices, the adjacency matrix $\mathbf{A} \in \mathbb{R}^{n \times n}$ has $n$ rows and $n$ columns corresponding to the vertices. The elements $A_{ij}$ of the adjacency matrix $\mathbf{A}$ takes unit value when there is an edge between vertices $i$ and $j$ and zero otherwise, i.e.,

$$A_{ij} = \begin{cases} 1, & \text{if } i \sim j \text{ and } i \neq j, \\ 0, & \text{otherwise.} \end{cases}$$

Here $i \sim j$ denotes the existence of an edge between vertex $i$ and $j$. From the definition of adjacency matrix, if a graph is directed, then, in general, the graph is asymmetric and the adjacency matrix does not have a special structure. In particular, it is not symmetric, i.e., $\mathbf{A} \neq \mathbf{A}^T$. For undirected graphs, the adjacency matrix $\mathbf{A}$ is symmetric. If all the vertices in a graph $G = (\mathcal{X}_n, E)$ are isolated, i.e., $A_{ij} = 0$ for all $i, j \in \mathcal{X}_n$, the graph is called a *null* graph.

A second important matrix associated to graphs is the Laplacian matrix which plays a major role on dynamical processes. Recall that the degree $d_i$ of a vertex $i$ is the number of edges attached to it. It is given by the cardinality of the set $\{j : j \sim i\}$ or, equivalently, in terms of the adjacency matrix elements expressed as follows

$$d_i = \sum_j A_{ij}.$$

The Laplacian matrix of a graph is a real symmetric $n \times n$ matrix defined by the following difference matrix

$$\mathbf{L} = \mathbf{D} - \mathbf{A}.$$

Here, $\mathbf{D} \in \mathbb{R}^{n \times n}$ is the diagonal $n \times n$ matrix of vertex degrees such that $D_{ij} = d_i \delta_{ij}$, where $\delta_{ij}$ denotes the Kronecker's delta. Let us consider a simple graph. Since the diagonal elements of the adjacency matrix are zero for a simple graph, the elements of the graph Laplacian matrix are given by

$$L_{ij} = \begin{cases} d_i, & \text{if } i = j, \\ -1, & \text{if } i \sim j, \\ 0, & \text{otherwise.} \end{cases}$$

The matrix $\mathbf{L}$ is called **combinatorial Laplacian** in order to distinguish it from slightly different matrices called **symmetric normalized Laplacian** $\boldsymbol{\mathcal{L}}$ and the **transition matrix** of a RW $\mathbf{P}$. Let $\mathbf{I}_n$ be the $n \times n$ identity matrix. The normalized Laplacian matrix $\boldsymbol{\mathcal{L}}$ is defined as

$$\begin{aligned} \boldsymbol{\mathcal{L}} &= \mathbf{D}^{-1/2} \mathbf{L} \mathbf{D}^{-1/2} \\ &= \mathbf{I}_n - \mathbf{D}^{-1/2} \mathbf{A} \mathbf{D}^{-1/2}, \end{aligned}$$

and has elements

$$\mathcal{L}_{ij} = \begin{cases} 1, & \text{if } i = j, \\ -\dfrac{1}{\sqrt{d_i d_j}}, & \text{if } i \sim j, \\ 0, & \text{otherwise.} \end{cases}$$

The RW normalized Laplacian matrix is defined as

$$\begin{aligned}\boldsymbol{\mathcal{L}}^{\mathrm{RW}} &= \mathbf{D}^{-1}\mathbf{L} = \mathbf{I}_n - \mathbf{D}^{-1}\mathbf{A} \\ &= \mathbf{D}^{-1/2}(\mathbf{I}_n - \mathbf{D}^{-1/2}\mathbf{A}\mathbf{D}^{-1/2})\mathbf{D}^{1/2} \\ &= \mathbf{D}^{-1/2}\boldsymbol{\mathcal{L}}\mathbf{D}^{1/2},\end{aligned} \tag{2.2}$$

and has elements

$$\mathcal{L}_{ij}^{\mathrm{RW}} = \begin{cases} 1, & \text{if } i = j, \\ -\dfrac{1}{d_i}, & \text{if } i \sim j, \\ 0, & \text{otherwise.} \end{cases}$$

The name of the RW normalized Laplacian comes from the fact that this matrix is $\boldsymbol{\mathcal{L}}^{\mathrm{RW}} = \mathbf{I}_n - \mathbf{P}$, where $\mathbf{P} = \mathbf{D}^{-1}\mathbf{A}$ is simply the transition matrix of a random walker on the graph.

The transition matrix of the RW $\mathbf{P}$ defined by $\mathbf{P} = \mathbf{D}^{-1}\mathbf{A}$ has elements

$$P_{ij} = \begin{cases} \dfrac{1}{d_i}, & \text{if } i \sim j \text{ and } i \neq j, \\ 0, & \text{otherwise.} \end{cases}$$

For undirected graphs $G$, the transition matrix $\mathbf{P}$ is a column-stochastic matrix in which the sum across each column is 1. The transition matrix $\mathbf{P}$ plays a key role in the analysis of RWs on graphs.

The incidence matrix $\mathbf{B}$ for a directed graph describing a network's structure is defined as

$$B_{ij} = \begin{cases} -1, & \text{if edge } j \text{ starts at vertex } i, \\ +1, & \text{if edge } j \text{ ends at vertex } i, \\ 0, & \text{otherwise.} \end{cases}$$

In the case of undirected graphs, the incidence matrix is obtained by assigning an arbitrary direction to each edge. The incidence matrix provides an alternative way to define the graph Laplacian matrix

$$\mathbf{L} = \mathbf{B}\mathbf{B}^T.$$

Let $G = (\mathcal{X}_n, E)$ be a simple undirected graph with a vertex set $\mathcal{X}_n = \{x_1, x_2, ...x_n\}$ and edge set $E$ and $\mathbf{A}$ be an $n \times n$ matrix representation of the graph $G$. For a square

matrix $\mathbf{A} \in \mathbb{R}^{n \times n}$, the eigenvalues $\lambda_i(\mathbf{A})$ are defined as values such that there exist vectors $\mathbf{v}_i \in \mathbb{R}^{n \times 1}$, $\mathbf{v}_i \neq 0$ with

$$\mathbf{A}\mathbf{v}_i = \lambda_i \mathbf{v}_i. \tag{2.3}$$

The pair $(\lambda_i, \mathbf{v}_i)$ is known as the eigenvalue-vector pair. In general the number $\lambda_i$ can be complex, but if $\mathbf{A}$ is symmetric, then $\mathbf{A}$ has real eigenvalues $\lambda_1, ..., \lambda_n$, and $\mathbb{R}^n$ has an orthonormal basis $\mathbf{v}_1, ..., \mathbf{v}_n$, where each vector $\mathbf{v}_i$ is an eigenvector of $\mathbf{A}$ with eigenvalue $\lambda_i$. Then,

$$\mathbf{A} = \mathbf{H}\mathbf{D}\mathbf{H}^{-1}, \tag{2.4}$$

where $\mathbf{H}$ is the matrix whose columns are $\mathbf{v}_1, ..., \mathbf{v}_n$, and $\mathbf{D}$ is the diagonal matrix whose diagonal entries are $\lambda_1, ..., \lambda_n$. Since the vectors $\mathbf{v}_1, ..., \mathbf{v}_n$ can be chosen to be orthonormal, the matrix $\mathbf{H}$ is orthogonal, i.e., $\mathbf{H}^T\mathbf{H} = \mathbf{I}_n$, thus we can alternatively write the above equation as

$$\mathbf{A} = \mathbf{H}\mathbf{D}\mathbf{H}^T. \tag{2.5}$$

The spectral radius of a matrix $\mathbf{A}$ is the non-negative real number given by

$$\rho(\mathbf{A}) = \max\{|\lambda_i| : 1 \leq i \leq n\},$$

The set $\{\lambda_i : 1 \leq i \leq n\}$ is called the spectrum of $\mathbf{A}$.

Let $\mathbf{A}$ be an $m \times n$ matrix. The matrix $\mathbf{A}^T\mathbf{A}$ is evidently a symmetric $n \times n$ matrix, and thus its eigenvalues are real. The singular values of $\mathbf{A}$ are the square roots of the eigenvalues of $\mathbf{A}^T\mathbf{A}$.

Let $\lambda_i$ be an eigenvalue of $\mathbf{L}$ with the corresponding normalized eigenvector, $\mathbf{v}_i$, $\mathbf{L}\mathbf{v}_i = \lambda_i\mathbf{v}_i$. Then,

$$\lambda_i = \mathbf{v}_i^T(\lambda_i\mathbf{v}_i) = \mathbf{v}_i^T(\mathbf{L}\mathbf{v}_i) = \mathbf{v}_i^T(\mathbf{B}\mathbf{B}^T\mathbf{v}_i) = (\mathbf{v}_i^T\mathbf{B})(\mathbf{B}^T\mathbf{v}_i) = (\mathbf{B}^T\mathbf{v}_i)^T(\mathbf{B}^T\mathbf{v}_i),$$

which corresponds to the inner product of the real vector $\mathbf{B}^T\mathbf{v}_i$ with itself. Therefore, the eigenvalues of the graph Laplacian are non-negative

$$\lambda_i \geq 0.$$

Since all the rows of the Laplacian matrix sum up to zero, the constant vector $\mathbf{1} = (1, 1, ..., 1)$ is a Laplacian eigenvector which corresponds to the zero eigenvalue. Then, the zero eigenvalue is always present in the Laplacian matrix spectrum and the eigenvalues are usually ordered as

$$\lambda_1 \geq \lambda_2 \geq ... \geq \lambda_n = 0.$$

The spectrum of $\boldsymbol{\mathcal{L}}$ has also non-negative real eigenvalues and its smallest eigenvalues is equal to zero, i.e., $\lambda_n = 0$. The eigenvalues of the normalized Laplacian matrix $\boldsymbol{\mathcal{L}}$ satisfy $0 = \lambda_n \leq \lambda_1 \leq 2$. The multiplicity of $\lambda_i = 0$ corresponds to the number of connected components of the graph. In addition, the smallest non-zero eigenvalue of the matrices $\mathbf{L}$

and $\boldsymbol{\mathcal{L}}$ is referred to as the *spectral gap*, a key property for graphs, related to the connectivity and the dynamics of numerous processes on the graph such as RWs. Furthermore, a larger spectral gap of the Laplacian matrix implies a more highly intertwined subgraph structure [41]. In other words, a large value of the smallest non-zero eigenvalue implies that there is a high number of links between any two possible pairs of clusters in the graph.

From (2.2), we note that the RW normalized Laplacian $\boldsymbol{\mathcal{L}}^{\mathrm{RW}}$ and the symmetric normalized Laplacian $\boldsymbol{\mathcal{L}}$ have the same spectrum. To see the connection between the probability transition matrix $\mathbf{P}$ and the normalized Laplacian matrix $\boldsymbol{\mathcal{L}}$, note that

$$\mathbf{D}^{-1/2}(\mathbf{I}_n - \boldsymbol{\mathcal{L}})\mathbf{D}^{1/2} = \mathbf{D}^{-1/2}(\mathbf{D}^{-1/2}\mathbf{A}\mathbf{D}^{-1/2})\mathbf{D}^{1/2} = \mathbf{P}.$$

As a consequence, if $\lambda_i$ is an eigenvalue of $\boldsymbol{\mathcal{L}}$ then $1 - \lambda_i$ is an eigenvalue of $\mathbf{P}$. In particular, the value one is always an eigenvalue of $\mathbf{P}$ since zero is always an eigenvalue of $\boldsymbol{\mathcal{L}}$.

In the following subsection, we provide preliminary definitions and an overview of different concepts on random matrices.

## 2.3 Random Matrix Theory (RMT)

As announced in the introduction, in this section, we review the main analytical tool that is RMT by recalling some of its basic concepts. The study of random matrices began with the work of Wishart in 1928 [42], who was interested in the distribution of the so-called empirical covariance matrices, which ultimately led to the Marcenko-Pastur distribution in 1967. Random matrices were utilized by Wigner in the 1950's as a statistical tool to model energy levels of heavy nuclei [43], and led to the well-known Wigner semi-circle distribution. Branching off from these early physical and statistical applications, RMT has become a vibrant research field of its own, with scores of beautiful results in the last decades. In the next chapter we provide the formal definition of the famous Marcenko-Pastur and Wigner semi-circle distributions.

We will only consider concepts of RMT necessary for the study of random graphs, and leave aside many topics. For more detailed and comprehensive introductions to RMT, see [44], [45], [46].

### 2.3.1 Types of Random Matrices

#### Wishart Matrix

Historically, the first defined random matrix is the well-known Wishart matrix. Let $\mathbf{x}_1 ... \mathbf{x}_n \in \mathbb{C}^p$ be independent and identically distributed (i.i.d) $p-$dimensional random vectors distributed as Gaussian with zero mean and variance $\boldsymbol{\Sigma}$, i.e., $\mathrm{N}(0, \boldsymbol{\Sigma})$. Then, the

Wishart distribution is the probability distribution of the eigenvalues of the $p \times p$ random matrix $\mathbf{C}_p$, i.e.,

$$\mathbf{C}_p = \frac{1}{n} \sum_{k=1}^{n} \mathbf{x}_k \mathbf{x}_k^H.$$

Historically, this was the first random matrix studied by John Wishart who provided the joint distribution of the eigenvalues of $\mathbf{C}_p$.

### Wigner Matrix

After the introduction of Wishart matrices, Eugene Wigner [43] studied the eigenspetrum of large Hermitian matrices, a kind of random matrices, known nowadays as Wigner matrices used to model the nuclei of heavy atoms. Wigner matrices, denoted in the following by $\mathbf{X}$ satisfy the following properties:

- $\mathbf{X}$ is an $n \times n$ random Hermitian matrix.
- The upper-triangular entries $X_{ij}$, $1 \leq i \leq j \leq n$, are i.i.d.(complex) random variables with zero mean and unit variance.
- The diagonal entries are i.i.d. real random variables.

### Euclidean Random Matrix (ERM)

In many physical applications, pairwise interactions can depend on distance, such that the strength or probability of interaction related to physical distance via a function over an Euclidean space. Random matrices that incorporate this constraint are known as Euclidean random matrices (ERM) [47], and have been used to model physical phenomena such as diffusion [48] and wave propagation [49].

The Euclidean random matrix is a relevent class of random matrices introduced by Mézard, Parisi and Zee [47]. An ERM is an $n \times n$ matrix $\mathbf{M}_n$, whose entries are a function of the distance of pairs of random points distributed according to some probability distribution in a compact set $\Omega$ of $\mathbb{R}^d$ represented as

$$M_{ij} = f(\|\mathbf{x}_i - \mathbf{x}_j\|_p) - u\delta_{ij} \sum_k f(\|\mathbf{x}_i - \mathbf{x}_k\|_p), \tag{2.6}$$

where $u$ is a real parameter which enables us to interpolate between the two most interesting cases $u = 0, 1$. The case where $u = 0$ is the simplest mathematical problem with correlated matrix elements and the case where $u = 1$ is the natural problem which appears when studying for instance vibration modes of an amorphous solid, instantaneous normal modes of a liquid. The function $f$ is a measurable mapping from $\mathbb{R}^d$ to $\mathbb{C}$, $\mathbf{x}_i$ are the positions of $n$ points, $\delta_{ij}$ is the Kronecker symbol, and $u \in \mathbb{R}$.

The adjacency and Laplacian matrices of RGGs belong to the class of ERMs. Indeed, when $u = 0$ and $f(\mathbf{x}) = \mathbf{1}_{(0\leq\|\mathbf{x}\|\leq r)}$, then $\mathbf{M}_n$ is the adjacency matrix of the RGG. This leads us to the field of graph theory.

There are many problems that involve Toeplitz-like structures. In the following, we define toeplitz and circulant matrices that play a fundamental role in developing the results of this thesis.

### Toeplitz and Circulant Matrices

Toeplitz structure is very interesting in itself for all the rich theoretical properties it involves, but at the same time it is important for the impact that it has in applications. Much of the theory of weakly stationary processes involves applications of Toeplitz matrices. Toeplitz matrices also arise in solutions to differential and integral equations, spline functions, problems in physics, mathematics, statistics, and signal processing. The most common and complete reference about Toeplitz matrices is given by Grenander and Szegö [50]. A more recent work devoted to the subject is Gray [51].

A Toeplitz matrix is an $n\times n$ matrix $\mathbf{T}_n$ with elements $t_{k,j} = t_{k-j}$ for $k, j = 0, 1, ..., n-1$, defined as

$$\mathbf{T}_n = \begin{bmatrix} t_0 & t_{-1} & \dots & t_{-(n-1)} \\ t_1 & t_0 & \dots & t_{n-2} \\ \vdots & \ddots & \ddots & \vdots \\ t_{n-1} & \ddots & \dots & t_0 \end{bmatrix}.$$

The most famous and arguably the most important result describing Toeplitz matrices is Szegö's theorem for sequences of Toeplitz matrices $\{\mathbf{T}_n\}$ which deals with the behavior of the eigenvalues as $n$ goes to infinity.

A common special case of Toeplitz matrices is when every row of the matrix is a right cyclic shift of the row above it, i.e.,

$$t_k = t_{-(n-k)} = t_{k-n}, \text{ for, } k = 1, 2, ..., n-1.$$

A matrix of this form is called a *circulant matrix* and is defined as

$$\mathbf{C}_n = \begin{bmatrix} c_0 & c_1 & \dots & c_{(n-1)} \\ c_{(n-1)} & c_0 & \dots & c_{n-2} \\ \vdots & \ddots & \ddots & \vdots \\ c_1 & c_2 & \dots & c_0 \end{bmatrix}.$$

Circulant matrices arise, for example, in applications involving the discrete Fourier transform (DFT) and the study of cycle codes for error correction. Block circulant matrices are defined similarly, except that the structure refers to block, rather than elements. In general, the blocks are free to have any structure.

### 2.3.2 Empirical distribution of eigenvalues

In RMT, random matrices are often studied in asymptotic conditions when their size tends to infinity. Although asymptotic conditions are obviously not a realistic assumption for practical problems where one rather deals with large matrices but finite of size $n$, nonetheless, working in the $n \to \infty$ limit leads to very precise approximations of the properties of large but finite matrices.

Due to the large size of real-world systems, the performance analysis of many applications requires the knowledge of the eigenvalue distribution of large random matrices. For example, in multivariate statistics, suppose that we have a very large dataset with correlated variables. A common technique to deal with this large dataset is to reduce the dimension of the problem using for instance a principal component analysis, obtained by diagonalizing the covariance matrix of different variables. But one can wonder whether the obtained eigenvalues and their associated eigenvectors are reliable or not (in a statistical sense). Hence, the characterization of eigenvalues is an example of features that one would like to study. In addition, the eigenvalues of the adjacency matrix have many applications in graph theory. For example, they describe certain topological features of a graph, such as connectivity and enumerate the occurrences of sub-graphs [19]. Eigenvalues of the Laplacian matrix provide information about diffusion, and have many applications in studying random walks on graphs and approximation algorithms [19].

The distribution of the eigenvalues can be characterized through the empirical spectral distribution (ESD). In the following, we define the empirical and the limiting distribution of the eigenvalues.

**Definition 19** (Empirical Spectral Distribution)**.** *Let $\{\mathbf{X}_n\}_{n=1}^{\infty}$ be a sequence of $n \times n$ random Hermitian matrices. Suppose that $\lambda_1, ..., \lambda_n$ are the real eigenvalues of $\mathbf{X}_n$. The ESD of $\mathbf{X}_n$ is defined as*

$$F_n^{\mathbf{X}_n}(x) = \frac{1}{n} \sum_{i=1}^{n} \mathbf{1}_{\lambda_i \leq x}.$$

The empirical spectral distribution of the $n \times n$ matrix is the probability measure which puts mass $1/n$ at each of its eigenvalues. One important and useful property of large random matrices is that often the ESD converges to a unique and deterministic limit, i.e., $F_n^{\mathbf{X}_n} \to F^{\mathbf{X}_n}$ as $n \to \infty$. This limiting function is called limiting spectral distribution (LSD).

In addition to the different definitions of the convergence of random sequences introduced in Section 2.2, the convergence of the ESD of Hermitian matrices to a LSD can be

shown using the *Levy distance*. The Levy distance is a metric on the space of cumulative distribution functions of one dimensional random variables. It is named after the French mathematician Paul Levy. In the following, we define the Levy distance, and provide an upper bound of the Levy distance between two distribution functions.

**Definition 20** (Levy Distance, [52]). *Let $F_n^{\boldsymbol{A}}$ and $F_n^{\boldsymbol{B}}$ be two distribution functions on $\mathbb{R}$. The Levy distance $L(F_n^{\boldsymbol{A}}, F_n^{\boldsymbol{B}})$ is defined as the infimum of all positive $\epsilon$ such that, for all $x \in \mathbb{R}$,*

$$F_n^{\boldsymbol{A}}(x-\epsilon) - \epsilon \leq F_n^{\boldsymbol{B}}(x) \leq F_n^{\boldsymbol{A}}(x+\epsilon) + \epsilon.$$

The following lemma provides an upper bound on the Levy distance between two empirical spectral distribution functions of two matrices depending on the trace of the difference of the respective matrices.

**Lemma 6** (Difference Inequality, [53], page 614). *Let $\boldsymbol{A}$ and $\boldsymbol{B}$ be two $n \times n$ Hermitian matrices with eigenvalues $\lambda_1, ..., \lambda_n$ and $\mu_1, ..., \mu_n$, respectively. Then,*

$$\sum_{k=1}^{n} |\lambda_k - \mu_k|^2 \leqslant \mathrm{trace}(\boldsymbol{A} - \boldsymbol{B})^2,$$

*and*

$$L^3(F_n^{\boldsymbol{A}}, F_n^{\boldsymbol{B}}) \leqslant \frac{1}{n}\mathrm{trace}(\boldsymbol{A} - \boldsymbol{B})^2,$$

*where $L(F_n^{\boldsymbol{A}}, F_n^{\boldsymbol{B}})$ denotes the Levy distance between the empirical distribution functions $F_n^{\boldsymbol{A}}$ and $F_n^{\boldsymbol{B}}$ of the eigenvalues of $\boldsymbol{A}$ and $\boldsymbol{B}$, respectively.*

Throughout this thesis, we utilize several concentration inequalities which show that a random variable with large probability assumes values in a small neighborhood of its mean. We will write $\mathbb{E}[x]$ to denote the expectation of $x$. In the same way, we denote the variance of a random variable $x$ by $\mathrm{Var}(x)$. We use $\mathrm{Bin}(n,p)$, $\mathrm{Pois}(\lambda)$ and $\mathrm{N}(\mu, \sigma^2)$ to denote the binomial, Poisson and normal distributions, respectively.

In the following we review well-known and relevant concentration inequalities.

### 2.3.3 Concentration Inequalities

Concentration and large deviation inequalities are very useful tools to study large matrices. A fundamental inequality is the Markov inequality given in the following theorem.

**Theorem 7** (Markov inequality). *Let $x \geq 0$ be a non-negative random variable with $\mathbb{E}[x] < \infty$. Then*

$$\mathbb{P}(x \geq t) \leq \frac{\mathbb{E}[x]}{t}, \qquad t > 0.$$

Markov inequality is a fundamental result to derive numerous concentration inequalities. In the following, we provide the Chebyshev inequality that controls fluctuations of a random variable around its mean.

**Theorem 8** (Chebyshev Inequality)**.** *Let $x$ be a non negative random variable with $\mathbb{E}[x^2] < \infty$. Then, for any $t > 0$*

$$\mathbb{P}(|x - \mathbb{E}[x]| \geq t) \leq \frac{\mathrm{Var}(x)}{t^2}.$$

The bounds provided by the Markov and the Chebyshev inequalities decay as $t^{-1}$ and $t^{-2}$, respectively. However, the Markov inequality can be applied to derive an exponentially decaying bound known as the *Chernoff bound.*

**Lemma 9** (Chernoff Bound)**.** *Define the log-moment generating function $\psi$ of a random variable $x$ and its Legendre dual $\psi^*$ as*

$$\psi(\lambda) = \log \mathbb{E}[e^{\lambda(x - \mathbb{E}[x])}], \qquad \psi^*(t) = \sup_{\lambda}\{\lambda t - \psi(\lambda)\}.$$

*Then*

$$\mathbb{P}(x - \mathbb{E}[x] \geq t) \leq e^{-\psi^*(t)} \quad \text{for all } t \geq 0.$$

*Proof.* Let us apply the Markov inequality to the random variable $e^{\lambda(x-\mathbb{E}[x])} > 0$. Then, for any $\lambda \geq 0$, we obtain

$$\begin{aligned} \mathbb{P}(x - \mathbb{E}[x] \geq t) &= \mathbb{P}\left(e^{\lambda(x-\mathbb{E}[x])} \geq e^{\lambda t}\right) \\ &\leq e^{-\lambda t}\mathbb{E}[e^{\lambda(x-\mathbb{E}[x])}] \\ &= e^{-\{\lambda t - \psi(\lambda)\}}. \end{aligned} \tag{2.7}$$

As the left hand side of (2.7) does not depend on the choice of $\lambda \geq 0$, the bound holds also for $\lambda$ which maximizes the exponent $\lambda t - \psi(\lambda)$, yielding the statement of Lemma 9. □

Note that Chernoff bound provides a bound only for the probability $\mathbb{P}(x \geq \mathbb{E}[x] + t)$, that is the probability that the random variable $x$ exceeds its mean $\mathbb{E}[x]$ by a fixed amount $t$. However, we can obtain an inequality for the lower tail by applying the Chernoff bound to the random variable $-x$, as

$$\mathbb{P}(x \leq \mathbb{E}[x] - t) = \mathbb{P}(-x \geq \mathbb{E}[-x] + t).$$

In particular, given an upper and lower tail bounds, we can obtain a bound on the magnitude of the fluctuations using the union bound

$$\begin{aligned} \mathbb{P}(|x - \mathbb{E}[x]| \geq t) &= \mathbb{P}\left((x \geq \mathbb{E}[x] + t) \text{ or } (x \leq \mathbb{E}[x] - t)\right) \\ &\leq \mathbb{P}(x \geq \mathbb{E}[x] + t) + \mathbb{P}(-x \geq \mathbb{E}[-x] + t). \end{aligned} \tag{2.8}$$

In numerous cases, the proof of a bound for the upper tail can be straightforward extended to derive a bound for the lower tail, and a global bound can be obtained by applying (2.8). In some cases, bounds for the upper and lower tail are proved under assumptions that are not invariant under negation. For example, if we prove an upper tail bound for a convex function $f(x)$, this bound does not automatically imply a bound for the lower tail since $-f(x)$ is concave and not convex. In such cases, a bound for the lower tail must be proved separately.

Chernoff bound is very useful and can be easy to manipulate. In fact the log-moment generating function $\lambda \to \psi(\lambda)$ is a continuous function and can therefore be investigated using calculus which makes the Chernoff bound very flexible and powerful.

In the following, we show an additional useful inequality involving sums of independent random variables known as Hoeffding inequality. Consider a sum of independent random variables

$$x = x_1 + ... + x_n,$$

where $x_i$ are i.i.d. centered random variables. Intuitively, while $x$ can take values of order $\mathcal{O}(n)$, very likely it is of order $\mathcal{O}(\sqrt{n})$, i.e., the order of its standard deviation. In the following, we state Hoeffding inequality.

**Theorem 10** (Hoeffding inequality)**.** *Let $x_1, ..., x_n$ be independent bounded random variables, i.e., $|x_i| \leq a$ and $\mathbb{E}[x_i] = 0$. Then, for $t > 0$*

$$\mathbb{P}\left\{\left|\sum_{i=1}^{n} x_i\right| > t\right\} \leq 2\exp\left(-\frac{t^2}{2na^2}\right).$$

This inequality implies that fluctuations larger than $\mathcal{O}(\sqrt{n})$ have small probability. For example, for $t = a\sqrt{2n\log(n)}$ we get that the probability is at most $\frac{2}{n}$.

The following inequality referred to as Bernstein inequality [54], uses the variance of the summands to obtain a tighter bound compared to Hoeffding inequality.

**Theorem 11** (Bernstein Inequality)**.** *Let $x_1, ..., x_n$ be independent centered bounded random variables, i.e., $|x_i| \leq a$ and $\mathbb{E}[x_i] = 0$, with variance $\mathbb{E}[x_i^2] = \sigma^2$. Then, for $t > 0$*

$$\mathbb{P}\left\{\left|\sum_{i=1}^{n} x_i\right| > t\right\} \leq 2\exp\left(-\frac{t^2}{2n\sigma^2 + \frac{2}{3}at}\right).$$

Numerous additional upper bounds for $\mathbb{E}[e^{\lambda x}]$ are derived from Bernstein or Markov inequality. In the following, we state several strong inequalities under more restrictive assumptions.

**Lemma 12** ([55])**.** *Let $x \sim \mathrm{Bin}(n, p)$, $\mathbb{E}[x] = np$. Then, for $t \geq 0$*

$$\mathbb{P}\left\{x \geq \mathbb{E}[x] + t\right\} \leq \exp\left(-\frac{t^2}{2\left(\mathbb{E}[x] + t/3\right)}\right).$$

A global upper bound for a binomial distribution is given under more restrictive assumptions in the following lemma.

**Lemma 13** ([55]). *Let $x \sim \mathrm{Bin}(n,p)$, $\mathbb{E}[x] = np$ and $0 < t \leq \frac{3}{2}$. Then,*

$$\mathbb{P}\left\{|x - \mathbb{E}[x]| \geq t\mathbb{E}[x]\right\} \leq 2\exp\left(-\frac{t^2}{3}\mathbb{E}[x]\right).$$

An additional and more general upper bound applicable to any random variable $x$, is obtained using its corresponding probability generating function.

**Lemma 14.** *Let $x$ be a random variable. Then, for any $t > 0$*

$$\mathbb{P}\{x \geq t\} \leq \frac{F(a)}{a^t},$$

*where $F(a)$ is the probability generating function and $a \geq 1$.*

In the following, we introduce the Hölder, Cauchy-Schwarz and Minkowski inequalities.

**Lemma 15** (Hölder Inequality). *For $p > 1$ and $\frac{1}{p} + \frac{1}{q} = 1$, the Hölder inequality is given by*

$$\sum_{i=1}^{n} |x_i y_i| \leq \left(\sum_{i=1}^{n} |x_i|^p\right)^{1/p} \left(\sum_{i=1}^{n} |y_i|^q\right)^{1/q}.$$

*For $p = 2$, it reduces to the Cauchy-Schwarz inequality.*

**Lemma 16** (Minkowski Inequality). *For $p \geq 1$, the triangle inequality for the $\ell_p$-norm is given by*

$$\left(\sum_{i=1}^{n} (|x_i + y_i|)^p\right)^{1/p} \leq \left(\sum_{i=1}^{n} |x_i|^p\right)^{1/p} + \left(\sum_{i=1}^{n} |y_i|^p\right)^{1/p}.$$

The following inequalities hold for all $x \in \mathbb{R}^d$ or $x \in \mathbb{C}^d$.

- $\|x\|_\infty \leq \|x\|_1 \leq d\|x\|_\infty$.
- $\|x\|_\infty \leq \|x\|_2 \leq \sqrt{d}\|x\|_\infty$.
- $\|x\|_\infty \leq \|x\|_2 \leq \|x\|_1 \leq \sqrt{d}\|x\|_2$.

### 2.3.4 Asymptotic Behavior of Matrices

The major use of this section is to provide tools in order to relate the asymptotic behavior of two sequences of matrices and introduce the concept of asymptotic equivalence of sequences of matrices.

We will be considering sequences of $n \times n$ matrices that are equivalent as $n$ becomes large. To measure the distance between two matrices, we use the weak norm of the difference of two matrices.

**Lemma 17** ([51]). *Two sequences of $n \times n$ matrices $\{\mathbf{A}_n\}$ and $\{\mathbf{B}_n\}$ are said to be asymptotically equivalent if*

1. *$\mathbf{A}_n$ and $\mathbf{B}_n$ are uniformly bounded in strong (and hence in weak) norm:*

$$\|\mathbf{A}_n\|, \|\mathbf{B}_n\| \leq M < \infty, \quad n = 1, 2, ...$$

*and*

2. *$\mathbf{A}_n - \mathbf{B}_n = \mathbf{D}_n$ goes to zero in weak norm as $n \to \infty$*

$$\lim_{n\to\infty} \|\mathbf{A}_n - \mathbf{B}_n\|_{\text{HS}} = \lim_{n\to\infty} \|\mathbf{D}_n\|_{\text{HS}} = 0.$$

We use the abbreviation $\mathbf{A}_n \sim \mathbf{B}_n$ for the asymptotic equivalence of the sequences $\{\mathbf{A}_n\}$ and $\{\mathbf{B}_n\}$. Several properties exist that relate the asymptotic equivalence between two matrices and their corresponding eigenvalues.

The following result shows that if the weak norm of the difference between two symmetric matrices is small, then the sums of the eigenvalues of each must be close.

**Lemma 18** ([51]). *Given two square symmetric matrices $\mathbf{A}$ and $\mathbf{B}$ with ordered eigenvalues $\alpha_k$ and $\beta_k$, respectively, then*

$$|\frac{1}{n}\sum_{k=0}^{n-1} \alpha_k - \frac{1}{n}\sum_{k=0}^{n-1} \beta_k| \leq \|\mathbf{A} - \mathbf{B}\|_{\text{HS}}.$$

An immediate consequence of the lemma is the following corollary.

**Corollary 2** ([51]). *Given two sequences of asymptotically equivalent square symmetric matrices $\{\mathbf{A}_n\}$ and $\{\mathbf{B}_n\}$ with eigenvalues $\alpha_{n,k}$ and $\beta_{n,k}$, respectively, then*

$$\lim_{n\to\infty} \frac{1}{n}\sum_{k=0}^{n-1} (\alpha_{n,k} - \beta_{n,k}) = 0,$$

*and hence if either limit exists individually,*

$$\lim_{n\to\infty} \frac{1}{n}\sum_{k=0}^{n-1} \alpha_{n,k} = \lim_{n\to\infty} \frac{1}{n}\sum_{k=0}^{n-1} \beta_{n,k}.$$

The following theorem is a fundamental result concerning asymptotic eigenvalue behavior of asymptotically equivalent sequences of matrices [51].

**Theorem 19** ([51]). *Let* $\{\mathbf{A}_n\}$ *and* $\{\mathbf{B}_n\}$ *be asymptotically equivalent sequences of square symmetric matrices with ordered eigenvalues* $\alpha_{n,k}$ *and* $\beta_{n,k}$*, respectively. Then, for any positive integer* $s$ *the sequences of matrices* $\{\mathbf{A}_n^s\}$ *and* $\{\mathbf{B}_n^s\}$ *are also asymptotically equivalent,*

$$\lim_{n\to\infty}\frac{1}{n}\sum_{k=0}^{n-1}(\alpha_{n,k}^s-\beta_{n,k}^s)=0,$$

*and hence if either limit exists individually,*

$$\lim_{n\to\infty}\frac{1}{n}\sum_{k=0}^{n-1}\alpha_{n,k}^s=\lim_{n\to\infty}\frac{1}{n}\sum_{k=0}^{n-1}\beta_{n,k}^s. \tag{2.9}$$

Since the previous theorem holds for any positive integer $s$, by adding sums corresponding to different values of $s$ to each side of (2.9). This observation leads to the following corollary.

**Corollary 3** ([51]). *Suppose that* $\{\mathbf{A}_n\}$ *and* $\{\mathbf{B}_n\}$ *are asymptotically equivalent sequences of square symmetric matrices with ordered eigenvalues* $\alpha_{n,k}$ *and* $\beta_{n,k}$*, respectively and let* $f(x)$ *be any polynomial. Then,*

$$\lim_{n\to\infty}\frac{1}{n}\sum_{k=0}^{n-1}(f(\alpha_{n,k})-f(\beta_{n,k}))=0,$$

*and hence if either limit exists individually,*

$$\lim_{n\to\infty}\frac{1}{n}\sum_{k=0}^{n-1}f(\alpha_{n,k})=\lim_{n\to\infty}\frac{1}{n}\sum_{k=0}^{n-1}f(\beta_{n,k}). \tag{2.10}$$

Additional key result from matrix theory is the Wielandt-Hoffman theorem [56] stated in the following

**Theorem 20** (Wielandt-Hoffman Theorem, [56]). *Given two Hermitian matrices* $\mathbf{A}$ *and* $\mathbf{B}$ *with eigenvalues* $\alpha_k$ *and* $\beta_k$*, respectively, then*

$$\frac{1}{n}\sum_{k=0}^{n-1}|\alpha_k-\beta_k|^2\le\|\mathbf{A}-\mathbf{B}\|_{\mathrm{HS}}^2.$$

The Cauchy-Schwarz inequality applied to the Wielandt-Hoffman Theorem yields the following stronger lemma.

**Lemma 21** ([51]). *Given two Hermitian matrices* $\mathbf{A}$ *and* $\mathbf{B}$ *with eigenvalues* $\alpha_k$ *and* $\beta_k$*, in nonincreasing order, respectively, then*

$$\frac{1}{n}\sum_{k=0}^{n-1}|\alpha_k-\beta_k|\le\|\mathbf{A}-\mathbf{B}\|_{\mathrm{HS}}.$$

In order to analyze the spectra of random graphs, the knowledge of the spectrum of several fundamental random matrices is required. In the following section, we recall well-known results on the LSD of relevant matrices.

# Chapter 3

# State of the Art

## 3.1 Introduction

In this chapter, we review fundamental results concerning asymptotic eigenvalue behavior of asymptotically equivalent sequences of matrices. Then, we provide a survey of fundamental results from spectral graph theory (SGT) domain. Finally, we provide results related to network dynamics and introduce an important concept for the characterization of diffusion behaviors in graphs called spectral dimension (SD).

## 3.2 Spectral Graph Theory (SGT)

SGT is the study of eigenvalues and eigenvectors of graph matrices. Questions about spectral properties are very important in graph theory to understand various properties of random graphs. Therefore, spectral graph methods have become a fundamental tool in the analysis of large complex networks. The results can be utilized in a broad range of applications in machine learning, data mining, web search and ranking. In particular, spectral analysis of the adjacency matrix or related matrices are of prior interest in graph theory. For example the probability of hitting times of RWs on graphs is governed by the spectrum of the transition matrix [18]. In network epidemics, the time evolution of the infected population is also govened by the spectral radius and spectral gap of the adjacency matrix [16], [57], [58].

The spectra of random matrices and random graphs have been extensively studied in the literature, see [59], [53], [60], [61], [46]. In this section, we review relevant eigenvalue properties of some random graphs.

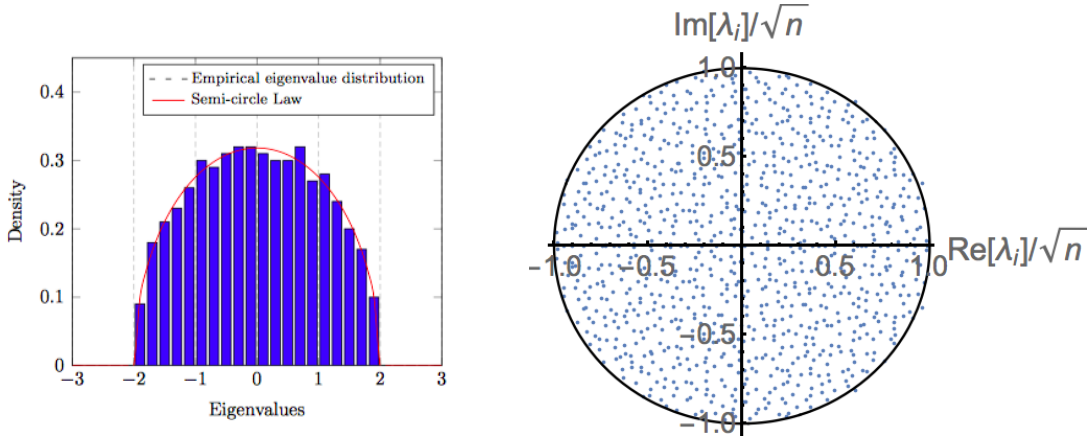


(a) Histogram of the eigenvalues of Wigner matrices and the semi-circle law, for $n = 500$.

(b) Illustration of the real and imaginary parts scaled by $\sqrt{1000}$ of the eigenvalues of a $1000 \times 1000$ matrix with independent, standard normal entries.

Figure 3.1: Illustration of the semi-circle law and the full circle law.

### 3.2.1 Spectrum of ER Random Graph

In Chapter 2, we have introduced ensembles of random matrices with i.i.d. entries. The ESD of a random Hermitian matrix has a very complicated form when the order of the matrix is large. In particular, it seems very difficult to characterize the LSD of an arbitrary given sequence of random Hermitian matrices [59], [62]. A pioneering and famous work on the spectral distribution of random Hermitian matrices owes to Wigner, which is now known as *Wigner's semicircle law* [43], [63].

In the following, we recall the well-known results due to Wigner concerning the convergence of the ESD of the aforementioned Wigner matrices.

**Theorem 22** (Wigner's Semicircle Law, Theorem 2.5 and Theorem 2.9 [59])**.** *Consider an $n \times n$ symmetric matrix $\mathbf{X}$ with independent entries $\frac{1}{\sqrt{n}}X_{ij}$ such that $\mathbb{E}[X_{ij}] = 0$, $\mathbb{E}[|X_{ij}|^2] = 1$ and $\mathbb{E}[|X_{ij}|^{2+\epsilon}] < \infty$ for an $\epsilon > 0$. Then, as $n \to \infty$, $F_n^{\mathbf{X}} \Rightarrow F$ almost surely, where*

$$\frac{dF}{dx} = \frac{1}{2\pi}\sqrt{4 - x^2 1_{(|x|\leq 2)}}$$

*and $F_n^{\mathbf{X}}$ is the ESD of $\mathbf{X}$.*

Moreover, if the elements $X_{ij}$ are identically distributed, the result holds without the need for the existence of the moment $\mathbb{E}[|X_{ij}|^{2+\epsilon}]$ for an $\epsilon > 0$. The LSD of Wigner matrices with independent and identically distributed upper-diagonal $X_{ij} \sim \mathrm{N}(0, \frac{1}{n})$ entries, is shown in Figure 3.1 (a). For non-symmetric matrices, the LSD follows the full-circle law [64], which is exemplified in Figure 3.1 (b).

Let us consider again the Wishart or the sample covariance matrix
$textbfC_p$. The convergence of the ESD of the sample covariance matrix with i.i.d. entries

of zero mean and variance normalized to $n$ to a LSD was studied in [65]. This LSD is known as Marchenko-Pastur law. In the following, we recall the well-known Marchenko-Pastur theorem.

**Theorem 23** (Marchenko-Pastur Law, [65]). *Consider a matrix $\mathbf{X} \in \mathbb{R}^{p\times n}$ with i.i.d. entries $\frac{1}{\sqrt{n}}X_{ij}$, such that $X_{ij}$ has zero mean and unit variance. As $n, p \to \infty$ with $\frac{p}{n} \to c \in (0, \infty)$, the ESD of $\boldsymbol{C}_p = \mathbf{X}\mathbf{X}^T$ converges weakly and almost surely to a non-random distribution function $F$ given by*

$$\frac{dF}{dx} = (1 - c^{-1})\delta(x) + \frac{1}{2\pi cx}\sqrt{(x-a)1_{(x\geq a)}(b-x)1_{(x\leq b)}}$$

*where $a = (1-\sqrt{c})^2$, $b = (1+\sqrt{c})^2$ and $\delta(x) = \mathbf{1}_0(x)$, i.e., delta function at zero (Dirac).*

Random matrices in Wigner's setup correspond to the adjacency matrix of ER random graph where edges appear independently with probability $p$, i.e., $G(n, p)$ [6]. If $p$ is held constant as $n \to \infty$, then the setup is equivalent to Wigner's random matrix setting. However, in graph theory, we are often interested in graphs where $p$ decreases with $n$.

As mentioned in Chapter 2, the ER graph $G(n, p)$ are classified in different regimes depending on the value of $p$. In the following, we discuss some results and observations related to the LSD of $G(n, p)$ in the different regimes.

In the case when $p = w(\frac{1}{n})$ and $p \leq \frac{1}{2}$, the LSD of $G(n, p)$ is the semi-circle distribution. It can be proved by the method of moments, and the proof follows along the lines of the proof for Wigner's matrices. We state the result in the following theorem and the detailed proof can be found in [66], [67] or [68].

**Theorem 24** ([66], Theorem 3.4). *Assume $p = w(\frac{1}{n})$ and $p \leq \frac{1}{2}$. Let $\mathbf{A}$ be the adjacency matrix of a random graph $G(n, p)$. Then, as $n \to \infty$, the ESD of the matrix $\frac{1}{\sqrt{np(1-p)}}\mathbf{A}$ converges in distribution to the semi-circle distribution function which has a density function*

$$f(x) = \frac{1}{2\pi}\sqrt{4 - x^2},$$

*with support $[-2, 2]$.*

In the case when $p = \frac{c}{n}$ and $c$ is fixed, i.e., $p = \mathcal{O}(\frac{1}{n})$, the ESD of $G(n, p)$ does not converge to the semi-circle distribution. Instead, the spectrum is a composition of two components: a discrete component consisting of spikes and a continuous component [69]. For small values of $c$, the discrete spectrum is dominant whereas, for large values of $c$, the continuous spectrum is dominant. The continuous spectrum approaches the semi-circle distribution as $c$ gets larger. This asymptotic behavior can be explained by the continuity between the regimes with $w(\frac{1}{n})$ and $\mathcal{O}(\frac{1}{n})$ modeled by $c \to \infty$. In fact, the LSD is given in Theorem 24. The presence of the discrete spectrum depends on the structure of the graph for different values of $c$. When $p = \frac{c}{n}$ with $c < 1$, the spectrum is characterized entirely by trees. The dominance of trees determines the appearance of mass points

in the spectrum. We could approximate the LSD by computing the spectra of small trees. When $c > 1$, there exists a giant component, which determines the appearance of the continuous component of the spectra. Nevertheless, for $c > 1$ there exist also small connected components, mostly trees, that determine the appearance of the discrete component of the spectrum, see Theorem 3.

### 3.2.2 Spectrum of Random Geometric Graph (RGG)

In this section, we provide existing results on spectrum of RGGs. First, the work in [70] investigates numerically the combinatorial Laplacian spectra of RGGs. The spectra consist of both a discrete and a continuous part. The discrete part is a collection of Dirac delta peaks at integer values. The peaks appear mainly due to the existence of symmetric motifs[1]. The symmetric motifs are numerous in RGGs and they determine the appearance of sharp and distinct peaks in the spectra of Laplacian and adjacency matrices, a feature often found in the spectrum of matrices associated to graphs of real-world networks. By contrast, similar peaks are not visible in the Laplacian spectrum of non-spatial random graph models such as ER graphs. In [71] the symmetric motifs in RGGs are analyzed and the probabilities of their appearance in both the connectivity and thermodynamic limits are studied. In the thermodynamic regime, the probability that the closest nodes are inter-changeable approaches one, whilst in the dense regime of fixed connection radius, this probability depends upon the dimension of the Euclidean space.

As mentionned in Section 2.3, the adjacency and Laplacian matrices of RGGs are in the class of Euclidean random matrices. The work in [72] analyzed the spectra of Euclidean random matrices when both the number of vertices $n$ and the dimension of the Euclidean space $d$ go to infinity proportionally. However, this result cannot be applied to our problem as we assume that $n$ grows large whereas the space dimension $d$ is fixed.

Jiang in [73] studied the LSD of Euclidean random matrices $\mathbf{M}_n$ when the dimension $d$ remains fixed and $n \to \infty$. In the following theorem, we recall the result showing that the ESD of Euclidean random matrices with $d$ fixed converges to the Dirac distribution at zero as $n \to \infty$.

**Theorem 25** (LSD of Euclidean Random Matrix, [73])**.** *Let $d \geq 1$ be fixed and $\mathbf{M}_n$ be as in (2.6) with $u = 0$, i.e.,*

$$M_{ij} = f(\|\mathbf{x}_i - \mathbf{x}_j\|_2^2).$$

*Let $\{\mathbf{x}_i : i \geq 1\}$ be $\mathbb{R}^d$-valued random variables with $\max_{i\geq 1} \mathbb{E}[e^{t_0\|\mathbf{x}_i\|^\alpha}] < \infty$ for some constants $\alpha > 2$ and $t_0 > 0$. Suppose $f \in [0, \infty)$ with $w_m = \sup_{x\geqslant 0} |f^{(m)}(x)|$ satisfying $\log(w_m) = o(m)\log(m)$ as $m \to \infty$. Then, with probability one, the ESD converges weakly to $\delta_0$ as $n \to \infty$.*

In addition, the work in [49] studied the probability distributions of eigenvalues of Hermitian and non-Hermitian Euclidean random matrices. The analysis in [49] focuses in

[1] Symmetric motifs are subsets of nodes which have the same adjacencies.

a class of functions where the real symmetric $n \times n$ Euclidean matrix $\mathbf{M}$ have elements defined through some specific function $f$ such as the cardinal sine (sinc) defined as $M_{ij} = \frac{\sin(|\mathbf{x}_i - \mathbf{x}_j|)}{|\mathbf{x}_i - \mathbf{x}_j|}$, or the cardinal cosine (cosc) defined as $M_{ij} = \frac{\cos(|\mathbf{x}_i - \mathbf{x}_j|)}{|\mathbf{x}_i - \mathbf{x}_j|}$, where vectors $\mathbf{x}_i$ define positions of $n$ randomly chosen points inside a three-dimensional cube.

The results in Theorem 25 and in [49] require the continuity of the function $f$ defining the Euclidean matrix. Thus, they cannot be applied to the step function considered in this work.

Regarding spectral properties of the adjacency matrix of RGGs, in [74] and [75], the authors show that the spectral distribution of the adjacency matrix converges to a deterministic LSD in the thermodynamic regime as $n \to \infty$. Due to the difficulty to compute exactly this spectral measure in the thermodynamic regime, the work in [74] proposes an approximation for it as the average vertex degree $\gamma \to \infty$. Additionally, Bordenave in [74] characterizes the spectral measure of the adjacency matrix normalized by $n$ in the dense regime. In the dense regime and as $n \to \infty$, due to the normalization factor $n$, all the finite eigenvalues of the adjacency matrix vanish and only the eigenvalues scaling as $n$ in the adjacency matrix do not vanish in the normalized adjacency matrix. In order to analyze the behavior of the finite eigenvalues of the adjacency matrix, in this work we study the LSD of the RGG adjacency matrices without normalization in the connectivity and dense regimes.

In [16], a closed form expression for the asymptotic spectral moments of the adjacency matrix of an RGG $G(\mathcal{X}_n, r_n)$ is derived in the connectivity regime. Then, an analytical upper bound for the spectral radius is given in order to study the behavior of the viral infection in an RGG. We have the following closed-form expression for the asymptotic expected spectral moments of RGGs.

**Theorem 26.** *Consider set of $n$ nodes distributed uniformly and independently on the $d$-dimensional unit torus $\mathbb{T}^d \equiv [0,1]^d$. Then, we form an RGG $G(n, r_n)$ by adding an edge between two vertices when the distance between them does not exceed a certain threshold $r_n$. When the average vertex degree $a_n = \Omega(\log(n))$, the asymptotic expected spectral moments are given as*

$$\mathbb{E}[m_k] = (nr_n)^{k-1} \frac{1}{2(k-1)!} \sum_{j=1}^{k-2} \binom{k-1}{j-1} E_{k-1,j},$$

*where $E_{k-1,j}$ are the Eulerian numbers[2] and $m_k$ is the $k$-th spectral moment of the $G(n, r_n)$.*

Furthermore, the author in [77] shows that, in the connectivity regime, the spectral measures of the transition probability matrix of the RW in an RGG and in a deterministic geometric graph (DGG) with nodes in a grid converge to the same limit as $n \to \infty$. However, this convergence is not studied for the full range of the connectivity regime. More specifically, the proof in [77] is based on a condition on the radius $r_n$. The condition enforced on $r_n$ in [77] implies that for $\epsilon > 0$, the result holds only for RGGs with an

[2]The Eulerian number $E_{n,k}$ gives the number of permutations of $\{1, 2, ..., n\}$ having $k$ permutation ascents [76].

average vertex degree $a_n$ that scales as $\Omega\left(\log^{\epsilon}(n)\sqrt{n}\right)$, when $d = 1$, as $\Omega\left(\log^{\frac{3}{2}+\epsilon}(n)\right)$ when $d = 2$, as $\Omega\left(\log^{1+\epsilon}(n)\right)$ for $d \geq 3$.

Compared to [77], in this thesis we study the LSD of the normalized Laplacian matrix of RGGs in the connectivity regime for a wider range of scaling laws of the average vertex degree $a_n$, or equivalently a wider range of scaling laws of the radius $r_n$. More specifically, for $d \geq 1$, we show that the LSDs of the normalized Laplacian matrix of RGGs and for DGGs converge to same limit when $a_n = \Omega(\log(n))$. Additionnaly, we extend the work in [77] and study the LSD of the normalized Laplacian for RGGs under on any $\ell_p$-metric with $p \in [1, \infty]$. Moreover, we study the LSD of the normalized Laplacian matrix of RGGs in the thermodynamic regime. To overcome the problem of singularities due to isolated nodes in the thermodynamic regime, we investigate the LSD of the normalized Laplacian on a modified graph by adding auxiliary edges among all the nodes with an arbitrary eventually vanishing weight. The corresponding normalized Laplacian is known as the regularized normalized Laplacian [78].

In the following section, we briefly review spectrum of circulant matrices useful for the analyzes in Chapter 4.

### 3.2.3 Spectrum of Circulant Matrices

The eigenvalues and eigenvectors of circulant matrices are related to the discrete Fourier transform (DFT). For a sequence of $n$ complex numbers $a_0, a_1, ..., a_{n-1}$, the DFT is defined as follows

$$\alpha_m = \sum_{k=0}^{n-1} a_k e^{-2\pi i m k/n}. \tag{3.1}$$

Recall that an $n \times n$ matrix $\mathbf{C}_n$ is circulant if each row is a cyclic shift of the row above it. In the following, we show that the eigenvalues of a circulant matrix are given by the DFT of the first row of the matrix and the normalized eigenvectors of a circulant matrix are the Fourier modes.

Using the circulant structure of the matrix, we write the eigenvalues equation $\mathbf{C}_n\mathbf{v} = \lambda\mathbf{v}$ as a set of $n$ difference equations [70]

$$\sum_{k=0}^{n-1-m} c_k v_{k+m} + \sum_{k=n-m}^{n-1} c_k v_{k-(n-m)} = \lambda v_m \text{ for } m = 0, 1, ...n-1.$$

Assuming solutions of the form $v_k = \rho^k$ yields,

$$\sum_{k=0}^{n-1-m} c_k \rho^k + \rho^{-n} \sum_{k=n-m}^{n-1} c_k \rho^k = \lambda.$$

If we choose $\rho^{-1} = 1$, that is, $\rho$ is one of the complex $n$-th roots of unity such that $\rho_m = e^{-2\pi im/n}$ for $m = 0, 1, ..., n-1$ we have an eigenvalue

$$\lambda = \sum_{k=0}^{n-1} c_k e^{-2\pi imk/n}, \tag{3.2}$$

with the corresponding eigenvector

$$\mathbf{v} = \frac{1}{\sqrt{n}}(1, e^{-2\pi im/n}, ..., e^{-2\pi im(n-1)/n}).$$

Comparing (3.1) and (3.2) shows that the eigenvalues are given by the DFT of the first row of the matrix.

The 2d DFT of the $n \times n$ matrix $\mathbf{A}$ is the matrix $\boldsymbol{\alpha}$ of the same size with entries

$$\alpha_{lm} = \sum_{g=0}^{n-1}\sum_{h=0}^{n-1} A_{gh} e^{-2\pi igl/n} e^{-2\pi ihm/n} \text{ for } l, m = 0, 1, ..., n-1. \tag{3.3}$$

Let $\mathbf{B}$ denote a symmetric $n_1 n_2 \times n_1 n_2$ block circulant matrix with circulant blocks. The matrix $\mathbf{B}$ has $n_1 \times n_1$ circulant blocks each of size $n_2 \times n_2$. The eigenvalues of $\mathbf{B}$ can be found by taking the 2d DFT of the $n_1 \times n_2$ matrix formed by arranging the elements of the first row of $\mathbf{B}$ [70]. To see that, we use the spectral decomposition of $\mathbf{B}$

$$\mathbf{B} = \mathbf{F}^{\mathrm{H}} \boldsymbol{\Lambda} \mathbf{F}, \tag{3.4}$$

where $\boldsymbol{\Lambda}$ is a diagonal matrix whose entries are the eigenvalues of $\mathbf{B}$ and $\mathbf{F}$ is the 2d DFT matrix. That is, $\mathbf{F} = \mathbf{F}_{n_1} \otimes \mathbf{F}_{n_2}$ where $\mathbf{F}_{n_1}$ is the $n_1-$point DFT matrix.

Multiplying both sides of (3.4) by $\mathbf{F}$ gives

$$\mathbf{FB} = \boldsymbol{\Lambda}\mathbf{F}.$$

Consider only the first column in the above equation

$$\mathbf{FB}_1 = \boldsymbol{\Lambda}\mathbf{F}_1. \tag{3.5}$$

Note that every entry in the first column of $\mathbf{F}$ is 1. Therefore,

$$\mathbf{FB}_1 = \lambda. \tag{3.6}$$

Thus, to find the eigenvalues of $\mathbf{B}$, arrange the elements of its first row in a $n_1 \times n_2$ matrix row-wise and using (3.3) take the 2d DFT. The elements of the resulting matrix are the eigenvalues.

This procedure is generalized to find the eigenvalues of symmetric matrix $\mathbf{B}$ with any number of levels of circulant structure. The author in [70] shows that the eigenvalues of

$\mathbf{B}$ are found by taking the $d$-dimensional DFT of an $n_1 \times n_2 \times ... \times n_d$ tensor of rank $d$ obtained from the first block row of $\mathbf{B}$.

Given the simplicity of circulant matrices, an obvious approach to study asymptotic properties of sequences of Toeplitz matrices is to approximate them by sequences asymptotically equivalent of circulant matrices and then applying the results developed for circulant matrices. Such results are most easily derived when strong assumptions are placed on the sequence of Toeplitz matrices, which keep the structure of the matrices simple and allow them to be well approximated. For example, assumptions where the sequence $\{t_{k,j}\}$ is assumed to be absolutely summable and also the case of sequences of banded Toeplitz matrices. Under such assumptions, the basic approach is to find a sequence of circulant matrices $\mathbf{C}_n$ that is asymptotically equivalent to the sequence of Toeplitz matrices $\mathbf{T}_n$. The choice of an appropriate sequence of circulant matrices to approximate a sequence of Toeplitz matrices is not unique. An example of such circulant matrix is constructed and can be found in [51].

The most famous and arguably the most important result of this type is Szego's theorem for sequences of Toeplitz matrices $\{\mathbf{T}_n\}$ which deals with the behavior of the eigenvalues as $n$ goes to infinity.

## 3.3 Diffusion Dynamics and Spectral Dimension (SD)

The theory of dynamical processes on complex networks combines concepts of graph theory and non-linear dynamics. It studies elements or agents whose states evolve following a dynamical rule. This dynamical rule models interactions with neighboring elements. Here, these elements or the agents are modeled by the vertices of a graph $G = (\mathcal{X}_n, E)$ and the edges specify their interactions. The study of dynamical processes on complex networks differs from the characterization of structural network properties of complex networks presented in the previous sections but they are related. In the following, we show the relation between diffusion processes, normalized Laplacian matrix and spectral dimension.

In the following section, we briefly survey spreading processes and the SD useful for the analyzes in Chapter 6.

### 3.3.1 Diffusion Dynamics and Laplacian Matrix

In general, a dynamical process on a graph with $n$ vertices is a $n$-dimensional dynamical process. The state of the system at time $t$ is described by the vector $(x_1(t), ..., x_n(t))$ where each $x_i(t)$ characterizes the state of vertex $i$ at time $t$. The time evolution of $x_i(t)$ is determined by its own value and the values of $x_j(t)$, the adjacent vertices $j \in \{1, ..., n\}$ only. The graph structure describes this interaction pattern. The variable $x_i(t)$ itself is usually a real or complex number or an element of some discrete set, but can also be a more complex mathematical object.

The first distinction between dynamical processes is whether the time $t$ is a discrete or a continuous variable. In the case of a discrete time $t \in \mathbb{N}$, the dynamics are governed by an equation of the form

$$x_i(t+1) = f_i\left(x_i(t), \{x_j(t) |\ \ j \sim\ i\}\right), \tag{3.7}$$

where the function $f_i$, which describes the time evolution of the vertex $i$, consists of a component depending on $x_i(t)$ and another component depending on the set of neighbors of $i$.

When the graph is undirected, in the case of a continuous time $t \in \mathbb{R}$, the real-valued state variable $x_i$ is generally described by a differential equation of the form

$$\frac{dx_i}{dt} = h_i(x_i(t)) + \sum_{j \in \mathcal{X}_n} A_{ij} g_{ij}(x_i(t), x_j(t)).$$

In this case, the function $h_i$ specifies the intrinsic dynamics of vertex $i$ as if it was isolated from all other vertices and $g_{ij}$ describes the influence of the neighbors $j$ on the dynamics of $i$. Many important processes, such as synchronization and spreading dynamics, fall into this class of dynamics.

A simple but generic class of dynamics consists of diffusion processes. It is a linear process, without intrinsic dynamics, i.e., $f(x) = 0$, and the coupling function $g_{ij}(x_i(t), x_j(t))$ is the difference between the two variables, i.e., $g_{ij}(x_i(t), x_j(t)) = x_j(t) - x_i(t)$. Despite its simplicity, diffusion is rather generic because it is a paradigmatic model for all kinds of spreading dynamics.

Traditionally, diffusion in physics describes the movement of a gas from regions with high concentration to regions with low concentration along some gradient, for example in pressure or temperature. However, also other types of spreading dynamics are modeled as diffusion processes. The spread of infectious diseases in a population, the transfer of information or fads from individual to individual without a common broadcaster, the change of opinions in a society, and the exploration of the World Wide Web by random searching are just some examples. A possible picture of diffusion are RWs. On a graph, consider a particle that moves randomly along the edges from vertex to vertex in discrete steps. The diffusion process is recovered from the RW by either considering a number of random walkers $n$ which tends to infinity and let $x_i(t)$ describe their density at vertex $i$ or, equivalently, let $x_i(t)$ simply be the probability of a random walker to be at vertex $i$ at time $t$.

The interplay between dynamic and structure of a network is of central interest. We consider dynamics at the nodes of the graph that are coupled via the graph Laplacian matrix.

In the context of diffusion, the state variable $x_i(t)$ describes, for example, the amount of substance at vertex $i$. The substance will flow along the edges from vertices with a high value to vertices with a lower value. Hence, $x_i(t)$ changes with time according to

$$\frac{dx_i}{dt} = c \sum_{j \in \mathcal{X}_n} A_{ij}(x_i(t) - x_j(t)). \tag{3.8}$$

The constant $c$ is a diffusion coefficient. The term $A_{ij}$ describes the adjacencies between nodes. Splitting the two terms in the sum yields

$$\frac{dx_i}{dt} = -c \sum_j L_{ij} x_j(t). \tag{3.9}$$

In matrix notation, (3.9) can be rewritten in terms of the Laplacian matrix, as

$$\frac{d\mathbf{x}}{dt} + c\mathbf{L}\mathbf{x}(t) = 0.$$

This equation has the form of a continum diffusion equation with the Laplace operator [79] replaced by $-\mathbf{L}$, the reason why it is called the graph Laplacian.

The time evolution is described by (3.9) which corresponds to a random walker in discrete time that jumps to the next vertex at each time step. Now, we consider the jump rate across each edge normalized by $d_i$, the degree of the vertex that the random walker is currently occupying, i.e., the rate to jump from vertex $i$ to vertex $j$ is $d_i^{-1}$. Thus, the corresponding diffusion equation is given by

$$\frac{dx_i}{dt} = c \sum_{j \in \mathcal{X}_n} A_{ij} \left( \frac{x_j(t)}{d_j} - \frac{x_i(t)}{d_i} \right).$$

The sum on the right hand side can be split, which leads to the matrix form

$$\frac{dx_i}{dt} = c \sum_j A_{ij} \frac{x_j(t)}{d_j} - c x_i(t) \frac{d_i}{d_i} = c \sum_j \left( \frac{A_{ij}}{d_j} - \delta_{ij} \right) x_j(t) = -c \sum_j \mathcal{L}_{ij}^{\mathrm{RW}} x_j(t). \tag{3.10}$$

In matrix notation, (3.10) can be rewritten in terms of the RW normalized Laplacian matrix $\boldsymbol{\mathcal{L}}^{\mathrm{RW}}$, as

$$\frac{d\mathbf{x}}{dt} + c\boldsymbol{\mathcal{L}}^{\mathrm{RW}}\mathbf{x}(t) = 0.$$

In this case, the RW normalized Laplacian matrix $\boldsymbol{\mathcal{L}}^{\mathrm{RW}}$ is the time evolution operator of the diffusion process which is obviously the reason why it is called the RW normalized Laplacian.

An additional important quantity to characterize diffusion processes is the probability $P_0(t)$ that a walker returns to its starting point after $t$ steps. Shortly refer to as *return probability*. On a finite graph, there is always a finite probability for a random walker

to visit any site of the connected component it started in. In the limit of $t \to \infty$, the random walker returns to its starting vertex at some point in time with probability one. In a graph with infinite nodes, this probability can be less than one and the RW is called transient.

The return probability $P_0(t)$ is directly linked to the normalized Laplacian eigenvalue distribution function $\rho(\lambda)$, also called the spectral density function of the RW normalized Laplacian $\boldsymbol{\mathcal{L}}^{\mathrm{RW}}$, or equivalently, the normalized Laplacian matrix $\boldsymbol{\mathcal{L}}$ by the following equation

$$P_0(t) = \int_0^\infty e^{-\lambda t}\rho(\lambda)d\lambda. \tag{3.11}$$

A derivation of this relation can be found in [80] and [80]. Equation (3.11) relates the behavior of $P_o(t)$ to the spectral density function of the normalized Laplacian matrix $\boldsymbol{\mathcal{L}}$. In particular, the long time limit of $P_o(t)$ is directly linked to the behavior of $\rho(\lambda)$ for $\lambda \to \infty$ [81].

When the ED follows a power-law tail asymptotics, i.e., $\rho(\lambda) \sim \lambda^{\gamma-1}$, $\gamma > 0$ for $\lambda \to 0$ then, for $t \to \infty$, we get

$$\mathrm{P}_0(t) \sim t^{-\gamma}. \tag{3.12}$$

This result can be obtained by substituting the spectral density function of the normalized Laplacian in the expression of the return probability $P_0(t)$ given in (3.11) and using Gamma function with $y = \lambda t$ defined as follows

$$\Gamma(x) = \int_0^\infty e^{-y}y^{x-1}dy = t^x \int_0^\infty e^{-\lambda t}(\lambda)^{x-1}d\lambda. \tag{3.13}$$

Then

$$P_0(t) = t^{-\gamma}t^\gamma \int_0^\infty e^{-\lambda t}\lambda^{\gamma-1}d\lambda = t^{-\gamma}\Gamma(\lambda). \tag{3.14}$$

Let us consider some examples. In a $d$-dimensional regular lattice, the low eigenvalue density is given by $\rho(\lambda) \sim \lambda^{d/2-1}$. Then, the use of (3.12) yields the well known result [80]

$$\mathrm{P}_0(t) \sim t^{-d/2}.$$

For the case of a random ER graph in [82] is proven that for $\lambda \to 0$, the spectral density of the normalized Laplacian matrix has the form $\rho(\lambda) \sim e^{\frac{-c}{\sqrt{\lambda}}}$, with $c$ a constant, which yields the expression of the long time behavior given by

$$P_0(t) \sim e^{-at^{1/3}}, \tag{3.15}$$

where $a$ is constants depending on the specific network.

### 3.3.2 Spectral Dimension

In a graph in which a particle moves randomly along edges from a vertex to another vertex in discrete steps, the diffusion process can be thought as a stochastic RW. Then, the SD $d_s$ is defined in terms of the return probability $\mathrm{P}(t)$ of the diffusion [83]

$$d_s = -2\frac{\mathrm{d}\ln \mathrm{P}(t)}{\mathrm{d}\ln(t)},$$

$t$ being the diffusion time. The spectral dimension, $d_s$, defined above is a measure of how likely a random walker return to the starting point after time $t$. In contrast to the topological dimension, $d_s$ need not be an integer. Note that this definition is independent of the particular initial point.

When Alexander and Orbach introduced the SD, it was considered as a useful tool to characterize the low-frequency vibration spectrum of fractals [84]. Nowadays, the SD is considered by many as the appropriate generalization of the Euclidean dimension of regular lattices to irregular structures in general, whether fractals or not. These irregular structures includes polymers, proteins, glasses, percolation clusters. In this thesis, we investigate the SD of random geometric graphs.

When the spectral density function of the normalized Laplacian matrix scales as a power-law, the spectrum of the graph Laplacian provides a second way to define the SD of a network by its asymptotic behavior for $\lambda \to 0$. This justifies why this quantity is called "spectral". For an infinite network, the definition of the SD is given by the relation

$$\frac{d_s}{2} = \lim_{\lambda\to 0}\frac{\log(F(\lambda))}{\log(\lambda)} = 1 + \lim_{\lambda\to 0}\frac{\log(\rho(\lambda))}{\log(\lambda)}, \tag{3.16}$$

where $F(\lambda)$ and $\rho(\lambda)$ are the ESD and the empirical spectral density of the normalized Laplacian matrix $\boldsymbol{\mathcal{L}}$ of the graph, respectively.

Exact values of $d_s$ are only known for a rather limited class of models. For instance, Euclidean lattices in dimension $d$ have SD $d_s = d$. In the case of the percolation problem, Alexander and Orbach conjectured that the SD of a percolating cluster is $d_s = 4/3$ [84]. In [85], the SD of an additional random geometry, called random combs is studied. Random combs are special tree graphs composed of an infinite linear chain with a number of linear chains attached according to some probability distribution. In this particular case, the SD is found to be $d_s = 3/2$.

In chapter 6, we study the return-to-origin probability of RWs $P_0(t)$ and the SD of RGGs.

# Chapter 4

# Spectrum of the Normalized Laplacian of RGGs

## 4.1 Spectrum of the Normalized Laplacian of RGGs

In this chapter, using tools from random matrix theory and probability theory, we analyze the spectrum of RGGs in the connectivity and thermodynamic regime. In particular, we analyze the eigenvalues and LSD of the normalized Laplacian matrix of RGGs and its regularized version in the connectivity and the thermodynamic regimes under any $\ell_p$-metric, with $p \in [1, \infty]$ and under any dimension $d \geq 1$ finite. Unlike ER graphs, the RGG is an inherently harder model to work with since the nature of the graph induces dependencies between edges. Therefore, the classical spectral methods might fail as the edges of the RGG are not independent.

To the best of our knowledge, explicit expressions for the LSD or the eigenvalues of the combinatorial Laplacian and normalized Laplacian for RGGs are still not known in the full range of the scaling laws for the radius $r_n^d$ in the connectivity regime, nor in the thermodynamic regime. In this work, we first extend the work in [77] by proposing another sequence of matrices called deterministic geometric graph (DGG) with nodes in a grid as an approximation for the actual RGG. Then, we provide a bound on the Hilbert-Schmidt norm of the difference between the RGG and the DGG regularized normalized Laplacian matrices in both the connectivity and thermodynamic regime.

In the connectivity regime, i.e., $a_n = \Omega(\log(n))$, we prove that the normalized Laplacian matrices for RGGs and DGGs are asymptotically equivalent with high probability. Then, we use the regular structure of the DGG to show that the LSD of the RGG normalized Laplacian converges with high probability to the Dirac distribution at one in the full range of the connectivity regime as $n \to \infty$. We give the rate of convergence for different cases depending on the chosen average vertex degree $a_n$. More precisely, we show that when $a_n \geq \log^{1+\epsilon}(n)$ for $\epsilon > 0$, the rate of convergence is $\mathcal{O}\left(1/n^{(a_n/12\log(n))-1)}\right)$. In particular, we show that, when $a_n = c\log(n)$, for $c > 24$, the rate of convergence is

$\mathcal{O}\left(1/n^{c/12-1}\right)$, and when $c \leq 24$, a slower rate of convergence holds and scales as $\mathcal{O}\left(1/n\right)$. When the graph is dense, i.e., $a_n$ scales as $\Omega(n)$, the LSD of the normalized Laplacian for an RGG converges with the rate of convergence $\mathcal{O}\left(ne^{-n/12}\right)$.

In the thermodynamic regime, we show that the spectrum of the regularized normalized Laplacian of an RGG obtained by using any $\ell_p$-metric can be approximated by the spectrum of the regularized normalized Laplacian of a DGG, with an error bound dependent upon the average vertex degree $a_n = \gamma$. Finally, using the regular structure of the DGG, we provide an analytical approximation for the eigenvalues of the RGG regularized normalized Laplacian matrix.

## 4.2 Preliminaries

This section recalls the graph model under study, which is the RGG, and provides preliminary technical results.

Let us precisely define the RGG studied in this work. We consider a finite set $\mathcal{X}_n$ of $n$ nodes, $x_1, ..., x_n$, distributed uniformly and independently on the $d$-dimensional torus $\mathbb{T}^d \equiv [0,1]^d$. Taking a torus $\mathbb{T}^d$ instead of a cube allows us not to consider boundary effects. Given a geographical distance $r_n > 0$, we form a graph by connecting two nodes $x_i, x_j \in \mathcal{X}_n$ if the $\ell_p$-distance between them is at most $r_n$, i.e., $\|x_i - x_j\|_p \leq r_n$ with $p \in [1, \infty]$ (that is, either $p \in [1, \infty)$ or $p = \infty$), see Figure 4.1(a). Such graphs, denoted by $G(\mathcal{X}_n, r_n)$, are called RGGs and are extensively discussed in [29]. Typically, the function $r_n$ is chosen such that $r_n \to 0$ when $n \to \infty$.

Two different scaling regimes for $a_n$ are of particular interest in this chapter. The first one is the connectivity regime, in which the average vertex degree $a_n$ grows logarithmically in $n$ or faster, i.e., $\Omega(\log(n))$ [29]. The second scaling regime of interest is the thermodynamic regime, in which the average vertex degree is a constant $\gamma$, i.e., $a_n \equiv \gamma$ [29].

In general, it is a challenging task to derive exact Laplacian eigenvalues for complex graphs. We remark that for this purpose, the use of deterministic structures is of much help. Therefore, we introduce an auxiliary graph called the deterministic geometric graph (DGG) with nodes in a grid useful for the study of the LSD of RGGs [77].

As for RGGs, we let $\mathcal{D}_n$ be the set of $n$ grid nodes that are at the intersections of all parallel hyperplanes with separation $n^{-1/d}$, and define a deterministic graph $G(\mathcal{D}_n, r_n)$ in the grid by connecting two nodes $x'_i$, $x'_j \in \mathcal{D}_n$ if $\|x'_i - x'_j\|_p \leq r_n$ for $p \in [1, \infty]$, see Figure 4.1(b). Given two nodes in $G(\mathcal{X}_n, r_n)$ or in $G(\mathcal{D}_n, r_n)$, we assume that there is always at most one edge between them. There is no edge from a vertex to itself. Moreover, we assume that the edges are not directed. In the following, we define the normalized Laplacian matrix for $G(\mathcal{X}_n, r_n)$ and $G(\mathcal{D}_n, r_n)$.

Let $\mathcal{N}(x_i)$ be the set of neighbors of vertex $x_i$ in $G(\mathcal{X}_n, r_n)$ and $\mathcal{N}(x'_i)$ be the set of neighbors of vertex $x'_i$ in $G(\mathcal{D}_n, r_n)$. Let $\mathcal{L}(\mathcal{X}_n)$ and $\mathcal{L}(\mathcal{D}_n)$ be the normalized Laplacian

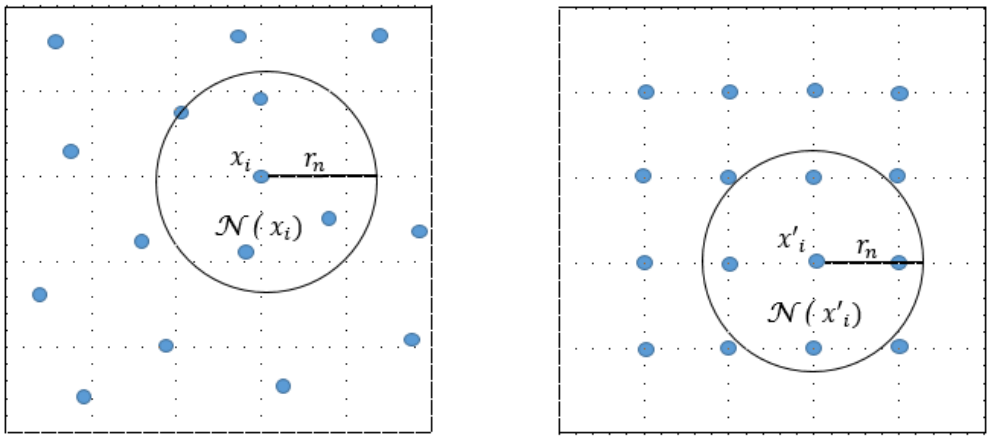


Figure 4.1: Illustration of an RGG (a) and a DGG (b) for $n = 16$.

matrices for $G(\mathcal{X}_n, r_n)$ and $G(\mathcal{D}_n, r_n)$, respectively, with entries,

$$\mathcal{L}(\mathcal{X}_n)_{ij} = \delta_{ij} - \frac{\chi[x_i \sim x_j]}{\sqrt{\mathbf{N}(x_i)\mathbf{N}(x_j)}}, \qquad \mathcal{L}(\mathcal{D}_n)_{ij} = \delta_{ij} - \frac{\chi[x'_i \sim x'_j]}{\sqrt{\mathbf{N}(x'_i)\mathbf{N}(x'_j)}}, \tag{4.1}$$

where $\mathbf{N}(x_i)$ and $\mathbf{N}(x'_i)$ are the sizes of the two sets $\mathcal{N}(x_i)$ and $\mathcal{N}(x'_i)$, respectively, and $\delta_{ij}$ is the Kronecker delta function. The term $\chi[x_i \sim x_j]$ takes unit value when there is an edge between nodes $x_i$ and $x_j$ in $G(\mathcal{X}_n, r_n)$ and zero otherwise, i.e.,

$$\chi[x_i \sim x_j] = \begin{cases} 1, & \|x_i - x_j\|_p \leq r_n, \quad i \neq j \\ 0, & \text{otherwise.} \end{cases}$$

A similar definition holds for $\chi[x'_i \sim x'_j]$ defined over the nodes in $G(\mathcal{D}_n, r_n)$. Recall that $a_n$ denotes the average vertex degree in $G(\mathcal{X}_n, r_n)$ and, in particular, in the thermodynamic regime $a_n \equiv \gamma$ for a constant $\gamma$. In $G(\mathcal{D}_n, r_n)$, the number of neighbors of each vertex is the same. For simplicity, we denote this number by $a'_n = \mathbf{N}(x'_i)$. In particular, in the thermodynamic regime $\mathbf{N}(x'_i) = \gamma'$. We have also $\mathbf{N}(x_i, x'_i) = \sum_j \chi[x_i \sim x_j]\chi[x'_i \sim x'_j] \leq a'_n \ \forall\ i, j$.

Note that the above formal definition of the normalized Laplacian in (4.1) requires $G(\mathcal{X}_n, r_n)$ and $G(\mathcal{D}_n, r_n)$ not to have isolated vertices. To overcome the problem of singularities due to isolated vertices in the termodynamic regime, we follow the scheme proposed in [78]. It corresponds to the normalized Laplacian matrix on a modified graph constructed by adding auxiliary edges among all the nodes with weight $\frac{\alpha}{n} > 0$. Specifically, the entries of the normalized Laplacian matrices are modified as

$$\hat{\mathcal{L}}(\mathcal{X}_n)_{ij} = \delta_{ij} - \frac{\chi[x_i \sim x_j] + \frac{\alpha}{n}}{\sqrt{(\mathbf{N}(x_i) + \alpha)(\mathbf{N}(x_j) + \alpha)}}, \qquad \hat{\mathcal{L}}(\mathcal{D}_n)_{ij} = \delta_{ij} - \frac{\chi[x'_i \sim x'_j] + \frac{\alpha}{n}}{\sqrt{(a'_n + \alpha)(a'_n + \alpha)}}. \tag{4.2}$$

The corresponding matrices are referred to as the regularized normalized Laplacian matrices [78]. Observe that for $\alpha = 0$, (4.2) reduces to (4.1).

## 4.3 Main Results

The matrices $\hat{\mathcal{L}}(\mathcal{X}_n)$ and $\hat{\mathcal{L}}(\mathcal{D}_n)$ are symmetric, and consequently, their spectra consist of real eigenvalues. We denote by $\{\hat{\mu}_i, i = 1, .., n\}$ and $\{\hat{\lambda}_i, i = 1, .., n\}$ the sets of all real eigenvalues of the real symmetric square matrices $\hat{\mathcal{L}}(\mathcal{X}_n)$ and $\hat{\mathcal{L}}(\mathcal{D}_n)$ of order $n$, respectively. Then, the empirical spectral distribution functions of $\hat{\mathcal{L}}(\mathcal{X}_n)$ and $\hat{\mathcal{L}}(\mathcal{D}_n)$ are defined as

$$F^{\hat{\mathcal{L}}(\mathcal{X}_n)}(x) = \frac{1}{n}\sum_{i=1}^{n} \mathbf{1}_{\hat{\mu}_i \leq x}, \quad \text{and} \quad F^{\hat{\mathcal{L}}(\mathcal{D}_n)}(x) = \frac{1}{n}\sum_{i=1}^{n} \mathbf{1}_{\hat{\lambda}_i \leq x},$$

To show that $F^{\hat{\mathcal{L}}(\mathcal{D}_n)}$ is a good approximation for $F^{\hat{\mathcal{L}}(\mathcal{X}_n)}$ when $n$ is large in both the connectivity and thermodynamic regimes, we provide a bound on Hilbert-Schmidt norm of the difference between the RGG and the DGG normalized Laplacian matrices.

### 4.3.1 Upper Bound the Hilbert-Schmidt norm of the Difference Between two Regularized Normalized Laplacian Matrices

In the following Lemma 27, we upper bound the Hilbert-Schmidt norm of the difference between the matrices $\hat{\mathcal{L}}(\mathcal{X}_n)$ and $\hat{\mathcal{L}}(\mathcal{D}_n)$ for any average vertex degree $a_n$.

**Lemma 27** (Upper Bound on the Hilbert-Schmidt norm of the difference between $\hat{\mathcal{L}}(\mathcal{X}_n)$ and $\hat{\mathcal{L}}(\mathcal{D}_n)$)**.** *For $d \geqslant 1$ and $p \in [1, \infty]$, the Hilbert-Schmidt norm of the difference between $\hat{\mathcal{L}}(\mathcal{X}_n)$ and $\hat{\mathcal{L}}(\mathcal{D}_n)$ is upper bounded as follows:*

$$\begin{aligned}\|\hat{\mathcal{L}}(\mathcal{X}_n) - \hat{\mathcal{L}}(\mathcal{D}_n)\|_{\mathrm{HS}}^2 \leq & \left| \frac{1}{n}\sum_i \sum_j \frac{\left(\chi[x_i \sim x_j] + \frac{\alpha}{n}\right)^2}{(\mathbf{N}(x_i) + \alpha)(\mathbf{N}(x_j) + \alpha)} - \frac{b}{n(a'_n + \alpha)^2} \right| \\ & + \left| \frac{2b}{n(a'_n + \alpha)^2} - \frac{2\left(\sum_i \mathbf{N}(x_i, x'_i) + \frac{\alpha}{n}\sum_i \mathbf{N}(x_i) + \alpha a'_n + \alpha^2\right)}{n(a'_n + \alpha)\left(\sum_i \sqrt{\mathbf{N}(x_i) + \alpha}\right)^2} \right|,\end{aligned}$$

*where $b = na'_n + \alpha^2 + 2\alpha a'_n$.*

*Proof.* To upper bound the Hilbert-Schmidt norm of the difference between the regularized normalized Laplacian matrices $\hat{\mathcal{L}}(\mathcal{X}_n)$ and $\hat{\mathcal{L}}(\mathcal{D}_n)$, we first give the following lemma.

**Lemma 28.** *If $a_i \geq 0$ and $b_i > 0$ for all $i$, and there exists an $a_i > 0$, then*

$$\sum_{i=1}^{n} \frac{a_i}{b_i} > \frac{\sum_{i=1}^{n} a_i}{\sum_{i=1}^{n} b_i}.$$

By using Lemma 6, we upper bound the Hilbert-Schmidt norm of the difference between $\hat{\mathcal{L}}(\mathcal{X}_n)$ and $\hat{\mathcal{L}}(\mathcal{X}_n)$ as

$$\begin{aligned}
\|\hat{\mathcal{L}}(\mathcal{X}_n) - \hat{\mathcal{L}}(\mathcal{D}_n)\|_{\text{HS}}^2 &= \frac{1}{n}\text{Trace}\left[\hat{\mathcal{L}}(\mathcal{X}_n) - \hat{\mathcal{L}}(\mathcal{D}_n)\right]^2 \\
&= \frac{1}{n}\sum_i\sum_j \left[\frac{\chi[x_i \sim x_j] + \frac{\alpha}{n}}{\sqrt{(\mathbf{N}(x_i)+\alpha)(\mathbf{N}(x_j)+\alpha)}} - \frac{\chi[x_i' \sim x_j'] + \frac{\alpha}{n}}{\sqrt{(a_n'+\alpha)(a_n'+\alpha)}}\right]^2 \\
&= \frac{1}{n}\sum_i\sum_j \left[\frac{\left(\chi[x_i \sim x_j] + \frac{\alpha}{n}\right)^2}{(\mathbf{N}(x_i)+\alpha)(\mathbf{N}(x_j)+\alpha)} + \frac{\left(\chi[x_i' \sim x_j'] + \frac{\alpha}{n}\right)^2}{(a_n'+\alpha)^2}\right] \\
&\quad - \frac{2}{n}\sum_i\sum_j \frac{\left(\chi[x_i \sim x_j] + \frac{\alpha}{n}\right)\left(\chi[x_i' \sim x_j'] + \frac{\alpha}{n}\right)}{(a_n'+\alpha)\sqrt{(\mathbf{N}(x_i)+\alpha)(\mathbf{N}(x_j)+\alpha)}}.
\end{aligned}$$

We notice from the last equation that $\sum_j \chi[x_i \sim x_j] = \mathbf{N}(x_i)$ corresponds to the number of neighbors of vertex $x_i$ in the RGG, and similarly $\sum_j \chi[x_i' \sim x_j'] = a_n'$ corresponds to the number of neighbors of vertex $x_i'$ in the DGG. Let $b = na_n' + 2\alpha a_n' + \alpha^2$ and $\mathbf{N}(x_i, x_i') = \sum_j \chi[x_i \sim x_j]\chi[x_i' \sim x_j']$. Then, by applying Lemma 28 we get the following upper bound.

$$\begin{aligned}
\|\hat{\mathcal{L}}(\mathcal{X}_n) - \hat{\mathcal{L}}(\mathcal{D}_n)\|_{\text{HS}}^2 \leq \frac{b}{n(a_n'+\alpha)^2} &- \frac{2\left(\sum_i \mathbf{N}(x_i, x_i') + \frac{\alpha}{n}\sum_i \mathbf{N}(x_i) + \alpha a_n' + \alpha^2\right)}{n(a_n'+\alpha)\left(\sum_i \sqrt{\mathbf{N}(x_i)+\alpha}\right)^2} \\
&+ \frac{1}{n}\sum_i\sum_j \frac{\left(\chi[x_i \sim x_j] + \frac{\alpha}{n}\right)^2}{(\mathbf{N}(x_i)+\alpha)(\mathbf{N}(x_j)+\alpha)}.
\end{aligned}$$

Using the triangle inequality, the result follows. □

Note that in the thermodynamic regime, for $d \geqslant 1$, the Hilbert-Schmidt norm of the difference between the matrices $\hat{\mathcal{L}}(\mathcal{X}_n)$ and $\hat{\mathcal{L}}(\mathcal{D}_n)$ is upper bounded as in Lemma 27 by letting $a_n \equiv \gamma$ being a positive constant. When the graph is connected, it is not necessary to work with the regularized normalized Laplacian, but we consider only the normalized Laplacian in (4.1) by enforcing $\alpha = 0$ in (4.2). Therefore, in the connectivity regime, the

Hilbert-Schmidt norm of the difference between the matrices $\mathcal{L}(\mathcal{X}_n)$ and $\mathcal{L}(\mathcal{D}_n)$ is bounded as follows:

$$\|\mathcal{L}(\mathcal{X}_n) - \mathcal{L}(\mathcal{D}_n)\|_{\mathrm{HS}}^2 \leq \left| \frac{1}{n} \sum_i \sum_j \frac{\chi[x_i \sim x_j]^2}{\mathbf{N}(x_i)\mathbf{N}(x_j)} - \frac{1}{a'_n} \right| + \left| \frac{2}{a'_n} - \frac{2\sum_i \mathbf{N}(x_i, x'_i)}{na'_n \left( \sum_i \sqrt{\mathbf{N}(x_i)} \right)^2} \right|.$$

Next, we state a general theorem on the concentration of the regularized normalized Laplacian for any average vertex degree $a_n$. Then, we specify the result for both the connectivity and thermodynamic regimes.

**Theorem 29** (Concentration Theorem for the Regularized Normalized Laplacian Matrix in RGGs)**.** *For $d \geq 1$, $p \in [1, \infty]$ and $t > \max\left[\frac{4(n+2\alpha)a'_n+4\alpha^2}{n(a'_n+\alpha)^2}, \frac{8(n+2\alpha)a_n+4\alpha^2}{n(a_n+\alpha)^2}\right]$, the inequality take place:*

$$\begin{aligned}\mathbb{P}\left\{\|\hat{\mathcal{L}}(\mathcal{X}_n) - \hat{\mathcal{L}}(\mathcal{D}_n)\|_{\mathrm{HS}}^2 > t\right\} &\leq 2\mathbb{P}\left\{\left|\sum_i \mathbf{N}(x_i) - na_n\right| > \frac{tn(a_n+\alpha)^2 - 4\alpha^2}{8\left(1+\frac{2\alpha}{n}\right)} - na_n\right\} \\ &+ 2\mathbb{P}\left\{\left|\sum_i \mathbf{N}(x_i) - na_n\right| > \frac{tn(a_n+\alpha)}{16}\right\} + \mathbb{P}\left\{\sum_i |a_n - \mathbf{N}(x_i)|^2 > \frac{tn(a_n+\alpha)^2}{8}\right\}.\end{aligned} \tag{4.3}$$

*Proof.* See Appendix A.1. □

Based on Theorem 29, we state the following corollary on the concentration of the regularized normalized Laplacian in RGGs specific to the thermodynamic regime.

**Corollary 4** (Concentration of the Regularized Normalized Laplacian in the Thermodynamic Regime)**.** *In the thermodynamic regime, i.e., $a_n \equiv \gamma$ finite, for $d \geq 1$, $p \in [1, \infty]$ and $t > \max\left[\frac{4(n+2\alpha)\gamma'+4\alpha^2}{n(\gamma'+\alpha)^2}, \frac{8(n+2\alpha)\gamma+4\alpha^2}{n(\gamma+\alpha)^2}\right]$, we get*

$$\mathbb{P}\left\{\|\hat{\mathcal{L}}(\mathcal{X}_n) - \hat{\mathcal{L}}(\mathcal{D}_n)\|_{\mathrm{HS}}^2 > t\right\} \leq \frac{320(n-1)\vartheta}{tn^2(\gamma+\alpha)^2},$$

*where $\vartheta = \left[\theta^{(d)} + 2(n-2)(\theta^{(d)})^2 r_n^d\right]$.*

*Under the conditions described above, for every $t > \max\left[\frac{4\gamma'}{(\gamma'+\alpha)^2}, \frac{8\gamma}{(\gamma+\alpha)^2}\right]$ as $n \to \infty$,*

$$\lim_{n\to\infty} \mathbb{P}\left\{\|\hat{\mathcal{L}}(\mathcal{X}_n) - \hat{\mathcal{L}}(\mathcal{D}_n)\|_{\mathrm{HS}}^2 > t\right\} = 0.$$

*Proof.* See Appendix A.3. □

In the thermodynamic regime, the previous corollary states that $\hat{\mathcal{L}}(\mathcal{D}_n)$ approximates $\hat{\mathcal{L}}(\mathcal{X}_n)$ with an error bound of $\max\left[\frac{4}{\gamma'}, \frac{8}{\gamma}\right]$ when $n \to \infty$ and $\alpha \to 0$, which in particular implies that the error bound becomes small for large values of the degree.

In the following Lemma 30, we provide a lower bound on the degree of the vertices in $G(\mathcal{D}_n, r_n)$, useful for the following studies.

**Lemma 30** (Lower Bound on the Vertex Degree of the DGG)**.** *For any chosen $\ell_p$-metric with $p \in [1, \infty]$, $d \geq 1$ and $a_n \geq \frac{2d^{1+1/p}}{2d-1}$, we have*

$$a'_n \geq \frac{a_n}{2d^{1+1/p}},$$

*where $a_n$ is the average vertex degree of $G(\mathcal{X}_n, r_n)$ and $a'_n$ is the degree of each vertex in $G(\mathcal{D}_n, r_n)$.*

*Proof.* See Appendix A.2. □

The following theorem shows that the Hilbert-Schmidt norm of the difference between the normalized Laplacian matrices $\mathcal{L}(\mathcal{D}_n)$ and $\mathcal{L}(\mathcal{X}_n)$ converges to zero in probability as $n \to \infty$.

**Theorem 31** (Concentration of the Hilbert-Schmidt norm of the difference of the Normalized Laplacian for RGG and DGG in the Connectivity Regime)**.** *In the connectivity regime, i.e., $a_n = \Omega(\log(n))$, for $a_n \geq \frac{2d^{1+1/p}}{2d-1}$, $d \geq 1$, $p \in [1, \infty]$ and $t > \frac{8d^{1+1/p}}{a_n}$, we have*

$$\mathbb{P}\left\{\|\mathcal{L}(\mathcal{X}_n) - \mathcal{L}(\mathcal{D}_n)\|_{\mathrm{HS}}^2 > t\right\} \leq \min\left[\frac{320(n-1)\vartheta}{tn^2(\gamma+\alpha)^2}, 6n\exp\left(-\frac{(a_n - r_n)}{12}\right)\right],$$

*where $\vartheta = \left[\theta^{(d)} + 2(n-2)(\theta^{(d)})^2 r_n^d\right]$.*

*Under the conditions described above, for every $t > 0$,*

$$\lim_{n\to\infty} \mathbb{P}\left\{\|\mathcal{L}(\mathcal{X}_n) - \mathcal{L}(\mathcal{D}_n)\|_{\mathrm{HS}}^2 > t\right\} = 0.$$

*Proof.* See Appendix A.3. □

This result show the concentration of the Hilbert–Schmidt norm of the difference between the normalized Laplacian matrices $\mathcal{L}(\mathcal{D}_n)$ and $\mathcal{L}(\mathcal{X}_n)$ as $n \to \infty$. In addition, we observe that the normalized Laplacian matrices are bounded in the strong norm. Hence, by applying Lemma 17, we conclude that the matrices $\mathcal{L}(\mathcal{D}_n)$ and $\mathcal{L}(\mathcal{X}_n)$ are asymptotically equivalent in probability. Then, Corollary 3 guarantees the convergence in probability of the two LSDs.

In the following we provide the rate of convergence in the connectivity regime. We have $\vartheta < \theta^{(d)} a_n \left(\frac{1}{a_n} + 2\right)$ and $t > \frac{8d^{1+1/p}}{a_n}$ then,

$$A = \frac{320(n-1)\vartheta}{tn^2 a_n^2} < \frac{320\vartheta}{tna_n^2} < \frac{40\vartheta}{na_n d^{1+1/p}} = \frac{40\theta^{(d)}\left(\frac{1}{a_n} + 2\right)}{nd^{1+1/p}},$$

and

$$B = \frac{6n}{\exp\left(\frac{a_n}{12}\left[1-\frac{r_n}{a_n}\right]\right)} = \frac{6}{n^{\frac{a_n}{12\log(n)}\left[1-\frac{r_n}{a_n}\right]-1}},$$

therefore,

$$\mathbb{P}\left\{\|\mathcal{L}(\mathcal{X}_n)-\mathcal{L}(\mathcal{D}_n)\|_{\text{HS}}^2 > t\right\} < \min\left[\frac{40\theta^{(d)}\left(\frac{1}{a_n}+2\right)}{nd^{1+1/p}}, \frac{6}{n^{\frac{a_n}{12\log(n)}\left[1-\frac{r_n}{a_n}\right]-1}}\right].$$

Note that, when $a_n = c\log(n)$, $c > 24$, then $B < A$ and the rate of convergence is $\mathcal{O}\left(1/n^{c/12-1}\right)$, and when $c \leq 24$, the rate of convergence is $\mathcal{O}(1/n)$. For $\epsilon > 0$ and $a_n \geq \log^{1+\epsilon}(n)$, the rate of convergence is $\mathcal{O}\left(1/n^{(a_n/12\log(n))-1}\right)$. When the graph is dense, i.e., $a_n$ scales as $\Omega(n)$, the LSD of the normalized Laplacian matrix of the RGG converges to the Dirac measure at one with rate of convergence $\mathcal{O}\left(ne^{-n/12}\right)$. Hence, from the result in Theorem 31 and Corollary 3 follows that the LSDs of the normalized Laplacian matrix for $G(\mathcal{X}_n, r_n)$ and $G(\mathcal{D}_n, r_n)$ converge to the same limit as $n \to \infty$ under any chosen $\ell_p$-metric, and the convergence holds in the full range of the connectivity regime, i.e, $a_n = \Omega(\log(n))$.

### 4.3.2 Eigenvalues and LSD of the Regularized Normalized Laplacian of RGGs

In the following, we use the structure of the DGG to approximate the eigenvalues of the regularized normalized Laplacian matrix of $G(\mathcal{X}_n, r_n)$ in both the connectivity and thermodynamic regime using the Chebyshev distance. Let us consider a $d$-dimensional DGG with $n = \text{N}^d$ nodes and assume the use of the Chebyshev distance. Then, the degree of a vertex in $G(\mathcal{D}_n, r_n)$ is given as [70]

$$a'_n = (2k_n+1)^d - 1, \quad \text{with} \quad k_n = \lfloor \text{N}r_n \rfloor,$$

where $\lfloor x \rfloor$ is the integer part, i.e., the greatest integer less than or equal to $x$. Note that when $d = 1$, the Chebyshev distance and the Euclidean distance are the same.

In the following Lemma 32, by using the expression of the eigenvalues of the adjacency matrix for a DGG under the Chebyshev distance [70], we approximate the eigenvalues of the regularized normalized Laplacian matrix for $G(\mathcal{X}_n, r_n)$ when the number of nodes $n$ is fixed and for any $a_n$. Then, we utilize this result to determine the LSD of the normalized Laplacian matrix in the connectivity regime as $n \to \infty$ in Corollary 5, and we provide the analytical approximation for the eigenvalues in the thermodynamic regime as $n$ goes to infinity in Corollary 6.

**Lemma 32** (Eigenvalue Distribution of the Regularized Normalized Laplacian Matrix)**.** *When using the Chebyshev distance and $d \geq 1$, the eigenvalues of $\hat{\mathcal{L}}(\mathcal{D}_n)$ are given by*

$$\hat{\lambda}_{m_1,\ldots,m_d} = 1 - \frac{1}{(a'_n+\alpha)}\prod_{s=1}^{d}\frac{\sin(\frac{m_s\pi}{\text{N}}(a'_n+1)^{1/d})}{\sin(\frac{m_s\pi}{\text{N}})} + \frac{1-\alpha\delta_{m_1,\ldots,m_d}}{(a'_n+\alpha)}, \tag{4.4}$$

*with* $m_1, ..., m_d \in \{0, ...\mathrm{N}-1\}$ *and* $\delta_{m_1,...,m_d} = 1$ *when* $m_1, ..., m_d = 0$ *otherwise* $\delta_{m_1,...,m_d} = 0$. *In (4.4),* $n = \mathrm{N}^d$, $a'_n = (2k_n+1)^d - 1$ *and* $k_n = \lfloor \mathrm{N} r_n \rfloor$.

*Proof.* See Appendix A.4. □

In the following Corollary 5, we provide the eigenvalue distribution of the normalized Laplacian matrix for $G(\mathcal{X}_n, r_n)$ in the connectivity regime as $a_n \geq 2d^{1+1/p}$ and $n \to \infty$.

**Corollary 5** (Eigenvalue Distribution of the Normalized Laplacian Matrix in the Connectivity Regime)**.** *In the connectivity regime, i.e.,* $a_n = \Omega(\log(n))$, *using the Chebyshev distance,* $a_n \geq 2d^{1+1/p}$, $d \geq 1$, *and letting* $\alpha \to 0$, *the eigenvalues of* $\mathcal{L}(\mathcal{D}_n)$ *converge asymptotically to the limiting*

$$\lambda_{m_1,...,m_d} = 1 - \frac{1}{a'_n} \prod_{s=1}^{d} \frac{\sin(\frac{m_s \pi}{\mathrm{N}}(a'_n+1)^{1/d})}{\sin(\frac{m_s \pi}{\mathrm{N}})} + \frac{1}{a'_n}, \tag{4.5}$$

*with* $m_1, ..., m_d \in \{0, ...\mathrm{N}-1\}$. *In (5.3),* $n = \mathrm{N}^d$, $a'_n = (2k_n+1)^d - 1$ *and* $k_n = \lfloor \mathrm{N} r_n \rfloor$. *Then, in particular, as* $n \to \infty$, *the LSD of* $\mathcal{L}(\mathcal{D}_n)$ *converges to the Dirac measure at one.*

In the following Corollary 6, we provide the eigenvalues of the regularized normalized Laplacian matrix $\hat{\mathcal{L}}(\mathcal{D}_n)$ in the thermodynamic regime as $n \to \infty$.

**Corollary 6** (Eigenvalues of the Regularized Normalized Laplacian in the Thermodynamic Regime)**.** *In the thermodynamic regime, by using the Chebyshev distance,* $\gamma \geq 1$ *and* $d \geq 1$, *as* $n \to \infty$, *the eigenvalues of* $\hat{\mathcal{L}}(\mathcal{D}_n)$ *are given by*

$$\hat{\lambda}_{f_1,...,f_d} = 1 - \frac{1}{(\gamma'+\alpha)} \prod_{s=1}^{d} \frac{\sin(\pi f_s(\gamma'+1)^{1/d})}{\sin(\pi f_s)} + \frac{1-\alpha\delta_{f_1,...,f_d}}{(\gamma'+\alpha)}, \tag{4.6}$$

*where* $s \in \{1, ..., d\}$, $m_s \in \{0, ..., \mathrm{N}\}$ *and* $f_s = \frac{m_s}{\mathrm{N}}$ *in* $\mathbb{Q} \cap [0,1]$ *with* $\mathbb{Q}$ *denotes the set of rational numbers. Also,* $\gamma' = (2\lfloor \gamma^{1/d} \rfloor + 1)^d - 1$ *and* $\delta_{f_1,...,f_d} = 1$ *when* $f_1, ..., f_d = 0$ *otherwise* $\delta_{f_1,...,f_d} = 0$.

In Lemma 32, we generalize the results given in [77], [73] and [74]. On one hand, in [77], the author shows that the spectral measures of the transition probability matrix of the RW in RGGs and DGGs converge to the same limit in a specific range of the connectivity regime. On the other hand, in [73], the author shows that, for a fixed dimension $d$ and $n \to \infty$, the LSD of $\mathbf{M}_n = f(\|x_i - x_j\|_2)$ converges to the Dirac measure in zero under some conditions on the function $f$. However, the techniques used in [73] cannot be applied to geometric graphs since the function $f$ is required to be continuous. Additionally, Bordenave in [74], characterizes the spectral measure of a normalized adjacency matrix in the dense regime. In contrast, in this work we study the LSD of the normalized Laplacian matrix for an RGG formed by using any $\ell_p$-metric, $1 \leq p \leq \infty$, and we show that it converges to the same limit as for the normalized Laplacian matrix for a DGG in the full range of the connectivity regime as $n \to \infty$. In particular, we show that they converge to the Dirac measure at one as $n$ goes to infinity in the full range of the connectivity regime.

## 4.4 Numerical Simulations

In this section, we validate our analytical results obtained in the section above by numerical computations. More specifically, we corroborate our results on the spectrum of the regularized normalized Laplacian matrix of RGGs in the connectivity and thermodynamic regimes by comparing the simulated and the analytical spectra.

Figure 4.2(a) illustrates the empirical spectral distribution in the thermodynamic regime of a realization for an RGG with $n = 30000$ vertices, $\alpha = 0.001$ and the corresponding DGG. The illustrated theoretical distribution is obtained from the eigenvalues given in Corollary 6. We notice that the gap that appears between the eigenvalue distributions of the RGG and the DGG is upper bounded as in Corollary 4.

Here, we provide an additional example in the thermodynamic regime to quantify the error between $F^{\hat{\mathcal{L}}(\mathcal{X}_n)}$ and $F^{\hat{\mathcal{L}}(\mathcal{D}_n)}$ for different values of $\gamma$ using the Chebyshev distance.

1) When $\gamma = 100$ and $\alpha = 10^{-3}$, $d = 1$ then as $n \to \infty$

$$\mathbb{P}\left\{\|\hat{\mathcal{L}}(\mathcal{X}_n) - \hat{\mathcal{L}}(\mathcal{D}_n)\|_{\mathrm{HS}}^2 > \mathbf{0.019}\right\} \to 0.$$

2) When $\gamma = 120$ and $\alpha = 10^{-3}$, $d = 1$ then as $n \to \infty$

$$\mathbb{P}\left\{\|\hat{\mathcal{L}}(\mathcal{X}_n) - \hat{\mathcal{L}}(\mathcal{D}_n)\|_{\mathrm{HS}}^2 > \mathbf{0.015}\right\} \to 0.$$

From these examples, we notice that for $\gamma = 100$, the LSD of the regularized normalized Laplacian matrix in the RGG can be approximated by the LSD of a DGG with an error bound of 0.019 when $\alpha = 10^{-3}$. Then, as we increase the average vertex degree $\gamma$ to $\gamma = 120$, we can notice a certain improvement. Therefore, the larger the average vertex degree $\gamma$ is, the tighter the approximation becomes.

In Figure 4.2(b) we compare the spectral distribution of a DGG (continuous lines) with the one for an RGG with increasing the number of nodes $n$ (dashed line for $n = 500$ and star markers for $n = 30000$) in the connectivity regime. We notice that the curves corresponding to the RGG and the DGG match very well when $n$ is large which confirm the concentration result given in Theorem 31. Also, it appears that by increasing $n$, the eigenvalue distribution converges to the Dirac measure at one, which confirms the result obtained in Corollary 5.

## 4.5 Conclusions

In this chapter, we studied in details the spectrum of RGGs in both the connectivity and thermodynamic regime. We first proposed an approximation for the regularized normalized Laplacian matrix and obtained an upper bound on the Hilbert-Schmidt norm of

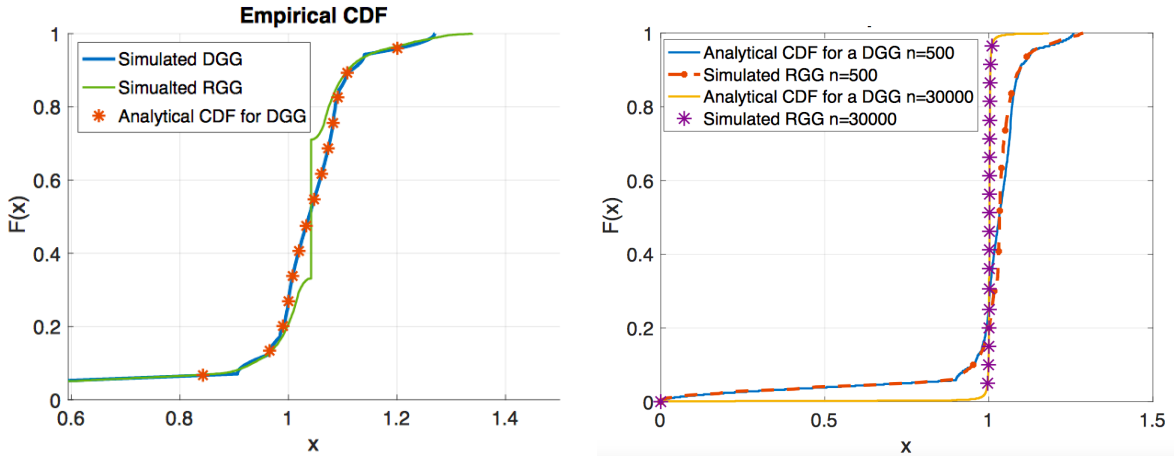


(a) Thermodynamic regime, $\gamma = 12$, $n = 30000$ and $\alpha = 0.001$.

(b) Connectivity regime for different $n$ and $r_n = \log^{\frac{3}{2}}(n)/n$.

Figure 4.2: Comparison between the simulated and the analytical spectral distributions of an RGG for $d = 1$.

the difference between this approximation and the RGG regularized normalized Laplacian matrix. In the connectivity, as $n \to \infty$, we found that the DGG and RGG regularized normalized Laplacian matrices are asymptotically equivalent with high probability. Then, using the structure of the DGG, we found the the LSD of the RGG normalized Lapalcian matrix converges to the Dirac measure at one in the full range of the connectivity regime. In the thermodynamic regime, we found that the spectrum of the RGG regularized normalized Laplacian matrix can be approximated by the spectrum of the DGG regularized normalized Laplacian matrix with the corresponding error bound. Then, with the regular structure of the DGG, we provided an analytical approximation for the eigenvalues of the RGG regularized normalized Lapalcian matrix.

# Chapter 5

# Spectrum of the Adjacency Matrix of RGGs

## 5.1 Introduction

In this chapter, we investigate spectral properties of the adjacency matrix of RGGs both theoretically and with simulations in the connectivity regime and without normalization by $n$. This contribution is motivated by the work of Bordenave in [74] that characterizes the spectral measure of the RGG adjacency matrix normalized by $n$ in the dense regime. Due to the normalization factor $n$, in the dense regime and as $n \to \infty$, all the finite eigenvalues of the adjacency matrix vanish and only the eigenvalues scaling as $n$ in the adjacency matrix do not vanish in the normalized adjacency matrix. Therefore, in order to analyze the behavior of the finite eigenvalues of the adjacency matrix, in this chapter we investigate the spectrum of adjacency matrices of RGGs without normalization in the connectivity and dense regimes.

Similarly to Chapter 4, we use the adjacency matrix of a DGG as an approximation for the adjacency matrix of an RGG. We provide an upper bound on the Hilbert-Schmidt norm of the difference between the adjacency matrices of the RGG and the DGG. More precisely, under some conditions on the average vertex degree $a_n$, we show that the Hilbert-Schmidt norm of the difference between two sequences of adjacency matrices of RGGs and DGGs converges to zero in probability as $n \to \infty$. Then, for $\epsilon > 0$, using this result, we show that the Levy distance between the eigenvalue distributions of the DGG and RGG adjacency matrices vanishes with high probability as $n \to \infty$ when the average vertex degree, $a_n$ scales as $\Omega(\log^{\epsilon}(n)\sqrt{n})$ for $d = 1$ and as $\Omega(\log^2(n))$ for $d \geq 2$. Then, under the $\ell_\infty$-metric we provide an analytical approximation for the eigenvalues of the adjacency matrix of RGGs by taking the $d$-dimensional discrete Fourier transform (DFT) of an $n = \mathrm{N}^d$ tensor of rank $d$ obtained from the first block row of the adjacency matrix of the DGG.

## 5.2 Mains Results

First, we introduce a property called the minimax grid matching problem useful for the following studies. Consider a square with area $n$ in the plane that contains $n$ grid points arranged in a regularly spaced $\sqrt{n} \times \sqrt{n}$ array and $n$ random points located independently and randomly according to the uniform distribution on the square. For any particular set of $n$ random points, let $\mathrm{M}_n$ denote the minimum length such that there exists a perfect matching of the (random) points to the grid points in the square for which the distance between every pair of matched points is at most $\mathrm{M}_n$. In other words, $\mathrm{M}_n$ is the minimum over all perfect matching of the maximum distance between any pair of matched points. Sharp bounds for $\mathrm{M}_n$ are given in [86], [87], [88]. We repeat them in the following lemma for convenience.

**Lemma 33.** *Under any $\ell_p$-norm, the bottleneck matching is*

- $\mathrm{M}_n = O\left(\left(\frac{\log n}{n}\right)^{1/d}\right)$, *when $d \geq 3$ [86].*
- $\mathrm{M}_n = O\left(\left(\frac{\log^{3/2} n}{n}\right)^{1/2}\right)$, *when $d = 2$ [87].*
- $\mathrm{M}_n = O\left(\sqrt{\frac{\log \epsilon^{-1}}{n}}\right)$, *with prob. $\geq 1 - \epsilon$, $d = 1$ [88].*

Let $\mathbf{A}(\mathcal{X}_n)$ be the adjacency matrix of $G(\mathcal{X}_n, r_n)$, with entries

$$\mathbf{A}(\mathcal{X}_n)_{ij} = \chi[x_i \sim x_j],$$

where the term $\chi[x_i \sim x_j]$ takes the value 1 when there is a connection between nodes $x_i$ and $x_j$ in $G(\mathcal{X}_n, r_n)$ and zero otherwise, represented as

$$\chi[x_i \sim x_j] = \begin{cases} 1, & \|x_i - x_j\|_p \leq r_n, \quad i \neq j, \quad p \in [1, \infty] \\ 0, & \text{otherwise.} \end{cases}$$

A similar definition holds for $\mathbf{A}(\mathcal{D}_n)$ defined over $G(\mathcal{D}_n, r_n)$. The matrices $\mathbf{A}(\mathcal{X}_n)$ and $\mathbf{A}(\mathcal{D}_n)$ are symmetric and their spectrum consists of real eigenvalues. We denote by $\{\lambda_i, i = 1, .., n\}$ and $\{\mu_i, i = 1, .., n\}$ the sets of all real eigenvalues of the real symmetric square matrices $\mathbf{A}(\mathcal{D}_n)$ and $\mathbf{A}(\mathcal{X}_n)$ of order $n$, respectively. The empirical spectral distribution functions $F^{\mathbf{A}(\mathcal{X}_n)}(x)$ and $F^{\mathbf{A}(\mathcal{D}_n)}$ of the adjacency matrices of an RGG and a DGG, respectively, are defined as $F_n(x)$ and $F'_n(x)$, respectively.

In the following, we first derive our result on the weak asymptotic equivalence of the sequences of the adjacency matrices of RGGs and DGGs as $n \to \infty$ in the connectivity regime.

### 5.2.1 Concentration of the RGG Adjacency Matrix

Let $a'_n$ be the degree of the nodes in $G(\mathcal{D}_n, r_n)$. In the following Lemma 34 we provide an upper bound for $a'_n$ under any $\ell_p$-metric.

**Lemma 34.** *For any chosen $\ell_p$-metric with $p \in [1, \infty]$ and $d \geq 1$, we have*

$$a'_n \leq d^{\frac{1}{p}} 2^d a_n \left(1 + \frac{1}{2a_n^{1/d}}\right)^d.$$

*Proof.* Here, we show how to upper bound the vertex degree $a'_n$ under any $\ell_p$-metric, $p \in [1, \infty]$. Assume that $G(\mathcal{X}_n, r_n)$ and $G(\mathcal{D}_n, r_n)$ are formed using the $\ell_\infty$-metric and let $a_n$ and $a'_n$ be their average vertex degree and vertex degree, respectively.

In this case, for a $d$-dimensional DGG with $n = \mathrm{N}^d$ nodes, the vertex degree $a'_n$ is given by [70]

$$a'_n = (2k_n + 1)^d - 1, \quad \text{with} \quad k_n = \lfloor \mathrm{N} r_n \rfloor \quad \text{and} \quad n = \mathrm{N}^d.$$

Therefore, for $\theta^{(d)} \geq 2$ and $d \geq 1$, we have

$$\begin{aligned} a'_n = (2k_n + 1)^d - 1 &\leq \frac{2^d a_n}{\theta^{(d)}} \left(1 + \frac{1}{2n^{1/d} r_n}\right)^d \\ &\leq 2^d a_n \left(1 + \frac{1}{2a_n^{1/d}}\right)^d. \end{aligned}$$

Now, let $b'_n$ and $b_n$ be the vertex degree and the average vertex degree in $G(\mathcal{D}_n, r_n)$ and $G(\mathcal{X}_n, r_n)$, respectively when using any $\ell_p$-metric, $p \in [1, \infty]$. Notice that for any $p \in [1, \infty]$, we have

$$\|x\|_\infty \leq \|x\|_p.$$

Then, the number of nodes $a'_n$ that falls in the ball of radius $r_n$ is greater or equal than $b'_n$, i.e., $a'_n \geq b'_n$. Hence,

$$\begin{aligned} b'_n \leq a'_n &\leq 2^d a_n \left(1 + \frac{1}{2n^{1/d} r_n}\right)^d \\ &= \frac{d^{1/p} 2^d a_n}{d^{1/p}} \left(1 + \frac{1}{2n^{1/d} r_n}\right)^d. \end{aligned}$$

It remains to show the relation between $b'_n$ and $b_n$.

Assume that the RGG is formed by connecting each two nodes when $d^{1/p}\|x_i - x_j\|_\infty \leq r_n$. This simply means that the graph is obtained using the $\ell_\infty$-metric with a radius equal to $\frac{r_n}{d^{1/p}}$. Then, the average vertex degree of this graph is $\frac{a_n}{d^{1/p}}$. In addition, we have

$$\|x\|_p \leq d^{\frac{1}{p}} \|x\|_\infty.$$

Therefore, we have the inequality

$$b'_n \leq d^{1/p} 2^d b_n \left(1 + \frac{1}{2n^{1/d} r_n}\right)^d,$$

and Lemma 34 follows. □

To prove our result on the concentration of the $\mathbf{A}(\mathcal{X}_n)$ of RGGs and investigate its relationship with $\mathbf{A}(\mathcal{D}_n)$ under any $\ell_p$-metric, we use the Hilbert-Schmidt norm of the difference between two matrices.

Let $\mathrm{M}_n$ be the minimum bottleneck matching distance defined in Lemma 33. Under the condition $\mathrm{M}_n = o(r_n)$, we provide an upper bound for the Hilbert-Schmidt norm of the difference between the adjacency matrices $\mathbf{A}(\mathcal{X}_n)$ and $\mathbf{A}(\mathcal{D}_n)$ in the following lemma.

**Lemma 35.** *For $d \geq 1$, $p \in [1, \infty]$ and $\mathrm{M}_n = o(r_n)$, the Hilbert-Schmidt norm of the difference between $\mathbf{A}(\mathcal{X}_n)$ and $\mathbf{A}(\mathcal{D}_n)$ is upper bounded as*

$$\begin{aligned} \|\mathbf{A}(\mathcal{X}_n) - \mathbf{A}(\mathcal{D}_n)\|^2_{\mathrm{HS}} &\leq d^{\frac{1}{p}} 2^{d+1} \left| \frac{1}{n} \sum_i \mathbf{N}(x_i) - a_n \right| \\ &+ d^{\frac{1}{p}} 2^{d+1} \left| a_n - \frac{2}{n} \sum_i \mathrm{L}_i \right| + a'_n, \end{aligned} \tag{5.1}$$

*where, $\mathbf{N}(x_i)$ denotes the degree of $x_i$ in $G(\mathcal{X}_n, r_n)$ and $\mathrm{L}_i \sim \mathrm{Bin}\left(n, \theta^{(d)}\left(r_n - 2\mathrm{M}_n\right)\right)$.*

*Proof.* Define $\mathbf{N}(x_i, x'_i) = \sum_j \chi[x_i \sim x_j]\chi[x'_i \sim x'_j]$ and let $\mathbf{N}(x_i) = \sum_j \chi[x_i \sim x_j]$ and $a'_n = \sum_j \chi[x'_i \sim x'_j]$. Then, by a straightforward application of Lemma 6, we have

$$\begin{aligned} \|\mathbf{A}(\mathcal{X}_n) - \mathbf{A}(\mathcal{D}_n)\|^2_{\mathrm{HS}} &= \frac{1}{n} \mathrm{Trace}\left[(\mathbf{A}(\mathcal{X}_n) - \mathbf{A}(\mathcal{D}_n)\right]^2 \\ &= \frac{1}{n} \sum_i \sum_j \left[\chi[x_i \sim x_j] - \chi[x'_i \sim x'_j]\right]^2 \\ &= \frac{1}{n} \sum_i \mathbf{N}(x_i) + a'_n - \frac{2}{n} \sum_i \mathbf{N}(x_i, x'_i). \end{aligned}$$

We notice that when $\|x_i - x_j\|_p \leq r_n - 2\mathrm{M}_n$, then $\|x'_i - x'_j\|_p \leq r_n$. So, all points within a radius of $r_n - 2\mathrm{M}_n$ of $x_i$ map to the neighbors of $x'_i$ [77]. Thus, $\mathbf{N}(x_i, x'_i)$ is stochastically greater than the random variable $\mathrm{L}_i \sim \mathrm{Bin}(n, \theta^{(d)}(r_n - 2\mathrm{M}_n))$. Hence,

$$\begin{aligned}\|\mathbf{A}(\mathcal{X}_n) - \mathbf{A}(\mathcal{D}_n)\|_{\text{HS}}^2 &\leq \frac{1}{n}\sum_i \mathbf{N}(x_i) + a'_n - \frac{2}{n}\sum_i \mathrm{L}_i \\ &\leq \left|\frac{1}{n}\sum_i \mathbf{N}(x_i) - \frac{2}{n}\sum_i \mathrm{L}_i\right| + a'_n \\ &\leq d^{\frac{1}{p}} 2^{d+1} \left|\frac{1}{n}\sum_i \mathbf{N}(x_i) - \frac{2}{n}\sum_i \mathrm{L}_i\right| + a'_n.\end{aligned}$$

□

The condition enforced on $r_n$, i.e., $\mathrm{M}_n = o(r_n)$ implies that for $\epsilon > 0$, (5.1) holds when $a_n$ scales as $\Omega(\log^{\epsilon}(n)\sqrt{n})$ for $d = 1$, as $\Omega(\log^{\frac{3}{2}+\epsilon}(n))$ for $d = 2$ and as $\Omega(\log^{1+\epsilon}(n))$ for $d \geq 3$.

Notice that the term $\sum_i \mathbf{N}(x_i)/2$ in Lemma 35 counts the number of edges in $G(\mathcal{X}_n, r_n)$. For convenience, we denote $\sum_i \mathbf{N}(x_i)/2$ as $\xi_n$. To show our main result, we apply the Chebyshev inequality given in Lemma 8 on the random variable $\xi_n$. For that, we need to determine $\mathrm{Var}(\xi_n)$.

**Lemma 36.** *When $x_1, ..., x_n$ are i.i.d. uniformly distributed in the d-dimensional unit torus $\mathbb{T}^d = [0, 1]$*

$$\mathrm{Var}\left(\xi_n\right) \leq [\theta^{(d)} + 2\theta^{(d)} a_n].$$

*Proof.* The proof follows along the same lines of Proposition A.1 in [89] when extended to a unit torus and applied to i.i.d. and uniformly distributed nodes. □

We can now state the main theorem on the concentration of the Hilbert-Schmidt norm of the difference between the adjacency matrices of RGGs and DGGs.

**Theorem 37.** *For $d \geq 1$, $p \in [1, \infty]$, $a \geq 1$, $\mathrm{M}_n = o(r_n)$ and $t > 0$, we have*

$$\mathbb{P}\{\|\mathbf{A}(\mathcal{X}_n) - \mathbf{A}(\mathcal{D}_n)\|_{\text{HS}}^2 > t\} \leq 2n \exp\left(\frac{-a_n\varepsilon^2}{3}\left(1 - \frac{2\mathrm{M}_n}{r_n}\right)\right)$$

$$+ \frac{n\left[\theta^{(d)}(r_n - 2\mathrm{M}_n)(a-1) + 1\right]^n}{a^{\left(\frac{t}{d^{\frac{1}{p}}2^{d+3}} + \frac{a_n(2-c)}{4}\right)}} + \frac{d^{\frac{2}{p}} 2^{2d+6}\left[\theta^{(d)} + 2\theta^{(d)} a_n\right]}{n^2 t^2},$$

*where* $\varepsilon = \left(\frac{t}{d^{\frac{1}{p}} 2^{d+2} a_n} + \frac{(2-c)}{4} - \frac{2\mathrm{M}_n}{r_n}\right)$ *and* $c = \left(1 + \frac{1}{2a_n^{1/d}}\right)^d$.

*In particular, for every $t > 0$, $a \geq 2$, $\epsilon > 0$ and $a_n$ that scales as $\Omega(\log^{\epsilon}(n)\sqrt{n})$ when $d = 1$, as $\Omega(\log^2(n))$ when $d \geq 2$, we have*

$$\lim_{n\to\infty} \mathbb{P}\left\{\|\mathbf{A}(\mathcal{X}_n) - \mathbf{A}(\mathcal{D}_n)\|_{\mathrm{HS}}^2 > t\right\} = 0.$$

*Proof.* We upper bound the probability that the Hilbert-Schmidt norm of the difference between $\mathbf{A}(\mathcal{X}_n)$ and $\mathbf{A}(\mathcal{D}_n)$ is higher than $t > 0$.

$$\mathbb{P}\left\{\|\mathbf{A}(\mathcal{X}_n) - \mathbf{A}(\mathcal{D}_n)\|_{\mathrm{HS}}^2 > t\right\} \leq \mathbb{P}\left\{ d^{\frac{1}{p}} 2^{d+1} \left| \frac{\sum_i \mathbf{N}(x_i)}{n} - a_n \right| + d^{\frac{1}{p}} 2^{d+1} \left| a_n - \frac{2\sum_i \mathrm{L}_i}{n} \right| + a'_n > t \right\}$$
$$\leq \mathbb{P}\left\{ \left| \sum_i \mathbf{N}(x_i) - n a_n \right| > \frac{nt}{d^{\frac{1}{p}} 2^{d+2}} \right\} + \mathbb{P}\left\{ \left| n a_n - 2\sum_i \mathrm{L}_i \right| > \frac{nt}{d^{\frac{1}{p}} 2^{d+2}} - \frac{n a'_n}{d^{\frac{1}{p}} 2^{d+1}} \right\}.$$

Let

$$\mathrm{A} = \mathbb{P}\left\{ \left| \sum_i \mathbf{N}(x_i) - n a_n \right| > \frac{nt}{d^{\frac{1}{p}} 2^{d+2}} \right\},$$

and

$$\mathrm{B} = \mathbb{P}\Big\{ \Big| n a_n - 2\sum_i \mathrm{L}_i \Big| > \frac{nt}{d^{\frac{1}{p}} 2^{d+2}} - \frac{n a'_n}{d^{\frac{1}{p}} 2^{d+1}} \Big\}.$$

We first upper bound the term A using Lemma 8 and 36.

$$\mathrm{A} = \mathbb{P}\left\{ \left| \sum_i \mathbf{N}(x_i) - n a_n \right| > \frac{nt}{d^{\frac{1}{p}} 2^{d+2}} \right\} = \mathbb{P}\left\{ |\xi_n - \mathbb{E}[\xi_n]| > \frac{nt}{d^{\frac{1}{p}} 2^{d+3}} \right\}$$
$$\leq \frac{d^{\frac{2}{p}} 2^{2d+6} \mathrm{Var}(\xi_n)}{n^2 t^2} \leq \frac{d^{\frac{2}{p}} 2^{2d+6} \left[\theta^{(d)} + 2\theta^{(d)} a_n\right]}{n^2 t^2}.$$

Next, we upper bound B.

$$\mathrm{B} = \mathbb{P}\left\{ \left| n a_n - 2\sum_i \mathrm{L}_i \right| > \frac{nt}{d^{\frac{1}{p}} 2^{d+2}} - \frac{n a'_n}{d^{\frac{1}{p}} 2^{d+1}} \right\} \leq n\mathbb{P}\left\{ a_n - 2\mathrm{L}_i > \frac{t}{d^{\frac{1}{p}} 2^{d+2}} - \frac{a'_n}{d^{\frac{1}{p}} 2^{d+1}} \right\}$$
$$+ n\mathbb{P}\left\{ 2\mathrm{L}_i - a_n > \frac{t}{d^{\frac{1}{p}} 2^{d+2}} - \frac{a'_n}{d^{\frac{1}{p}} 2^{d+1}} \right\}$$
$$\leq n\mathbb{P}\left\{ |a_n - \mathrm{L}_i| > \frac{t}{d^{\frac{1}{p}} 2^{d+3}} - \frac{a'_n}{d^{\frac{1}{p}} 2^{d+2}} + \frac{a_n}{2} \right\} + n\mathbb{P}\left\{ \mathrm{L}_i > \frac{t}{d^{\frac{1}{p}} 2^{d+3}} - \frac{a'_n}{d^{\frac{1}{p}} 2^{d+2}} + \frac{a_n}{2} \right\}$$
$$\overset{(a)}{\leq} n\mathbb{P}\left\{ |a_n - \mathrm{L}_i| > \frac{t}{d^{\frac{1}{p}} 2^{d+3}} + \frac{a_n(2-c)}{4} \right\} + n\mathbb{P}\left\{ \mathrm{L}_i > \frac{t}{d^{\frac{1}{p}} 2^{d+3}} + \frac{a_n(2-c)}{4} \right\}.$$

Step (a) follows by applying Lemma 34 and $c = \left(1 + \frac{1}{2a_n^{1/d}}\right)^d$. Then,

$$\begin{aligned}
\mathrm{B} &\leq n\mathbb{P}\left\{|\mathbb{E}[\mathrm{L}_i] - \mathrm{L}_i| > \frac{t}{d^{\frac{1}{p}}2^{d+3}} + \frac{a_n(2-c)}{4} - 2\theta^{(d)}n\mathrm{M}_n\right\} \\
&\quad + n\mathbb{P}\left\{\mathrm{L}_i > \frac{t}{d^{\frac{1}{p}}2^{d+3}} + \frac{a_n(2-c)}{4}\right\} \\
&\leq n\mathbb{P}\left\{|\mathbb{E}[\mathrm{L}_i] - \mathrm{L}_i| > a_n\varepsilon\right\} \\
&\quad + n\mathbb{P}\left\{\mathrm{L}_i > \frac{t}{d^{\frac{1}{p}}2^{d+3}} + \frac{a_n(2-c)}{4}\right\},
\end{aligned}$$

where

$$\varepsilon = \left(\frac{t}{d^{\frac{1}{p}}2^{d+2}a_n} + \frac{(2-c)}{4} - \frac{2\mathrm{M}_n}{r_n}\right).$$

We continue by letting

$$\mathrm{B}_1 = \mathbb{P}\left\{|\mathbb{E}[\mathrm{L}_i] - \mathrm{L}_i| > a_n\varepsilon\right\}.$$

$$\mathrm{B}_2 = \mathbb{P}\left\{\mathrm{L}_i > \frac{t}{d^{\frac{1}{p}}2^{d+3}} + \frac{a_n(2-c)}{4}\right\}.$$

For $n$ sufficiently large and consequently $a_n$ sufficiently large, we have $1 \leq c < 2$ and $0 < \varepsilon \leq \frac{3}{2}$. Therefore, by applying Lemma 13, we upper bound $\mathrm{B}_1$ as

$$\begin{aligned}
&\mathbb{P}\left\{|\mathbb{E}[\mathrm{L}_i] - \mathrm{L}_i| > a_n\varepsilon\right\} \\
&\leq \mathbb{P}\left\{|\mathbb{E}[\mathrm{L}_i] - \mathrm{L}_i| > (a_n - 2n\theta^{(d)}\mathrm{M}_n)\varepsilon\right\} \\
&\leq 2\exp\left(\frac{-\varepsilon^2}{3}\left(a_n - 2n\theta^{(d)}\mathrm{M}_n\right)\right).
\end{aligned}$$

The last term $\mathrm{B}_1$ is upper bounded by using the Chernoff bound in Lemma 14.

The probability generating function of the binomial random variable $\mathrm{L}_i$ is given by

$$\left[a\theta^{(d)}(r_n - 2\mathrm{M}_n) + 1 - \theta^{(d)}(r_n - 2\mathrm{M}_n)\right]^n.$$

Therefore, for $n$ sufficiently large, $1 \leq c < 2$ and $a \geq 1$, we have

$$\mathrm{B}_2 \leq \frac{\left[\theta^{(d)}(r_n - 2\mathrm{M}_n)(a-1) + 1\right]^n}{a^{\left(\frac{t}{d^{\frac{1}{p}}2^{d+3}} + \frac{a_n(2-c)}{4}\right)}}.$$

Finally, taking the upper bounds of A and B obtained from the upper bounds of $B_1$ and $B_2$ all together, Theorem 37 follows. □

This result shows the convergence in probability of the Hilbert-Schmidt norm of the difference between sequences of adjacency matrices of DGGs and RGGs by a straightforward application of Lemma 13 and 14 on the random variable $L_i$, then by applying Lemma 8 and 36 to $\xi_n$. Let us observe that the strong norms of adjacency matrices of DGGs and RGGs are not uniformly bounded and then the convergence of the Hilbert-Schmidt norm is not sufficient to prove the asymptotic equivalence of the sequences of adjacency matrices of DGGs and RGGs.

Therefore, for adjacency matrices, we consider a weaker form of convergence in probability in terms of the Levy distance introduced in Definition 20 between the eigenvalue distributions of the adjacency matrices of DGGs and RGGs as implied by the following inequality

$$\begin{aligned}\mathbb{P}\left(L^3(F^{\mathbf{A}(\mathcal{X}_n)}, F^{\mathbf{A}(\mathcal{D}_n)}) > t\right) &\leq \mathbb{P}\left(\frac{1}{n}\sum_{i}^{n}|\lambda_i - \mu_i|^2 > \epsilon\right) \\ &\leq \mathbb{P}\left(\|\mathbf{A}(\mathcal{X}_n) - \mathbf{A}(\mathcal{D}_n)\|_{\mathrm{HS}}^2 > \epsilon\right). \end{aligned} \tag{5.2}$$

In the limit, as $n \to \infty$, (5.2) goes to zero.

### 5.2.2 Eigenvalues of the Adjacency Matrix

In what follows, we provide the eigenvalues of $\mathbf{A}(\mathcal{D}_n)$ which approximates the eigenvalues of $\mathbf{A}(\mathcal{X}_n)$ for $n$ sufficiently large.

**Lemma 38.** *For $d \geq 1$ and using the $\ell_\infty$-metric, the eigenvalues of $\mathbf{A}(\mathcal{D}_n)$ are given by*

$$\lambda_{m_1,\ldots,m_d} = \prod_{s=1}^{d} \frac{\sin(\frac{m_s\pi}{\mathrm{N}}(a_n'+1)^{1/d})}{\sin(\frac{m_s\pi}{\mathrm{N}})} - 1, \tag{5.3}$$

*where, $m_1, ..., m_d \in \{0, ...\mathrm{N}-1\}$, $a_n' = (2k_n+1)^d - 1, k_n = \lfloor \mathrm{N}r_n \rfloor$ and $n = \mathrm{N}^d$. The term $\lfloor x \rfloor$ is the integer part, i.e., the greatest integer less than or equal to $x$.*

*Proof.* See Appendix A.4. □

The proof utilizes the result in [70] which shows that the eigenvalues of the adjacency matrix of a DGG in $\mathbb{T}^d$ are found by taking the $d$-dimensional DFT of an $\mathrm{N}^d$ tensor of rank $d$ obtained from the first block row of $\mathbf{A}(\mathcal{D}_n)$.

For $\epsilon > 0$, Theorem 37 shows that when $a_n$ scales as $\Omega(\log^{\epsilon}(n)\sqrt{n})$ for $d = 1$ and as $\Omega(\log^2(n))$ when $d \geq 2$, the LSD of the adjacency matrix of an RGG concentrate around

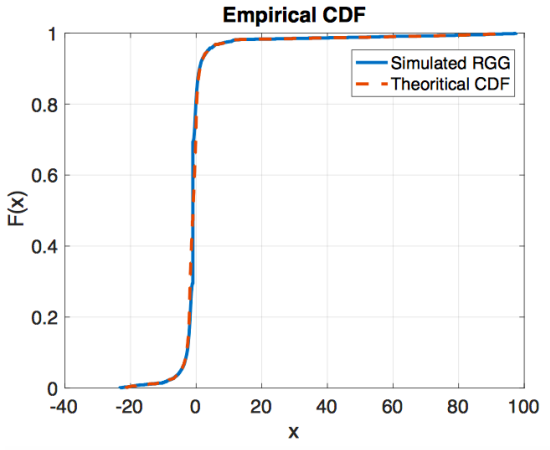


Figure 5.1: An illustration of the cumulative distribution function of the eigenvalues of the RGG adjacency matrix.

the LSD of the adjacency matrix of a DGG as $n \to \infty$. Therefore, for $n$ sufficiently large, the eigenvalues of the DGG given in (5.3) approximate very well the eigenvalues of the adjacency matrix of the RGG.

## 5.3 Numerical Results

We present simulations to validate the results obtained on the eigenvalues of the adjacency matrix of the RGG. More specifically, we corroborate the theoretical results on the spectrum of the adjacency matrix of RGGs in the connectivity regime by comparing the simulated and the analytical results.

Fig. 5.1 shows the cumulative distribution functions of the eigenvalues of the adjacency matrix of an RGG realization with $r_n = \frac{\log(n)}{\sqrt{n}}$ and $n = 2000$ vertices and the analytical spectral distribution in the connectivity regime. We notice that for the chosen average vertex degree $a_n = \log(n)\sqrt{n}$ and $d = 1$, the curves corresponding to the eigenvalues of the RGG and the DGG fit very well for a large value of $n$.

## 5.4 Conclusions

In this chapter, we studied the eigenvalues distribution of the adjacency matrix of RGGs in the connectivity regime. Under some conditions on the average vertex degree $a_n$, we showed that the LSDs of the adjacency matrices of an RGG and a DGG converge to the same limit as $n \to \infty$ in a weaker form of convergence in probability in terms of the Levy distance. Then, based on the regular structure of the DGG, we approximated the eigenvalues of $\mathbf{A}(\mathcal{X}_n)$ by the eigenvalues of $\mathbf{A}(\mathcal{D}_n)$ by taking the $d$-dimensional DFT of an $\mathrm{N}^d$ tensor of rank $d$ obtained from the first block row of $\mathbf{A}(\mathcal{D}_n)$.

# Chapter 6

# Spectral Dimension of RGGs

## 6.1 Introduction

The study of dynamical processes on complex networks is a diverse topic. One of the important dynamical processes identified by researchers is the process of diffusion on random geometric structures. It corresponds to the spread in time and space of a particular phenomenum. This concept is widely used and find application in a wide range of different areas of physics. For example, in percolation theory, the percolation clusters provide fluctuating geometries [90]. Additional applications are the spread of epidemics [91] and the spread of information on social networks [92], which are often modeled by random geometries.

In 1982, the spectral dimension (SD) is introduced for the first time to characterize the low-frequency vibration spectrum of geometric objects [84] and then has been widely used in quantum gravity [93]. We recall that in a graph in which a particle moves randomly along edges from a vertex to another vertex in discrete steps, the diffusion process can be thought as a stochastic RW. Then, the SD $d_s$ is defined in terms of the return probability $\mathrm{P}(t)$ of the diffusion [83]

$$d_s = -2\frac{\mathrm{d}\ln \mathrm{P}(t)}{\mathrm{d}\ln(t)}.$$

In many applications, an estimator of the SD can serve as an estimator of the intrinsic dimension of the underlying geometric space [94]. In the fields of pattern recognition and machine learning [95], the intrinsic dimension of a data set can be thought of as the number of variables needed in a minimal representation of the data. Similarly, in signal processing of multidimensional signals, the intrinsic dimension of the signal describes how many variables are needed to generate a good approximation of the signal. Therefore, an estimator of the SD of RGGs is relevant and can be used for the estimation of the intrinsic dimension in applications in which a complex network takes into account the proximity between nodes.

In this chapter, we provide an analytical expression for the spectral dimension of RGGs in the thermodynamic regime.

## 6.2 Main Results

The main purpose of this chapter is the study of the return-to-origin probability of RWs and SD on RGGs in the thermodynamic regime. In Chapter 4, we developed techniques for analyzing the LSD of the regularized normalized Laplacian of RGGs in the thermodynamic regime. In particular, we showed that the spectrum of the regularized normalized Laplacian of an RGG can be approximated by the spectrum of the regularized normalized Laplacian of a DGG with nodes in a grid. Then, we provided an analytical approximation for the normalized Laplacian eigenvalues of the RGG in the thermodynamic regime. In this chapter, we use this eigenvalues approximation to find the SD of RGGs in the thermodynamic regime. In particular, we use the eigenvalues in the neighborhood of $\lambda_1 = 0$ to find the spectral dimension $d_s$ of RGGs in the thermodynamic regime.

Recall that when the Laplacian spectral density follows a power-law tail, the spectral dimension $d_s$ can be described according to the asymptotic behavior of the normalized Laplacian operator spectral density

$$\frac{d_s}{2} = \lim_{\lambda \to 0} \frac{\log(F(\lambda))}{\log(\lambda)}, \tag{6.1}$$

with $F(\lambda)$ being the empirical spectral distribution function of the normalized Laplacian.

As shown in Chapter 3, the long time limit of the return probability $\mathrm{P}_0(t)$ or equivalently the SD is related to the normalized Laplacian ED in the neighborhood of $\lambda_1$. Therefore, to find the spectral dimension of RGGs in the thermodynamic regime, we need to analyze the behavior of the ED of the regularized normalized Laplacian of RGGs in a neighborhood of $\lambda_1$.

Recall that the eigenvalues of the regularized normalized Laplacian of DGGs in the thermodynamic regime are approximated in the limit as

$$\lambda(w) = \lambda_{w_1,\ldots,w_d} \approx 1 - \frac{1}{(\gamma' + \alpha)} \prod_{s=1}^{d} \frac{\sin(\pi w_s^{1/d}(\gamma' + 1)^{1/d})}{\sin(\pi w_s^{1/d})} + \frac{1 - \alpha \delta_{w_1,\ldots,w_d}}{(\gamma' + \alpha)}. \tag{6.2}$$

We have that he smallest eigenvalue $\lambda_1$ of the normalized Laplacian is always equal to zero, hence, $0 = \lambda_1 \leq \lambda_2 \leq \ldots \leq \lambda_n \leq 2$. The second smallest eigenvalue $\lambda_2$ is called the Fidler eigenvalue. In the following, we show that the the Fidler eigenvalue, $\lambda_2$ of the regularized normalized Laplacian of RGGs goes to zero for large networks, i.e., $\lambda_2 \to 0$ as $n \to \infty$.

**Lemma 39.** *The Fidler eigenvalue $\lambda_2$ of RGGs in the thermodynamic regime is approximated as*

$$\lambda_2 \approx \frac{1}{(\gamma'+\alpha)} + 1 - (1+\gamma')^{\frac{d-1}{d}} \frac{\sin(\frac{\pi}{\mathrm{N}}(\gamma'+1)^{1/d})}{(\gamma'+\alpha)\sin(\frac{\pi}{\mathrm{N}})}, \tag{6.3}$$

*where $n = \mathrm{N}^d$ and $\gamma' = (2\lfloor \gamma^{1/d} \rfloor + 1)^d - 1$. In particular, as $n \to \infty$, $\lambda_2 \to 0$.*

*Proof.* In general, the eigenvalues in (4.4) are unordered, but it is obvious that the smallest eigenvalue is $\lambda_{0\ldots0}$ and the next smallest one is $\lambda_{1,0\ldots0} = \ldots = \lambda_{0\ldots0,1}$. Therefore, for $n = \mathrm{N}^d$, we have

$$\begin{aligned}
\lambda_2 &= \lambda_{1,0\ldots0} \\
&\approx \lim_{m_s \to 0} \left( 1 - \frac{1}{(\gamma'+\alpha)} \frac{\sin(\frac{\pi}{\mathrm{N}}(\gamma'+1)^{1/d})}{\sin(\frac{\pi}{\mathrm{N}})} \prod_{s=2}^{d} \frac{\sin(\frac{m_s\pi}{\mathrm{N}}(\gamma'+1)^{1/d})}{\sin(\frac{m_s\pi}{\mathrm{N}})} + \frac{1}{(\gamma'+\alpha)} \right) \qquad (6.4) \\
&= 1 + \frac{1}{(\gamma'+\alpha)} - (1+\gamma')^{\frac{d-1}{d}} \frac{\sin(\frac{\pi}{\mathrm{N}}(\gamma'+1)^{1/d})}{(\gamma'+\alpha)\sin(\frac{\pi}{\mathrm{N}})}. \qquad (6.5)
\end{aligned}$$

In large RGGs, i.e., $n \to \infty$, we get

$$\begin{aligned}
\lim_{n\to\infty} \lambda_2 &\approx \lim_{n\to\infty} \left[ 1 + \frac{1}{(\gamma'+\alpha)} - (1+\gamma')^{\frac{d-1}{d}} \frac{\sin(\frac{\pi}{\mathrm{N}}(\gamma'+1)^{1/d})}{(\gamma'+\alpha)\sin(\frac{\pi}{\mathrm{N}})} \right] \\
&= 1 + \frac{1}{(\gamma'+\alpha)} - 1 - \frac{1}{(\gamma'+\alpha)} = 0.
\end{aligned}$$

□

This lemma shows that the spectral gap of the regularized normalized Laplacian in the thermodynamic regime closes as $n \to \infty$.

From Figure 6.1(a), we can notice that the eigenvalues of the DGG show a symmetry and the smallest ones are reached for small values of $w$. Additionally, for small and decreasing values of $w$, the eigenvalues of the regularized normalized Laplacian of DGGs decrease. Therefore, in the following, we show that the empirical distribution of the eigenvalues in a neighborhood of $\lambda_1$, or equivalently, the eigenvalues for small values of $w$ of the regularized normalized Laplacian of DGGs follow a power-law asymptotics.

The eigenvalues of the regularized normalized Laplacian of RGGs in a neighborhood of $\lambda_1$ are then approximated by

$$\lambda(w) \approx 1 - \frac{1}{(\gamma'+\alpha)} \left[ \frac{\sin(\pi w^{1/d}(\gamma'+1)^{1/d})}{\sin(\pi w^{1/d})} \right]^d + \frac{1-\alpha\delta_w}{(\gamma'+\alpha)},$$

for $w \to 0$.

The limiting distribution $F^{\mathcal{L}(\mathcal{D})}(x) = \lim_{n\to\infty} F^{\mathcal{L}(\mathcal{D}_n)}(x)$ exists and is given by

$$F^{\mathcal{L}(\mathcal{X})}(x) = \int_0^1 \mathbf{1}_{(-\infty,x]}\left(\lambda(w)\right) dw = \int_{\lambda(w)\leq x} dw, \tag{6.6}$$

where $\mathbf{1}_S(t)$ is the characteristic function on a set $S$ defined as

$$\mathbf{1}_S(t) = \begin{cases} 1 & \text{if } \ t \in S, \\ 0 & \text{if } \ t \notin S. \end{cases}$$

The quantity $\int_{\lambda(w)\leq x} dw$ is the measure of the set of all $w$ such that $\lambda(w) \leq x$. Therefore, to compute (6.6), we only need to find the location of the points $w$ for which $\lambda(w) \leq x$ by solving $\lambda(w) = x$. However, The expression of $\lambda(w)$ includes the Chebyshev polynomials of the 2nd kind. In general there is no closed-form solution for $w$ for this polynomial function. To find the spectral dimension, only small eigenvalues are of interest. Therefore, for $\gamma'$ finite, we use Taylor series expansion of degree 2 around zero, which is given by

$$\lambda(w) \approx \frac{\pi^2}{6(\gamma' + \alpha)} w^{2/d} (\gamma' + 1)^{\frac{d+2}{d}}.$$

Figure 6.1(b) validates this approximation and shows that it provides an accurate approximation. Hence, to compute (6.6), we only need to find the location of the points $w$ for which $\lambda(w) \leq x$, by solving the new equation

$$\lambda(w) = x \iff \frac{\pi^2}{6(\gamma' + \alpha)} w^{2/d} (\gamma' + 1)^{\frac{d+2}{d}} = x.$$

By solving with respect to $x$, we obtain

$$w = \frac{6^{d/2}(\gamma' + \alpha)^{\frac{d}{2}}}{\pi^d (1 + \gamma')^{(2+d)/2}} x^{d/2}.$$

Thus, the LSD of the normalized Laplacian of the RGG, $F^{\mathcal{L}(\mathcal{X}_n)}(x)$ for small $x$ is approximated by

$$F^{\mathcal{L}(\mathcal{X}_n)}(x) \approx \frac{6^{d/2}(1 + \gamma' + 1)^{-\frac{2+d}{2}}}{\pi^d} x^{d/2}. \tag{6.7}$$

From (6.7), it is apparent that the empirical distribution of the eigenvalues, $F^{\mathcal{L}(\mathcal{D}_n)}(x)$ of the regularized normalized Laplacian of a DGG in a neighborhood of $\lambda_1$ follows a power-law tail asymptotics.

Therefore, combining (6.1) and (6.7), we get the spectral dimension $d_s$ of RGGs in the thermodynamic regime as

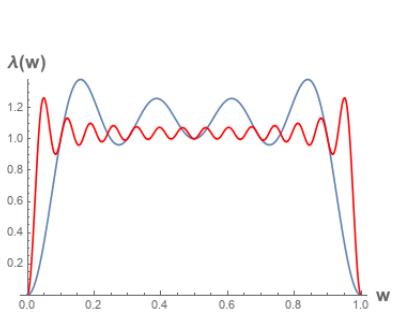


(a) Eigenvalues of the DGG for $\gamma = 8$ (blue line) and $\gamma = 28$ (red line), $d = 1$.

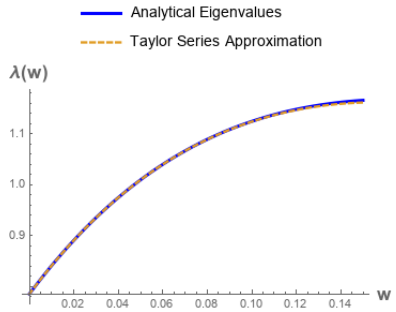


(b) Comparison between the Analytical eigenvalues (blue) and its Taylor series approximation of degree 2 around zero (dashed orange) for $\gamma = 12$, $\alpha = 0.1$, $d = 2$.

Figure 6.1: Eigenvalues of the DGG.

$$
\begin{aligned}
d_s &\approx \lim_{x \to 0} \frac{2 \log \left( F^{\mathcal{L}(\mathcal{X}_n)}(x) \right)}{\log (x)} \\
&= \lim_{x \to 0} \frac{2 \log \left( \dfrac{6^{d/2} (\gamma' + \alpha)^{\frac{d}{2}}}{\pi^d (1 + \gamma')^{(2+d)/2}} x^{d/2} \right)}{\log (x)} \\
&= d.
\end{aligned}
$$

This result generalizes the existing work on the standard lattice in which it has already been shown that its spectral dimension, $d_s$, and its Euclidean dimension coincide. In this work, we show that the spectral dimension in DGGs with nodes in a grid is equal to the space dimension $d$ and is an approximation for the spectral dimension of the RGG in the thermodynamic regime. Thus, by taking a vertex degree in the DGG corresponding to the standard lattice, we retrieve the result for the lattice.

## 6.3 Conclusions

This chapter investigates the spectral dimension of RGGs in the thermodynamic regime. The notion of spectral dimension could serve as an estimator of the intrinsic dimension of the underlying geometric space in many problems. The intrinsic dimension in RGGs is a technique that might be used to cope with high dimensionality data of networks modeled as RGGs. The spectral dimension can be described according to the LSD of the normalized Laplacian in a neighborhood of zero. Therefore, in this chapter we provided an analytical approximation for the eigenvalues of an RGG regularized normalized Laplacian

in a neighborhood of zero. Then, using Taylor series expansion around zero, we approximate the empirical distribution of low-eigenvalues which is useful for the derivation of the spectral dimension in thermodynamic regime. The study shows that the spectral dimension $d_s$ for RGGs is approximated by the Euclidean dimension $d$ in the thermodynamic regime.

# Chapter 7

# Conclusions and Perspectives

In this Ph.D. manuscript, we tackled the problem of spectral analysis of random geometric graphs in different regimes using techniques from random matrix theory and probability theory. In this chapter, we summarize the main contributions of this thesis and discuss some possible extensions.

## 7.1 Summary of Contributions

As mentioned in Chapter 1, one possible way of describing a complex system is to consider the system as a graph consisting of a set of vertices connected by links. In this case, the graph may be represented by several matrices, such as adjacency or Laplacian matrices. Then, the set of eigenvalues of one of these matrices is known as the network's spectrum and is utilized as a tool to understand topological and dynamical characteristics of a network.

This thesis focuses on the theoretical understanding of the spectrum of large RGGs in different regimes. The spectrum analysis of different matrices on RGGs allows us to provide improvements over the existing results. We tackled this problem by benefiting from a concentration phenomena in large size graphs in the connectivity and dense regime.

More precisely, in Chapter 4, we analyzed the spectrum of the regularized normalized Laplacian of RGGs in different regimes. First, we proposed an approximation for the RGG regularized normalized Laplacian matrix and obtained a bound on the probability that the Hilbert-Schmidt norm of the difference between the approximation and the actual matrix is greater than a certain threshold in both connectivity and thermodynamic regime. In particular, in the connectivity regime, we proved that the normalized Laplacian matrices of the RGG and the DGG are asymptotically equivalent with high probability. In the thermodynamic regime, we approximated the spectrum of the RGG regularized normalized Laplacian with the DGG regularized normalized Laplacian matrix, and we provided an upper bound for the approximation error. Therefore, we used the deterministic structure of the DGG to provide an analytical closed form approximation for the eigenvalues

of the RGG in both the connectivity and thermodynamic regime. In particular, In the connectivity regime, when $n \to \infty$, we showed that the LSD of the normalized Laplacian matrix of RGGs converges with high probability to the Dirac distribution at one in the full range of the connectivity regime.

In Chapter 5, we studied the spectrum of the adjacency matrix of RGGs in the connectivity regime. Under some conditions on the average vertex degree $a_n$, and using Hilbert-Schmidt norm, we showed that the Levy distance of the eigenvalue distributions of the adjacency matrix of RGGs and DGGs vanishes with high probability as $n \to \infty$. Then, for $n$ finite, based on the regular structure of the DGG, we approximated the eigenvalues of the adjacency matrix of the RGG by the ones of the DGG by taking the $d$-dimensional DFT of an $\mathrm{N}^d$ tensor of rank $d$ obtained from the first block row of $\mathbf{A}(\mathcal{D}_n)$.

Finally, due to the link between dynamical processes such as diffusion and the normalized Laplacian matrix, we apply the analysis in Chapter 4 to understand how the return probability distribution and spectral dimension of an RGG is affected by the RGG normalized Laplacian spectrum. More precisely, we investigated the spectral dimension of RGGs in the thermodynamic regime using the expression of eignevalues of the regularized normalized Laplacian found in Chapter 4. We derived an analytical approximation of the eigenvalues of the RGG regularized normalized Laplacian matrix in a neighborhood of $\lambda_1 = 0$. Then, using Taylor series expansion around zero, we approximated the empirical distribution of low-eigenvalues useful for the derivation of the spectral dimension in the thermodynamic regime. The analysis shows that the spectral dimension $d_s$ for RGGs is approximated by the Euclidean dimension $d$ in the thermodynamic regime.

## 7.2 Perspectives

The different contributions discussed in this manuscript can be extended in multifold directions and, used as a starting point to explore other and more efficient solutions. In the following, we give possible future research directions inspired by the findings presented in this thesis.

### 7.2.1 Spectrum Analysis of RGGs Using Free Probability Approach

In this thesis, we provided an approximation for the eigenvalues of the regularized normalized Laplacian of RGG asymptotically in both connectivity and thermodynamic regime. A limit of the analysis in the thermodynamic regime is that the obtained error bound requires an average vertex degree finite but large enough for a good approximation. This is because the trace norm bound shown in Chapter 4, which is, to the best of our knowledge, the tightest bound found in this regime, is still not tight enough. Therefore, one possible extension in this spirit is to investigate RGG spectrum using the free probability approximation proposed in [46], [96]. In RMT, free probability theory is a very powerful

tool in the understanding of diverse properties of matrices, most notably, statistics of matrix eigenvalues. Hence, it can be investigated whether free probability approach can be developed to provide more accurate spectrum.

### 7.2.2 RGGs in Hyperbolic Space

In this work, we studied the RGG which is an important model for spatial networks. However, RGGs do not fit perfectly on the real world spatial networks in every aspect. Therefore, various sophisticated RGGs are worth to be considered to improve this drawback.

Results in network science have shown that hyperbolic geometry in particular is well-suited for modeling complex networks [97]. Typical properties such as heterogeneous degree distributions and strong clustering can often be explained by assuming an underlying hierarchy which is well captured in hyperbolic space [97].

These observations offer new perspectives of analyzing RGG structural properties in non-Euclidean space, and led, for instance, to consider as an extension, RGGs with real-world properties by sampling nodes uniformly in the hyperbolic space. In such case, one can investigate if the results obtained in this thesis continue to hold, and if not, how they change.

### 7.2.3 Spectral Properties of Geometric Block Models (GBMs)

Another relevant extension of our analysis would be to consider and investigate a random graph for community detection analogous to the stochastic block model (SBM) [98], called the geometric block model (GBM) [99].

The SBM has been incredibly popular in theoritical and practical domains of community detection. However, one aspect that SBM does not take into account but GBM does is the so-called transitivity rule. Formally, the transitivity rule is defined as follows: if $x$, $y$ and $z$ are three vertices in the graph. Then, if $x$ and $y$ are connected or are in the same community and $y$ and $z$ are also connected by an edge or are in the same community, then it is more likely that $x$ and $z$ are connected by an edge. This phenomenon is seen in many real-world networks. For example, in social networks there is the phenomena that friends having common friends is translated by the transitivity rule.

Recently, there has been contributions on GBM community detection problem. The authors in [99] and [100] investigated the GBM community detection using the triangle counting technique. Then, they showed that the simple triangle counting algorithm to detect communities in the GBM is near-optimal in the regime where the average vertex degree of the graph grows logarithmically with the number of vertices. They found that the triangle counting algorithm performs extremely well compared to its application in SBM. In the future, we can investigate the community detection problem in GBM by analyzing the eigenvalues and eigenvectors of GBM normalized Laplacian matrix in both

connectivity and thermodynamic regime, and compare the performance of the spectral clustering algorithm with the triangle counting algorithm.

# Appendix A

# Supplementary Material Chapter 4

## A.1 Proof of Theorem 29

In this appendix, we provide an upper bound for the probability that the Hilbert-Schmidt norm of the difference between the regularized normalized Laplacian matrices $\hat{\mathcal{L}}(\mathcal{X}_n)$ and $\hat{\mathcal{L}}(\mathcal{D}_n)$ is higher than

$$t > \max\left[\frac{4\,(n+2\alpha)\,a'_n + 4\alpha^2}{n(a'_n+\alpha)^2}, \frac{8\,(n+2\alpha)\,a_n + 4\alpha^2}{n(a_n+\alpha)^2}\right]. \tag{A.1}$$

$$\begin{aligned}
\mathbb{P}\left\{\|\hat{\mathcal{L}}(\mathcal{X}_n) - \hat{\mathcal{L}}(\mathcal{D}_n)\|^2_{\mathrm{HS}} > t\right\} &\leq \mathbb{P}\left\{\left|\frac{1}{n}\sum_i\sum_j \frac{\left(\chi[x_i \sim x_j] + \frac{\alpha}{n}\right)^2}{(\mathbf{N}(x_i)+\alpha)(\mathbf{N}(x_j)+\alpha)} - \frac{b}{n(a'_n+\alpha)^2}\right|\right. \\
&\quad \left. + \left|\frac{2b}{n(a'_n+\alpha)^2} - \frac{2\left(\sum_i \mathbf{N}(x_i, x'_i) + \frac{\alpha}{n}\sum_i \mathbf{N}(x_i) + \alpha a'_n + \alpha^2\right)}{n(a'_n+\alpha)\left(\sum_i \sqrt{\mathbf{N}(x_i)+\alpha}\right)^2}\right| > t\right\} \\
&\leq \mathbb{P}\left\{\left|\frac{1}{n}\sum_i\sum_j \frac{\left(\chi[x_i \sim x_j] + \frac{\alpha}{n}\right)^2}{(\mathbf{N}(x_i)+\alpha)(\mathbf{N}(x_j)+\alpha)} - \frac{b}{n(a'_n+\alpha)^2}\right| > \frac{t}{2}\right\} + \\
&\mathbb{P}\left\{\left|\frac{2b}{n(a'_n+\alpha)^2} - \frac{2\left(\sum_i \mathbf{N}(x_i, x'_i) + \frac{\alpha}{n}\sum_i \mathbf{N}(x_i) + \alpha a'_n + \alpha^2\right)}{n(a'_n+\alpha)\left(\sum_i \sqrt{\mathbf{N}(x_i)+\alpha}\right)^2}\right| > \frac{t}{2}\right\}.
\end{aligned}$$

Define,

$$A = \left| \frac{2b}{n(a'_n + \alpha)^2} - \frac{2\left(\sum_i \mathbf{N}(x_i, x'_i) + \frac{\alpha}{n}\sum_i \mathbf{N}(x_i) + \alpha a'_n + \alpha^2\right)}{n(a'_n + \alpha)\left(\sum_i \sqrt{\mathbf{N}(x_i) + \alpha}\right)^2} \right|,$$

and

$$B = \left| \frac{1}{n}\sum_i \sum_j \frac{\left(\chi[x_i \sim x_j] + \frac{\alpha}{n}\right)^2}{(\mathbf{N}(x_i) + \alpha)(\mathbf{N}(x_j) + \alpha)} - \frac{b}{n(a'_n + \alpha)^2} \right|.$$

In the following, we upper bound $\mathbb{P}\left\{A > \frac{t}{2}\right\}$ and $\mathbb{P}\left\{B > \frac{t}{2}\right\}$.

First, we write $\mathbb{P}\left\{A > \frac{t}{2}\right\}$ as

$$\mathbb{P}\left\{A > \frac{t}{2}\right\} = \mathbb{P}\left\{ \left| \frac{2b}{n(a'_n + \alpha)^2} - \frac{2\left(\sum_i \mathbf{N}(x_i, x'_i) + \frac{\alpha}{n}\sum_i \mathbf{N}(x_i) + \alpha a'_n + \alpha^2\right)}{n(a'_n + \alpha)\left(\sum_i \sqrt{\mathbf{N}(x_i) + \alpha}\right)^2} \right| > \frac{t}{2} \right\}$$

$$\mathbb{P}\left\{A > \frac{t}{2}\right\} = \mathbb{P}\left\{ \left| 1 - \frac{(a'_n + \alpha)\left[\sum_i \mathbf{N}(x_i, x'_i) + \frac{\alpha}{n}\sum_i \mathbf{N}(x_i) + \alpha a'_n + \alpha^2\right]}{b\left(\sum_i \sqrt{\mathbf{N}(x_i) + \alpha}\right)^2} \right| > \frac{tn(a'_n + \alpha)^2}{4b} \right\}$$

$$\stackrel{(a)}{=} \mathbb{P}\left\{ b\left(\sum_i \sqrt{\mathbf{N}(x_i) + \alpha}\right)^2 - (a'_n + \alpha)\left[\sum_i \mathbf{N}(x_i, x'_i) + \frac{\alpha}{n}\sum_i \mathbf{N}(x_i) + \alpha a'_n + \alpha^2\right] > \frac{tn(a'_n + \alpha)^2}{4}\left(\sum_i \sqrt{\mathbf{N}(x_i) + \alpha}\right)^2 \right\}$$

$$= \mathbb{P}\left\{ \left(b - \frac{tn(a'_n + \alpha)^2}{4}\right)\left(\sum_i \sqrt{\mathbf{N}(x_i) + \alpha}\right)^2 > (a'_n + \alpha)\left[\sum_i \mathbf{N}(x_i, x'_i) + \frac{\alpha}{n}\sum_i \mathbf{N}(x_i) + \alpha a'_n + \alpha^2\right] \right\}.$$

Note that $\sum_i \mathbf{N}(x_i, x'_i) \le n a'_n$ and $\mathbf{N}(x_i) \le n$. Then, in step $(a)$ for $n$ sufficiently large, we remove the absolute value because

$$\frac{\sum_i \mathbf{N}(x_i, x_i') + \frac{\alpha}{n}\sum_i \mathbf{N}(x_i) + \alpha a_n' + \alpha^2}{b\left(\sum_i \sqrt{\mathbf{N}(x_i)+\alpha}\right)^2} \leq \frac{na_n' + \alpha n + \alpha a_n' + \alpha^2}{b\left(\sum_i \sqrt{\mathbf{N}(x_i)+\alpha}\right)^2}$$
$$\leq \frac{\left(1 + \frac{\alpha}{a_n'} + \frac{\alpha}{n} + \frac{\alpha^2}{na_n'}\right)}{\left(1 + \frac{2\alpha}{n} + \frac{\alpha^2}{na_n'}\right) n^2\alpha} \leq 1.$$

Notice from the last equality that, $\frac{tn(a_n'+\alpha)^2}{4} > b \Leftrightarrow t > \frac{4na_n' + 4\alpha^2 + 8\alpha a_n'}{n(a_n'+\alpha)^2}$. Then

$$\mathbb{P}\left\{A > \frac{t}{2}\right\} = 0 \quad \text{for} \quad t > \frac{4na_n' + 4\alpha^2 + 8\alpha a_n'}{n(a_n'+\alpha)^2}. \tag{A.2}$$

We continue further by bounding $\mathbb{P}\left\{B > \frac{t}{2}\right\}$ as

$$\mathbb{P}\left\{B > \frac{t}{2}\right\} = \mathbb{P}\left\{\left|\frac{1}{n}\sum_i\sum_j \frac{\left(\chi[x_i \sim x_j] + \frac{\alpha}{n}\right)^2}{(\mathbf{N}(x_i)+\alpha)(\mathbf{N}(x_j)+\alpha)} - \frac{b}{n(a_n'+\alpha)^2}\right| > \frac{t}{2}\right\}$$
$$= \mathbb{P}\left\{\left|\frac{1}{n}\sum_i\sum_j \left(\frac{\left(\chi[x_i \sim x_j] + \frac{\alpha}{n}\right)^2}{(\mathbf{N}(x_i)+\alpha)(\mathbf{N}(x_j)+\alpha)} - \frac{(\chi[x_i \sim x_j] + \frac{\alpha}{n})^2}{(a_n+\alpha)^2} + \frac{(\chi[x_i \sim x_j] + \frac{\alpha}{n})^2}{(a_n+\alpha)^2}\right) - \frac{b}{n(a_n'+\alpha)^2}\right| > \frac{t}{2}\right\}$$

$$\mathbb{P}\left\{B > \frac{t}{2}\right\} \leqslant \mathbb{P}\left\{\left|\frac{1}{n}\sum_i\sum_j \left(\frac{\left(\chi[x_i \sim x_j] + \frac{\alpha}{n}\right)^2}{(\mathbf{N}(x_i)+\alpha)(\mathbf{N}(x_j)+\alpha)} - \frac{(\chi[x_i \sim x_j] + \frac{\alpha}{n})^2}{(a_n+\alpha)^2}\right)\right| > \frac{t}{4}\right\}$$
$$+ \mathbb{P}\left\{\left|\frac{1}{n}\sum_i\sum_j \frac{(\chi[x_i \sim x_j] + \frac{\alpha}{n})^2}{(a_n+\alpha)^2} - \frac{b}{n(a_n'+\alpha)^2}\right| > \frac{t}{4}\right\}.$$

Let

$$B_1 = \left|\frac{1}{n}\sum_i\sum_j \frac{(\chi[x_i \sim x_j] + \frac{\alpha}{n})^2}{(a_n+\alpha)^2} - \frac{b}{n(a_n'+\alpha)^2}\right|,$$

and

$$B_2 = \left|\frac{1}{n}\sum_i\sum_j \left(\frac{(\chi[x_i \sim x_j] + \frac{\alpha}{n})^2}{(\mathbf{N}(x_i)+\alpha)(\mathbf{N}(x_j)+\alpha)} - \frac{(\chi[x_i \sim x_j] + \frac{\alpha}{n})^2}{(a_n+\alpha)^2}\right)\right|.$$

In the following, we upper bound the two probabilities $\mathbb{P}\left\{B_1 > \frac{t}{4}\right\}$ and $\mathbb{P}\left\{B_2 > \frac{t}{4}\right\}$.

First, we write $\mathbb{P}\left\{B_1 > \frac{t}{4}\right\}$ as

$$\begin{aligned}
\mathbb{P}\left\{B_1 > \frac{t}{4}\right\} &= \mathbb{P}\left\{\left|\frac{1}{n}\sum_i\sum_j \frac{(\chi[x_i \sim x_j] + \frac{\alpha}{n})^2}{(a_n+\alpha)^2} - \frac{b}{n(a'_n+\alpha)^2}\right| > \frac{t}{4}\right\} \\
&= \mathbb{P}\left\{\left|\sum_i\sum_j \left(\chi[x_i \sim x_j] + \frac{\alpha}{n}\right)^2 - \frac{b(a_n+\alpha)^2}{(a'_n+\alpha)^2}\right| > \frac{nt(a_n+\alpha)^2}{4}\right\} \\
&\overset{(a)}{\leq} \mathbb{P}\left\{\left|\sum_i \mathbf{N}(x_i) - na_n\right| > \frac{nt(a_n+\alpha)^2 - 4\alpha^2}{4\left(1+\frac{2\alpha}{n}\right)} - na_n\right\} \text{ for } t > \frac{4na'_n + 4\alpha^2 + 8\alpha a'_n}{n(a'_n+\alpha)^2}.
\end{aligned} \tag{A.3}$$

Step $(a)$ follows from $\sum_i\sum_j \left(\chi[x_i \sim x_j] + \frac{\alpha}{n}\right)^2 = \left(1+\frac{2\alpha}{n}\right)\sum_i \mathbf{N}(x_i) + \alpha^2$ and substituting the value of $b$.

We continue further by upper bounding the term $\mathbb{P}\left\{B_2 > \frac{t}{4}\right\}$ as

$$\begin{aligned}
\mathbb{P}\left\{B_2 > \frac{t}{4}\right\} &= \mathbb{P}\left\{\left|\sum_i\sum_j \left(\frac{(\chi[x_i \sim x_j] + \frac{\alpha}{n})^2}{(\mathbf{N}(x_i)+\alpha)(\mathbf{N}(x_j)+\alpha)} - \frac{(\chi[x_i \sim x_j] + \frac{\alpha}{n})^2}{(a_n+\alpha)^2}\right)\right| > \frac{tn}{4}\right\} \\
&= \mathbb{P}\left\{\sum_i\sum_j \frac{(\chi[x_i \sim x_j] + \frac{\alpha}{n})^2}{(\mathbf{N}(x_i)+\alpha)(\mathbf{N}(x_j)+\alpha)} - \sum_i\sum_j \frac{(\chi[x_i \sim x_j] + \frac{\alpha}{n})^2}{(a_n+\alpha)^2} > \frac{tn}{4}\right\} \\
&\quad + \mathbb{P}\left\{\sum_i\sum_j \frac{(\chi[x_i \sim x_j] + \frac{\alpha}{n})^2}{(a_n+\alpha)^2} - \sum_i\sum_j \frac{(\chi[x_i \sim x_j] + \frac{\alpha}{n})^2}{(\mathbf{N}(x_i)+\alpha)(\mathbf{N}(x_j)+\alpha)} > \frac{tn}{4}\right\}.
\end{aligned}$$

Define

$$C_1 = \sum_i\sum_j \frac{(\chi[x_i \sim x_j] + \frac{\alpha}{n})^2}{(a_n+\alpha)^2} - \sum_i\sum_j \frac{(\chi[x_i \sim x_j] + \frac{\alpha}{n})^2}{(\mathbf{N}(x_i)+\alpha)(\mathbf{N}(x_j)+\alpha)},$$

$$C_2 = \sum_i\sum_j \frac{(\chi[x_i \sim x_j] + \frac{\alpha}{n})^2}{(\mathbf{N}(x_i)+\alpha)(\mathbf{N}(x_j)+\alpha)} - \sum_i\sum_j \frac{(\chi[x_i \sim x_j] + \frac{\alpha}{n})^2}{(a_n+\alpha)^2}.$$

In the following, we upper bound $\mathbb{P}\left\{C_1 > \frac{tn}{4}\right\}$ and $\mathbb{P}\left\{C_2 > \frac{tn}{4}\right\}$.

We start first with $\mathbb{P}\left\{C_1 > \frac{tn}{4}\right\}$

$$\mathbb{P}\left\{C_1 > \frac{tn}{4}\right\} = \mathbb{P}\left\{\sum_i \sum_j \frac{(\chi[x_i \sim x_j] + \frac{\alpha}{n})^2}{(a_n+\alpha)^2} - \sum_i \sum_j \frac{(\chi[x_i \sim x_j] + \frac{\alpha}{n})^2}{(\mathbf{N}(x_i)+\alpha)(\mathbf{N}(x_j)+\alpha)} > \frac{tn}{4}\right\}$$

$$\overset{(a)}{\leq} \mathbb{P}\left\{\sum_i \sum_j \frac{(\chi[x_i \sim x_j] + \frac{\alpha}{n})^2}{(a_n+\alpha)^2} - \frac{\left(1+\frac{2\alpha}{n}\right)\sum_i \mathbf{N}(x_i) + \alpha^2}{\left(\sum_i \mathbf{N}(x_i) + n\alpha\right)\sum_j (\mathbf{N}(x_j)+\alpha)} > \frac{tn}{4}\right\}$$

$$= \mathbb{P}\left\{\sum_i \sum_j \frac{(\chi[x_i \sim x_j] + \frac{\alpha}{n})^2}{(a_n+\alpha)^2} - \frac{\alpha\left[\left(\frac{1}{\alpha}+\frac{2}{n}\right)\sum_i \mathbf{N}(x_i) + \alpha\right]}{n\left(\frac{1}{n}\sum_i \mathbf{N}(x_i) + \alpha\right)\sum_j (\mathbf{N}(x_j)+\alpha)} > \frac{tn}{4}\right\}$$

$$\overset{(b)}{\leq} \mathbb{P}\left\{\sum_{i,j} \frac{(\chi[x_i \sim x_j] + \frac{\alpha}{n})^2}{(a_n+\alpha)^2} - \frac{\alpha\left[\left(\frac{1}{\alpha}+\frac{2}{n}\right)\sum_i \mathbf{N}(x_i) + \alpha\right]}{n\left[\left(\frac{1}{\alpha}+\frac{2}{n}\right)\sum_i \mathbf{N}(x_i) + \alpha\right]\sum_j (\mathbf{N}(x_j)+\alpha)} > \frac{tn}{4}\right\}.$$

Step $(a)$ follows from Lemma 28 and step $(b)$ from $\left(\frac{1}{\alpha}+\frac{2}{n}\right)\sum_i \mathbf{N}(x_i)+\alpha > \frac{1}{n}\sum_i \mathbf{N}(x_i)+\alpha$.

$$\mathbb{P}\left\{C_1 > \frac{tn}{4}\right\} = \mathbb{P}\left\{(n+2\alpha)\sum_i \mathbf{N}(x_i) - \frac{\alpha(a_n+\alpha)^2}{\sum_j \mathbf{N}(x_j) + n\alpha} > \frac{tn^2(a_n+\alpha)^2}{4} - n\alpha^2\right\}$$

$$\leq \mathbb{P}\left\{(n+2\alpha)\left|\sum_i \mathbf{N}(x_i) - na_n\right| + \left|(n+2\alpha)\,na_n - \frac{\alpha(a_n+\alpha)^2}{\sum_j \mathbf{N}(x_j) + n\alpha}\right| > \frac{tn^2(a_n+\alpha)^2}{4} - n\alpha^2\right\}$$

$$\leq \mathbb{P}\left\{\left|(n+2\alpha)\,na_n - \frac{\alpha(a_n+\alpha)^2}{\sum_j \mathbf{N}(x_j) + n\alpha}\right| > \frac{tn^2(a_n+\alpha)^2 - 4n\alpha^2}{8}\right\}$$

$$+ \mathbb{P}\left\{\left|\sum_i \mathbf{N}(x_i) - na_n\right| > \frac{tn(a_n+\alpha)^2 - 4\alpha^2}{8\left(1+\frac{2\alpha}{n}\right)}\right\}.$$

Let

$$C_3 = \mathbb{P}\left\{\left|\sum_i \mathbf{N}(x_i) - na_n\right| > \frac{tn(a_n+\alpha)^2 - 4\alpha^2}{8\left(1+\frac{2\alpha}{n}\right)}\right\}, \tag{A.4}$$

and

$$D = \left|(n+2\alpha)\,na_n - \frac{\alpha(a_n+\alpha)^2}{\sum_j \mathbf{N}(x_j) + n\alpha}\right|.$$

$$\mathbb{P}\left\{D > \frac{tn^2(a_n+\alpha)^2 - 4n\alpha^2}{8}\right\} = \mathbb{P}\left\{\left|(n+2\alpha)\,na_n - \frac{\alpha(a_n+\alpha)^2}{\sum_j \mathbf{N}(x_j)+n\alpha}\right| > \frac{tn^2(a_n+\alpha)^2 - 4n\alpha^2}{8}\right\}$$
$$\overset{(a)}{\leq} \mathbb{P}\left\{\left[(n+2\alpha)\,na_n + \frac{4n\alpha^2 - tn^2(a_n+\alpha)^2}{8}\right] \times \left(\sum_j \mathbf{N}(x_j)+n\alpha\right) > \alpha(a_n+\alpha)^2\right\}.$$

Step $(a)$ follows from the inequality $(n+2\alpha)\,na_n > \dfrac{\alpha(a_n+\alpha)^2}{\sum_j \mathbf{N}(x_j)+n\alpha}$. Notice that $8\,(n+2\alpha)\,na_n + 4n\alpha^2 < tn^2(a_n+\alpha)^2 \Leftrightarrow t > \dfrac{8\,(n+2\alpha)\,a_n + 4\alpha^2}{n(a_n+\alpha)^2}$. Then,

$$\mathbb{P}\left\{D > \frac{tn^2(a_n+\alpha)^2 - 4n\alpha^2}{8}\right\} = 0 \quad \text{for} \quad t > \frac{8\,(n+2\alpha)\,a_n + 4\alpha^2}{n(a_n+\alpha)^2}. \tag{A.5}$$

Finally, we upper bound the remaining probability $\mathbb{P}\left\{C_2 > \dfrac{tn}{4}\right\}$ as

$$\begin{aligned}
\mathbb{P}\left\{C_2 > \frac{tn}{4}\right\} &= \mathbb{P}\left\{\sum_i\sum_j \frac{(\chi[x_i\sim x_j]+\frac{\alpha}{n})^2}{(\mathbf{N}(x_i)+\alpha)(\mathbf{N}(x_j)+\alpha)} - \sum_i\sum_j \frac{(\chi[x_i\sim x_j]+\frac{\alpha}{n})^2}{(a_n+\alpha)^2} > \frac{tn}{4}\right\} \\
&= \mathbb{P}\left\{\sum_i\sum_j \frac{(\chi[x_i\sim x_j]+\frac{\alpha}{n})}{(\mathbf{N}(x_i)+\alpha)}\frac{(\chi[x_i\sim x_j]+\frac{\alpha}{n})}{(\mathbf{N}(x_j)+\alpha)}\right. \\
&\qquad\qquad \left. - \sum_i\sum_j \frac{(\chi[x_i\sim x_j]+\frac{\alpha}{n})^2}{(a_n+\alpha)^2} > \frac{tn}{4}\right\} \\
&\overset{(a)}{\leq} \mathbb{P}\left\{\left(\sum_i\sum_j \frac{(\chi[x_i\sim x_j]+\frac{\alpha}{n})^2}{(\mathbf{N}(x_i)+\alpha)^2}\right)^{\frac{1}{2}}\left(\sum_i\sum_j \frac{(\chi[x_i\sim x_j]+\frac{\alpha}{n})^2}{(\mathbf{N}(x_j)+\alpha)^2}\right)^{\frac{1}{2}}\right. \\
&\qquad\qquad \left. - \sum_i\sum_j \frac{(\chi[x_i\sim x_j]+\frac{\alpha}{n})^2}{(a_n+\alpha)^2} > \frac{tn}{4}\right\} \\
&= \mathbb{P}\left\{\sum_i\sum_j \frac{\left(\chi[x_i\sim x_j]+\frac{\alpha}{n}\right)^2}{(\mathbf{N}(x_i)+\alpha)^2} - \sum_i\sum_j \frac{(\chi[x_i\sim x_j]+\frac{\alpha}{n})^2}{(a_n+\alpha)^2} > \frac{tn}{4}\right\}.
\end{aligned} \tag{A.6}$$

Step $(a)$ follows from applying Cauchy-Schwarz inequality. Then

$$\begin{aligned}
\mathbb{P}\left\{C_2 > \frac{tn}{4}\right\} &\leq \mathbb{P}\left\{\sum_i \sum_j \left(\chi[x_i \sim x_j] + \frac{\alpha}{n}\right)^2 \left|\frac{1}{(\mathbf{N}(x_i)+\alpha)^2} - \frac{1}{(a_n+\alpha)^2}\right| > \frac{tn}{4}\right\} \\
&\leq \mathbb{P}\left\{\sum_i \left|(a_n+\alpha)^2 - (\mathbf{N}(x_i)+\alpha)^2\right| > \frac{tn(a_n+\alpha)^2}{4}\right\} \\
&\leq \mathbb{P}\left\{\sum_i |a_n - \mathbf{N}(x_i)|^2 + 2(a_n+\alpha)\sum_i |a_n - \mathbf{N}(x_i)| > \frac{tn(a_n+\alpha)^2}{4}\right\} \\
&\leq \mathbb{P}\left\{\sum_i |a_n - \mathbf{N}(x_i)|^2 > \frac{tn(a_n+\alpha)^2}{8}\right\} + 2\mathbb{P}\left\{\left|\sum_i \mathbf{N}(x_i) - na_n\right| > \frac{tn(a_n+\alpha)}{16}\right\}.
\end{aligned} \tag{A.7}$$

Finally, $\mathbb{P}\left\{C_1 > \frac{tn}{4}\right\}$ is upper bounded by the sum of (A.4) and (A.5). We Use this result combined with the upper bound of $\mathbb{P}\left\{C_2 > \frac{tn}{4}\right\}$ given in (A.7) to upper bound the term $\mathbb{P}\left\{B_2 > \frac{t}{4}\right\}$. Then, apply the new upper bound with (A.2) and (A.3) to upper bound (4.3) and therefore Theorem 29 follows. □

## A.2 Proof of Lemma 30

In this appendix we show that for $a_n \geq \dfrac{2d^{1+1/p}}{2d-1}$ and any $\ell_p$-metric, $p \in [1,\infty]$, the vertex degree $a'_n$ of $G(\mathcal{D}_n, r_n)$ is lower bounded as

$$\frac{a_n}{2d^{1+1/p}} \leq a'_n. \tag{A.8}$$

First, we show that (A.8) holds under the Chebyshev distance. Let an RGG and a DGG be obtained by connecting two nodes if the Chebyshev distance between them is at most $r_n > 0$. Recall that the Chebyshev distance corresponds to the metric given by the $\ell_\infty$-norm. Then, the degree of a $d$-dimensional DGG with $n$ nodes formed by using the Chebyshev distance is given by [70]

$$\begin{aligned}
a'_n &= \left(2\lfloor n^{1/d} r_n \rfloor + 1\right)^d - 1 \\
&= \left(2\lfloor a_n^{1/d} \rfloor + 1\right)^d - 1,
\end{aligned}$$

where $\lfloor x \rfloor$ is the integer part, i.e., the greatest integer less than or equal to $x$.

For $p = \infty$, we have

$$\begin{aligned}
\frac{a_n}{2d} \leq a'_n \iff a_n \leq 2da'_n &\iff a_n \leq 2d\left(2\lfloor a_n^{1/d} \rfloor + 1\right)^d - 2d \\
&\iff (a_n + 2d) \leq 2d\left(2\lfloor a_n^{1/d} \rfloor + 1\right)^d.
\end{aligned}$$

Notice that $\lfloor a_n^{1/d} \rfloor \geq (a_n^{1/d} - 1)$, then it is sufficient to show that

$$(a_n + 2d) \leq 2d \left(2(a_n^{1/d} - 1) + 1\right)^d \iff (a_n + 2d) \leq 2d \left(2a_n^{1/d} - 1\right)^d$$
$$\iff \left(\frac{1}{2d} + \frac{1}{a_n}\right) \leq \left(2 - \frac{1}{a_n^{1/d}}\right)^d.$$

By taking the log in both sides of the last inequality, yields

$$\ln\left(\frac{1}{2d} + \frac{1}{a_n}\right) \leq d \ln\left(2 - \frac{1}{a_n^{1/d}}\right).$$

Consequently, under the Chebyshev distance, (A.8) holds for $a_n \geq \frac{2d}{2d-1}$.

Next, we show that (A.8) holds under any $\ell_p$-metric, $p \in [1, \infty]$. Let $b_n$ and $b'_n$ be the degrees of an RGG and a DGG formed by connecting each two nodes when $d^{1/p}\|x_i - x_j\|_\infty \leq r_n$. This simply means that the graphs are obtained using the Chebyshev distance with a radius equal to $\frac{r_n}{d^{1/p}}$. Then, the degree of the DGG can be written as

$$b'_n = \left(2 \lfloor b_n^{1/d} \rfloor + 1\right)^d - 1.$$

When $p = \infty$, we have that (A.8) holds. Therefore, we deduce that for $b_n \geq \frac{2d}{2d-1}$, we get

$$\frac{b_n}{2d} \leq b'_n.$$

Note that for any $\ell_p$-metric with $p \in [1, \infty)$ in $\mathbb{R}^d$, we have

$$\|x_i - x_j\|_p \leq d^{1/p}\|x_i - x_j\|_\infty.$$

Then the number of nodes $a'_n$ in the DGG that falls in the ball of radius $r_n$ is greater or equal than $b'_n$, i.e., $b'_n \leq a'_n$. Therefore,

$$\frac{b_n}{2d} = \frac{a_n}{2d^{1+1/p}} \leq b'_n \leq a'_n.$$

Hence, for $a_n \geq \frac{2d^{1+1/p}}{2d-1}$, we get

$$\frac{a_n}{2d^{1+1/p}} \leq a'_n.$$

□

## A.3 Proof of Corollary 4 and Theorem 31

In this Appendix, we show that the LSD of the regularized normalized Laplacian for a DGG is a good approximation for the LSD of the regularized normalized Laplacian for an RGG in both the connectivity and thermodynamic regimes.

To upper bound the terms obtained in Theorem 29, we use the Chebyshev inequality. Notice that $\sum_i \mathbf{N}(x_i)/2$ that appears in Theorem 29 counts the number of edges in $G(\mathcal{X}_n, r_n)$. For convenience, we denote $\sum_i \mathbf{N}(x_i)/2$ as $\xi_n$. In order to apply the Chebyshev inequality, we determine the variance of the number of edges, i.e.,$\mathrm{Var}(\xi_n)$.

Let $\vartheta = \left[\theta^{(d)} + 2(n-2)(\theta^{(d)})^2 r_n^d\right]$. In the following, we upper bound the probabilities given in Theorem 29 using Lemma 8 and 36.

We start by upper bounding the first term as follows:

$$\begin{aligned}
&\mathbb{P}\left\{\left|\sum_i \mathbf{N}(x_i) - na_n\right| > \frac{tn(a_n+\alpha)^2 - 4\alpha^2}{4\left(1+\frac{2\alpha}{n}\right)} - na_n\right\} = \\
&\mathbb{P}\left\{|\xi_n - \mathbb{E}[\xi_n]| > \frac{tn(a_n+\alpha)^2 - 4\alpha^2}{8\left(1+\frac{2\alpha}{n}\right)} - na_n\right\} \\
&\leq \frac{8^2\left(1+\frac{2\alpha}{n}\right)^2 \mathrm{Var}(\xi_n)}{\left[tn(a_n+\alpha)^2 - 4\alpha^2 - 8(1+\frac{2\alpha}{n})na_n\right]^2} \\
&= \frac{8^2\left(1+\frac{2\alpha}{n}\right)^2 (n-1)\vartheta}{n\left[tn(a_n+\alpha)^2 - 4\alpha^2 - 8(1+\frac{2\alpha}{n})na_n\right]^2},
\end{aligned} \tag{A.9}$$

and

$$\begin{aligned}
\mathbb{P}\left\{\left|\sum_i \mathbf{N}(x_i) - na_n\right| > \frac{tn(a_n+\alpha)}{16}\right\} &\leq \frac{32^2 \mathrm{Var}(\xi_n)}{t^2 n^2 (a_n+\alpha)^2} \\
&= \frac{32^2(n-1)\vartheta}{t^2 n^3 (a_n+\alpha)^2}.
\end{aligned} \tag{A.10}$$

Finally, we upper bound the last term as

$$\begin{aligned}
\mathbb{P}\left\{\sum_i |\mathbf{N}(x_i) - a_n|^2 > \frac{nt(a_n+\alpha)^2}{8}\right\} &\leq \mathbb{P}\left\{\left(\sum_i |\mathbf{N}(x_i) - a_n|\right)^2 > \frac{nt(a_n+\alpha)^2}{8}\right\} \\
&= \mathbb{P}\left\{\sum_i |\mathbf{N}(x_i) - a_n| > \frac{(a_n+\alpha)\sqrt{nt}}{2\sqrt{2}}\right\}.
\end{aligned}$$

Then,

$$\begin{aligned}\mathbb{P}\left\{\sum_i |\mathbf{N}(x_i)-a_n|^2 > \frac{nt(a_n+\alpha)^2}{8}\right\} &\leq 2\mathbb{P}\left\{\left|\sum_i \mathbf{N}(x_i)-na_n\right| > \frac{(a_n+\alpha)\sqrt{nt}}{2\sqrt{2}}\right\}\\ &= 2\mathbb{P}\left\{|\xi_n-\mathbb{E}[\xi_n]| > \frac{(a_n+\alpha)\sqrt{nt}}{4\sqrt{2}}\right\}\\ &\leq \frac{64(n-1)\vartheta}{tn^2(a_n+\alpha)^2}.\end{aligned} \tag{A.11}$$

Corollary 4 for the thermodynamic regime is obtained from upper bounding the terms in the r.h.s of (4.3) in Theorem 29 obtained in (A.9), (A.10) and (A.11). In addition, by letting $\alpha \to 0$, the provided upper bounds hold in the connectivity case.

In the following, we propose a tighter upper bound for the Hilbert-Schmidt norm of the difference between $\mathcal{L}(\mathcal{D}_n)$ and $\mathcal{L}(\mathcal{X}_n)$ in the connectivity regime. More precisely, the following upper bounds are tighter when the average vertex degree scales as $\Omega(\log^{1+\epsilon}(n))$ or for $a_n = c\log(n)$ when $c > 24$.

First, observe that the number of nodes that fall in an arbitrary interval of radius $r_n$ follows a binomial distribution. Then in order to derive the distribution of $\mathbf{N}(x_i)$, we need to derive the distribution of the nodes that fall in a ball centered in $x_i$. To derive the distribution of $\mathbf{N}(x_i)$ in the connectivity regime, we throw at random a node which will be in a random position and we are left with $n-1$ nodes. Then, we take a ball of size $2r_n$, centered around the thrown node. If we throw randomly the remaining $n-1$ nodes, then, $\mathbf{N}(x_i)$ will be a random variable binomially distributed with parameters $(n-1, \theta^{(d)}r_n)$, i.e.,

$$\mathbb{P}(\mathbf{N}(x_i)=k) = \binom{n-1}{k}(\theta^{(d)}r_n)^k(1-\theta^{(d)}r_n)^{n-k-1}, \quad \text{for} \quad k=0,...,n-1.$$

To upper bound the terms in the r.h.s of (4.3) given in Theorem 29, we use the upper bounds for a binomially distributed random variable $x$ given in Chapter 3 appropriate for large deviations. These results play a key role to establish the relation between $F^{\mathcal{L}(\mathcal{X}_n)}$ and $F^{\mathcal{L}(\mathcal{D}_n)}$.

We upper bound the first term in the r.h.s of (4.3) in Theorem 29 by using Lemmas

12 and 13 as follows:

$$\begin{aligned}
\mathbb{P}\left\{\left|\sum_i \mathbf{N}(x_i) - na_n\right| > \frac{tna_n^2}{4} - na_n\right\} &\overset{(a)}{\leq} \mathbb{P}\left\{\sum_i |\mathbf{N}(x_i) - a_n| > \frac{nta_n^2}{4} - na_n\right\} \\
&\overset{(b)}{\leq} n\mathbb{P}\left\{|\mathbf{N}(x_i) - a_n| > \frac{ta_n^2}{4} - a_n\right\} \\
&\leq n\mathbb{P}\left\{\mathbf{N}(x_i) > \frac{ta_n^2}{4}\right\} + n\mathbb{P}\mathbb{P}\left\{\mathbf{N}(x_i) < 2a_n - \frac{ta_n^2}{4}\right\} \\
&\leq n\exp\left(-\frac{(ta_n - 4)^2}{16\left(\frac{t}{6} - \frac{2r_n}{a_n^2} + \frac{4}{3a_n}\right)}\right), \qquad \text{for } \; t > \frac{8}{a_n}.
\end{aligned} \tag{A.12}$$

Step $(a)$ follows from $\left|\sum_i z_i\right| \leq \sum_i |z_i|$ and step $(b)$ from $\sum_i |\mathbf{N}(x_i) - a_n| \leq n\,|\mathbf{N}(x_i) - a_n|$.

Now, instead of upper bounding the two last probabilities given in Theorem 29, we go back to Appendix A.1 and upper bound (A.6) by letting $\alpha \to 0$.

$$\begin{aligned}
\mathbb{P}\left\{C_2 > \frac{tn}{4}\right\} &\leq \mathbb{P}\left\{\sum_i \sum_j \frac{\chi[x_i \sim x_j]^2}{\mathbf{N}(x_i)^2} - \sum_i \sum_j \frac{\chi[x_i \sim x_j]^2}{a_n^2} > \frac{tn}{4}\right\} \\
&\leq n\mathbb{P}\left\{\frac{1}{\mathbf{N}(x_i)} - \frac{\mathbf{N}(x_i)}{a_n^2} > \frac{t}{4}\right\}
\end{aligned}$$

$$\begin{aligned}
\mathbb{P}\left\{C_2 > \frac{tn}{4}\right\} &= n\mathbb{P}\left\{a_n^2 - \mathbf{N}(x_i)^2 > \frac{ta_n^2\mathbf{N}(x_i)}{4}\right\} \\
&= n\mathbb{P}\left\{\left[a_n^2 - \mathbf{N}(x_i)^2\right] + \frac{ta_n^2}{4}\left[a_n - \mathbf{N}(x_i)\right] > \frac{ta_n^3}{4}\right\} \\
&\leq n\mathbb{P}\left\{\left|a_n^2 - \mathbf{N}(x_i)^2\right| > \frac{ta_n^3}{8}\right\} + n\mathbb{P}\left\{|a_n - \mathbf{N}(x_i)| > \frac{a_n}{2}\right\} \\
&\leq n\mathbb{P}\left\{-\mathbf{N}(x_i)^2 > \frac{ta_n^3}{8} - a_n^2\right\} + n\mathbb{P}\left\{|a_n - r_n - \mathbf{N}(x_i)| > \frac{a_n - r_n}{2}\right\} \\
&\qquad + n\mathbb{P}\left\{\mathbf{N}(x_i) > a_n - r_n + \sqrt{\frac{ta_n^3}{8} + a_n^2} - a_n + r_n\right\} \\
&= n\mathbb{P}\left\{-\mathbf{N}(x_i)^2 > \frac{ta_n^3}{8} - a_n^2\right\} + n\mathbb{P}\left\{|\mathbf{N}(x_i) - \mathbb{E}[\mathbf{N}(x_i)]| > \frac{a_n - r_n}{2}\right\} \\
&\qquad + n\mathbb{P}\left\{\mathbf{N}(x_i) > \mathbb{E}[\mathbf{N}(x_i)] + \sqrt{\frac{ta_n^3}{8} + a_n^2} - a_n + r_n\right\}.
\end{aligned}$$

Then, applying Lemma 12 and 13, yields

$$\mathbb{P}\left\{C_2 > \frac{tn}{4}\right\} \leq 2n \exp\left(-\frac{(a_n - r_n)}{12}\right) + n \exp\left(\frac{-3a_n\left[\sqrt{\frac{t}{8}a_n + 1} - 1 + \frac{r_n}{a_n}\right]^2}{2\left[2 - \frac{2r_n}{a_n} + \sqrt{\frac{t}{8}a_n + 1}\right]}\right), \tag{A.13}$$

for $t > \dfrac{8}{a_n}$.

Finally, taking the upper bounds found by using the Chebyshev inequality in (A.9), (A.10) and (A.11) combined with the upper bounds found by using Lemmas 12 and 13, i.e., (A.12), (A.13) all together, then by applying Lemma 30 and letting $\alpha \to 0$, Theorem 31 follows. □

## A.4 Proof of Lemma 32 and Lemma 38

In this appendix, we provide the eigenvalues of the regularized normalized Laplacian matrix for a DGG using the Chebyshev distance. Then, the degree of a vertex in $G(\mathcal{D}_n, r_n)$ is given as [70]

$$a'_n = (2k_n + 1)^d - 1, \quad \text{with} \quad k_n = \lfloor \mathrm{N} r_n \rfloor,$$

where $\lfloor x \rfloor$ is the integer part, i.e., the greatest integer less than or equal to $x$. The regularized normalized Laplacian can be written as

$$\hat{\mathcal{L}}(\mathcal{D}_n) = \mathbf{I} - \frac{1}{(a'_n + \alpha)}\mathbf{A} - \frac{\alpha}{n(a'_n + \alpha)}\mathbf{1}\mathbf{1}^T, \tag{A}$$

where $\mathbf{I}$ is the identity matrix, $\mathbf{1}^T = [1, ..., 1]^T$ is the vector of all ones and $\mathbf{A}$ is the adjacency matrix defined as

$$\mathbf{A}_{ij} = \begin{cases} 1, & \|x_i - x_j\|_p \leq r_n, \quad i \neq j, \quad \text{and} \quad p \in [1, \infty], \\ 0, & \text{otherwise.} \end{cases}$$

When $d = 1$, the adjacency matrix $\mathbf{A}$ of a DGG in $\mathbb{T}^1$ with $n$ nodes is a circulant matrix. A well known result appearing in [51], states that the eigenvalues of a circulant matrix are given by the DFT of the first row of the matrix. When $d > 1$, the adjacency matrix of a DGG is no longer circulant but it is block circulant with $\mathrm{N}^{d-1} \times \mathrm{N}^{d-1}$ circulant blocks, each of size $\mathrm{N} \times \mathrm{N}$. The author in [70], pages 85-87, utilizes the result in [51], and shows that the eigenvalues of the adjacency matrix in $\mathbb{T}^d$ are found by taking the $d$-dimensional DFT of an $\mathrm{N}^d$ tensor of rank $d$ obtained from the first block row of (A)

$$\lambda_{m_1,...,m_d} = \sum_{h_1,...,h_d=0}^{\mathrm{N}-1} c_{h_1,...,h_d} \exp\left(-\frac{2\pi i}{\mathrm{N}}\mathbf{m}.\mathbf{h}\right), \tag{A.14}$$

where $\mathbf{m}$ and $\mathbf{h}$ are vectors of elements $m_i$ and $h_i$, respectively, with $m_1, ..., m_d \in \{0, 1, ..., \mathrm{N}-1\}$ and $c_{h_1,...,h_d}$ defined as [70]

$$c_{h_1,...,h_d} = \begin{cases} 0, & \text{for } \; k_n < h_1, ..., h_d \leq \mathrm{N} - k_n - 1 \text{ or } h_1, ...h_d = 0, \\ 1, & \text{otherwise.} \end{cases} \tag{A.15}$$

The eigenvalues of the block circulant matrix $\mathbf{A}$ follow the spectral decomposition [70], page 86,

$$\mathbf{A} = \mathbf{F}^H \mathbf{\Lambda} \mathbf{F},$$

where $\mathbf{\Lambda}$ is a diagonal matrix whose entries are the eigenvalues of $\mathbf{A}$, and $\mathbf{F}$ is the $d$-dimensional DFT matrix. It is well known that when $d = 1$, the DFT of an $n \times n$ matrix is the matrix of the same size with entries

$$\mathbf{F}_{m,k} = \frac{1}{\sqrt{n}} \exp\left(-2\pi i m k / n\right) \quad \text{for} \;\; m, k = \{0, 1, ..., n-1\}.$$

When $d > 1$, the block circulant matrix $\mathbf{A}$ is diagonalized by the $d$-dimensional DFT matrix $\mathbf{F} = \mathbf{F}_{\mathrm{N}_1} \bigotimes ... \bigotimes \mathbf{F}_{\mathrm{N}_d}$, i.e., tensor product, where $\mathbf{F}_{\mathrm{N}_d}$ is the $\mathrm{N}_d$-point DFT matrix.

Notice that all the matrices in (A) have a common eigenvector that is $\left(\frac{1}{\sqrt{n}}, ..., \frac{1}{\sqrt{n}}\right)$ and this eigenvector coincides with the first row and column of $\mathbf{F}$. Then, $\left(\frac{1}{\sqrt{n}}, ..., \frac{1}{\sqrt{n}}\right)$ is also an eigenvector of $\hat{\mathcal{L}}(\mathcal{D}_n)$.

The regularized normalized Laplacian can be expressed as

$$\begin{aligned} \hat{\mathcal{L}}(\mathcal{D}_n) &= \mathbf{I} - \frac{1}{(a'_n + \alpha)} \mathbf{F}^H \mathbf{\Lambda} \mathbf{F} - \frac{\alpha}{n(a'_n + \alpha)} \mathbf{1}\mathbf{1}^T \\ &= \mathbf{F}^H \left( \mathbf{I} - \frac{1}{(a'_n + \alpha)} \mathbf{\Lambda} - \frac{\alpha}{n(a'_n + \alpha)} \mathbf{F}\mathbf{1}\mathbf{1}^T\mathbf{F}^H \right) \mathbf{F} \\ &= \mathbf{F}^H \left( \mathbf{I} - \frac{1}{(a'_n + \alpha)} \mathbf{\Lambda} - \frac{n\alpha}{n(a'_n + \alpha)} \mathbf{e}_1^T \mathbf{e}_1 \right) \mathbf{F} \\ &= \mathbf{F}^H \mathbf{\Lambda}_1 \mathbf{F}, \end{aligned} \tag{A.16}$$

where $\mathbf{e}_1 = (1, 0...0)$ and $\mathbf{\Lambda}_1 = \left( \mathbf{I} - \frac{1}{(a'_n + \alpha)} \mathbf{\Lambda} - \frac{n\alpha}{n(a'_n + \alpha)} \mathbf{e}_1^T \mathbf{e}_1 \right)$ is a diagonal matrix whose diagonal elements are the eigenvalues of $\hat{\mathcal{L}}(\mathcal{D}_n)$. Then, from (A.16), the derivation of the eignevalues of $\hat{\mathcal{L}}(\mathcal{D}_n)$ reduces to the derivation of the eigenvalues of the normalized adjacency matrix $\mathbf{A}'$.

The normalized adjacency matrix $\mathbf{A}'$ is defined as

$$\mathbf{A}' = \frac{1}{(a'_n + \alpha)} \mathbf{A}.$$

By using (A.14) and (A.15), the eigenvalues of $\mathbf{A}'$ for a DGG in $\mathbb{T}^d$ are given as

$$\begin{aligned}\lambda'_{m_1,\ldots,m_d} &= \frac{1}{(a'_n+\alpha)}\left[\sum_{h_1,\ldots,h_d=0}^{\mathrm{N}-1}\exp\left(-\frac{2\pi i\mathbf{mh}}{\mathrm{N}}\right)-\sum_{h_1,\ldots,h_d=k_n+1}^{\mathrm{N}-k_n-1}\exp\left(-\frac{2\pi i\mathbf{mh}}{\mathrm{N}}\right)\right]-\frac{1}{(a'_n+\alpha)}\\ &= -\frac{1}{(a'_n+\alpha)}\sum_{h_1,\ldots,h_d=k_n+1}^{\mathrm{N}-k_n-1}\exp\left(-\frac{2\pi i\mathbf{mh}}{\mathrm{N}}\right)-\frac{1}{(a'_n+\alpha)}\end{aligned}$$

$$\begin{aligned}\lambda'_{m_1,\ldots,m_d} &= -\frac{1}{(a'_n+\alpha)}\prod_{s=1}^{d}\frac{\left(e^{\frac{-2im_s\pi}{\mathrm{N}}k_n}-e^{\frac{2im_s\pi}{\mathrm{N}}(1+k_n)}\right)}{\left(-1+e^{\frac{2im_s\pi}{\mathrm{N}}}\right)}-\frac{1}{(a'_n+\alpha)}\\ &= \frac{1}{(a'_n+\alpha)}\prod_{s=1}^{d}\frac{\left(e^{\frac{2im_s\pi}{\mathrm{N}}(1+k_n)}-e^{\frac{-2im_s\pi}{\mathrm{N}}k_n}\right)}{\left(-1+e^{\frac{2im_s\pi}{\mathrm{N}}}\right)}-\frac{1}{(a'_n+\alpha)}\\ &= \frac{1}{(a'_n+\alpha)}\prod_{s=1}^{d}\frac{\sin(\frac{m_s\pi}{\mathrm{N}}(2k_n+1))}{\sin(\frac{m_s\pi}{\mathrm{N}})}-\frac{1}{(a'_n+\alpha)}.\end{aligned}$$

Then, we conclude that the eigenvalues of $\hat{\mathcal{L}}(\mathcal{D}_n)$ for $n$ finite are given by

$$\begin{aligned}\hat{\lambda}_{m_1,\ldots,m_d} &= 1-\frac{1}{(a'_n+\alpha)}\prod_{s=1}^{d}\frac{\sin(\frac{m_s\pi}{\mathrm{N}}(2k_n+1))}{\sin(\frac{m_s\pi}{\mathrm{N}})}+\frac{1-\alpha\delta_{m_1,\ldots,m_d}}{(a'_n+\alpha)}\\ \hat{\lambda}_{m_1,\ldots,m_d} &= 1-\frac{1}{(a'_n+\alpha)}\prod_{s=1}^{d}\frac{\sin(\frac{m_s\pi}{\mathrm{N}}(a'_n+1)^{1/d})}{\sin(\frac{m_s\pi}{\mathrm{N}})}+\frac{1-\alpha\delta_{m_1,\ldots,m_d}}{(a'_n+\alpha)},\end{aligned}$$

with $m_1,\ldots,m_d\in\{0,\ldots\mathrm{N}-1\}$ and $\delta_{m_1,\ldots,m_d}=1$ when $m_1,\ldots,m_d=0$ otherwise $\delta_{m_1,\ldots,m_d}=0$.

In particular, as $\alpha\to 0$, the eigenvalues of $\mathcal{L}(\mathcal{D}_n)$ in the connectivity regime are given by

$$\lambda_{m_1,\ldots,m_d}=1-\frac{1}{a'_n}\prod_{s=1}^{d}\frac{\sin(\frac{m_s\pi}{\mathrm{N}}(a'_n+1)^{1/d})}{\sin(\frac{m_s\pi}{\mathrm{N}})}+\frac{1}{a'_n},\tag{A.17}$$

with $m_1,\ldots,m_d\in\{0,\ldots,\mathrm{N}-1\}$.

In the thermodynamic regime, for $s\in\{0,\ldots,d\}$ we let $f_s=\frac{m_s}{\mathrm{N}}$ then as $n\to\infty$, $f_s\in\mathbb{Q}\cap[0,1]$ where $\mathbb{Q}$ denotes the set of rational numbers. Therefore, for $\gamma\geq 1$, the eigenvalues of $\hat{\mathcal{L}}(\mathcal{X}_n)$ can be approximated by the eigenvalues of $\hat{\mathcal{L}}(\mathcal{D}_n)$ given as

$$\hat{\lambda}_{f_1,\ldots,f_d}=1-\frac{1}{(\gamma'+\alpha)}\prod_{s=1}^{d}\frac{\sin(\pi f_s(\gamma'+1)^{1/d})}{\sin(\pi f_s)}+\frac{1-\alpha\delta_{f_1,\ldots,f_d}}{(\gamma'+\alpha)},\tag{A.18}$$

where $\gamma'=(2\left\lfloor\gamma^{1/d}\right\rfloor+1)^d-1$ and $\delta_{f_1,\ldots,f_d}=1$ when $f_1,\ldots,f_d=0$, otherwise $\delta_{f_1,\ldots,f_d}=0$. □

# Bibliography


[1] D. I. Shuman, S. K. Narang, P. Frossard, A. Ortega, and P. Vandergheynst, "The emerging field of signal processing on graphs: Extending high-dimensional data analysis to networks and other irregular domains," *IEEE Signal Processing Magazine*, vol. 30, no. 3, pp. 83–98, 2013.

[2] M. E. Newman, "The structure and function of complex networks," *SIAM Review*, vol. 45, no. 2, pp. 167–256, 2003.

[3] S. H. Strogatz, "Exploring complex networks," *Nature*, vol. 410, no. 6825, p. 268, 2001.

[4] B. Bollobás, "Random graphs," in *Modern graph theory*. Springer, 1998, pp. 215–252.

[5] P. Erdos, "On random graphs," *Publicationes Mathematicae*, vol. 6, pp. 290–297, 1959.

[6] P. Erdős and A. Rényi, "On the evolution of random graphs," *Publ. Math. Inst. Hung. Acad. Sci*, vol. 5, no. 1, pp. 17–60, 1960.

[7] ——, "On the strength of connectedness of a random graph," *Acta Mathematica Hungarica*, vol. 12, no. 1-2, pp. 261–267, 1961.

[8] E. N. Gilbert, "Random graphs," *The Annals of Mathematical Statistics*, vol. 30, no. 4, pp. 1141–1144, 1959.

[9] R. Albert and A.-L. Barabási, "Statistical mechanics of complex networks," *Reviews of Modern Physics*, vol. 74, no. 1, p. 47, 2002.

[10] A.-L. Barabási and R. Albert, "Emergence of scaling in random networks," *Science*, vol. 286, no. 5439, pp. 509–512, 1999.

[11] D. J. Watts and S. H. Strogatz, "Collective dynamics of 'small-world' networks," *Nature*, vol. 393, no. 6684, p. 440, 1998.

[12] E. N. Gilbert, "Random plane networks," *Journal of the Society for Industrial and Applied Mathematics*, vol. 9, no. 4, pp. 533–543, 1961.

[13] C. Bettstetter, "On the minimum node degree and connectivity of a wireless multihop network," in *Proceedings of the 3rd ACM International Symposium on Mobile ad hoc Networking & Computing*, 2002, pp. 80–91.

[14] F. Baccelli, B. Błaszczyszyn *et al.*, "Stochastic geometry and wireless networks: Volume ii applications," *Foundations and Trends® in Networking*, vol. 4, no. 1–2, pp. 1–312, 2010.

[15] J. Yick, B. Mukherjee, and D. Ghosal, "Wireless sensor network survey," *Computer Networks*, vol. 52, no. 12, pp. 2292–2330, 2008.

[16] V. M. Preciado and A. Jadbabaie, "Spectral analysis of virus spreading in random geometric networks," *IEEE Conference on Decision and Control*, 2009.

[17] A. Ganesh, L. Massoulié, and D. Towsley, "The effect of network topology on the spread of epidemics," in *Proc. of IEEE Conference on Computer Communications (INFOCOM)*, 2005.

[18] L. Lovász *et al.*, "Random walks on graphs: A survey," *Combinatorics, Paul erdos is eighty*, vol. 2, no. 1, pp. 1–46, 1993.

[19] F. R. Chung and F. C. Graham, *Spectral graph theory*. American Mathematical Soc., 1997, no. 92.

[20] G. Bianconi, "Interdisciplinary and physics challenges of network theory," *EPL (Europhysics Letters)*, vol. 111, no. 5, p. 56001, 2015.

[21] V. Salnikov, D. Cassese, and R. Lambiotte, "Simplicial complexes and complex systems," *European Journal of Physics*, vol. 40, no. 1, p. 014001, 2018.

[22] D. Mulder and G. Bianconi, "Network geometry and complexity," *Journal of Statistical Physics*, vol. 173, no. 3-4, pp. 783–805, 2018.

[23] G. Bianconi and C. Rahmede, "Complex quantum network manifolds in dimension d> 2 are scale-free," *Scientific Reports*, vol. 5, p. 13979, 2015.

[24] J. Jost and S. Liu, "Ollivier's ricci curvature, local clustering and curvature-dimension inequalities on graphs," *Discrete & Computational Geometry*, vol. 51, no. 2, pp. 300–322, 2014.

[25] A. Muscoloni, J. M. Thomas, S. Ciucci, G. Bianconi, and C. V. Cannistraci, "Machine learning meets complex networks via coalescent embedding in the hyperbolic space," *Nature Communications*, vol. 8, no. 1, p. 1615, 2017.

[26] M. M. Bronstein, J. Bruna, Y. LeCun, A. Szlam, and P. Vandergheynst, "Geometric deep learning: going beyond Euclidean data," *IEEE Signal Processing Magazine*, vol. 34, no. 4, pp. 18–42, 2017.

[27] D. Ben-Avraham and S. Havlin, *Diffusion and reactions in fractals and disordered systems*. Cambridge University Press, 2000.

[28] J. Ambjørn, B. Durhuus, T. Jonsson, and O. Jonsson, *Quantum geometry: a statistical field theory approach*. Cambridge University Press, 1997.

[29] M. Penrose, *Random geometric graphs*. Oxford University Press, 2003.

[30] A. Frieze and M. Karoński, *Introduction to random graphs*. Cambridge University Press, 2016.

[31] M. E. Newman *et al.*, "Random graphs as models of networks," *Handbook of Graphs and Networks*, vol. 1, pp. 35–68, 2003.

[32] R. Albert, H. Jeong, and A.-L. Barabási, "Internet: Diameter of the world-wide web," *Nature*, vol. 401, no. 6749, p. 130, 1999.

[33] Z. J. Haas, J. Deng, B. Liang, P. Papadimitratos, and S. Sajama, "Wireless ad hoc networks," *Encyclopedia of Telecommunications*, 2002.

[34] M. Maier, M. Hein, and U. von Luxburg, "Optimal construction of k-nearest-neighbor graphs for identifying noisy clusters," *Theoretical Computer Science*, vol. 410, no. 19, pp. 1749–1764, 2009.

[35] M. D. Penrose, "On k-connectivity for a geometric random graph," *Random Structures & Algorithms*, vol. 15, no. 2, pp. 145–164, 1999.

[36] M. D. Penrose *et al.*, "The longest edge of the random minimal spanning tree," *The Annals of Applied Probability*, vol. 7, no. 2, pp. 340–361, 1997.

[37] P. Gupta and P. R. Kumar, "Critical power for asymptotic connectivity in wireless networks," in *Stochastic Analysis, Control, Optimization and Applications*. Springer, 1999, pp. 547–566.

[38] M. J. Appel and R. P. Russo, "The connectivity of a graph on uniform points on [0, 1] d," *Statistics & Probability Letters*, vol. 60, no. 4, pp. 351–357, 2002.

[39] J. Díaz, D. Mitsche, and X. Pérez, "Sharp threshold for hamiltonicity of random geometric graphs," *SIAM Journal on Discrete Mathematics*, vol. 21, no. 1, pp. 57–65, 2007.

[40] R. Meester and R. Roy, *Continuum percolation*. Cambridge University Press, 1996, vol. 119.

[41] N. Alon and V. D. Milman, "$\lambda 1$, isoperimetric inequalities for graphs, and superconcentrators," *Journal of Combinatorial Theory, Series B*, vol. 38, no. 1, pp. 73–88, 1985.

[42] J. Wishart, "The generalised product moment distribution in samples from a normal multivariate population," *Biometrika*, pp. 32–52, 1928.

[43] E. P. Wigner, "Characteristic vectors of bordered matrices with infinite dimensions i," in *The Collected Works of Eugene Paul Wigner*. Springer, 1993, pp. 524–540.

[44] G. Akemann, J. Baik, and P. Di Francesco, *The Oxford handbook of random matrix theory*. Oxford University Press, 2011.

[45] G. W. Anderson, A. Guionnet, and O. Zeitouni, *An introduction to random matrices*. Cambridge University Press, 2010, vol. 118.

[46] R. Couillet and M. Debbah, *Random matrix methods for wireless communications*. Cambridge University Press, 2011.

[47] M. Mézard, G. Parisi, and A. Zee, "Spectra of Euclidean random matrices," *Nuclear Physics B*, vol. 559, no. 3, pp. 689–701, 1999.

[48] A. Amir, Y. Oreg, and Y. Imry, "Localization, anomalous diffusion, and slow relaxations: A random distance matrix approach," *Physical Review Letters*, vol. 105, no. 7, p. 070601, 2010.

[49] S. Skipetrov and A. Goetschy, "Eigenvalue distributions of large Euclidean random matrices for waves in random media," *Journal of Physics A: Mathematical and Theoretical*, vol. 44, no. 6, 2011.

[50] U. Grenander and G. Szegö, *Toeplitz forms and their applications*. Univ of California Press, 1958.

[51] R. M. Gray, "Toeplitz and circulant matrices: A review," *Foundations and Trends® in Communications and Information Theory*, vol. 2, no. 3, pp. 155–239, 2006.

[52] J. C. Taylor, *An introduction to measure and probability*. Springer Science & Business Media, 2012.

[53] Z. D. Bai, "Methodologies in spectral analysis of large dimensional random matrices, a review," *Statistica Sinica*, vol. 9, pp. 611–677, 1999.

[54] S. Bernstein, "On a modification of chebyshev's inequality and of the error formula of laplace," *Ann. Sci. Inst. Sav. Ukraine, Sect. Math*, vol. 1, no. 4, pp. 38–49, 1924.

[55] S. Janson, T. Luczak, and A. Rucinski, *Random graphs*. John Wiley & Sons, 2011, vol. 45.

[56] A. J. Hoffman and H. W. Wielandt, "The variation of the spectrum of a normal matrix," in *Selected Papers Of Alan J Hoffman: With Commentary*. World Scientific, 2003, pp. 118–120.

[57] M. Draief, A. Ganesh, and L. Massoulié, "Thresholds for virus spread on networks," in *Proceedings of the 1st International Conference on Performance Evaluation Methodolgies and Tools*. ACM, 2006, p. 51.

[58] P. Van Mieghem, J. Omic, and R. Kooij, "Virus spread in networks," *IEEE/ACM Transactions on Networking (TON)*, vol. 17, no. 1, pp. 1–14, 2009.

[59] Z. Bai and J. W. Silverstein, *Spectral analysis of large dimensional random matrices*. Springer, 2010, vol. 20.

[60] I. J. Farkas, I. Derényi, A.-L. Barabási, and T. Vicsek, "Spectra of "real-world" graphs: Beyond the semicircle law," *Physical Review E*, vol. 64, no. 2, p. 026704, 2001.

[61] P. Van Mieghem, *Graph spectra for complex networks*. Cambridge University Press, 2010.

[62] M. L. Mehta, *Random matrices*. Elsevier, 2004, vol. 142.

[63] E. P. Wigner, "On the distribution of the roots of certain symmetric matrices," *Ann. Math*, vol. 67, no. 2, pp. 325–327, 1958.

[64] Z. Bai *et al.*, "Circular law," *The Annals of Probability*, vol. 25, no. 1, pp. 494–529, 1997.

[65] V. A. Marčenko and L. A. Pastur, "Distribution of eigenvalues for some sets of random matrices," *Mathematics of the USSR-Sbornik*, vol. 1, no. 4, p. 457, 1967.

[66] F. Chung, L. Lu, and V. Vu, "The spectra of random graphs with given expected degrees," *Internet Mathematics*, vol. 1, no. 3, pp. 257–275, 2004.

[67] L. V. Tran, V. H. Vu, and K. Wang, "Sparse random graphs: Eigenvalues and eigenvectors," *Random Structures & Algorithms*, vol. 42, no. 1, pp. 110–134, 2013.

[68] K. Avrachenkov, L. Cottatellucci, and A. Kadavankandy, "Spectral properties of random matrices for stochastic block model," in *2015 13th International Symposium on Modeling and Optimization in Mobile, Ad Hoc, and Wireless Networks (WiOpt)*. IEEE, 2015, pp. 537–544.

[69] A. Spiridonov, "Spectra of sparse graphs and matrices," *Preprint*, 2005.

[70] A. Nyberg, "The laplacian spectra of random geometric graphs," Ph.D. dissertation, 2014.

[71] C. P. Dettmann and G. Knight, "Symmetric motifs in random geometric graphs," *Journal of Complex Networks*, vol. 6, no. 1, pp. 95–105, 2017.

[72] N. El Karoui, "The spectrum of kernel random matrices," *The Annals of Statistics*, vol. 38, no. 1, pp. 1–50, 2010.

[73] T. Jiang, "Distributions of eigenvalues of large Euclidean matrices generated from lp balls and spheres," *Linear Algebra and its Applications*, vol. 473, pp. 14–36, 2015.

[74] C. Bordenave, "Eigenvalues of Euclidean random matrices," *Random Structures & Algorithms*, vol. 33, no. 4, pp. 515–532, 2008.

[75] P. Blackwell, M. Edmondson-Jones, and J. Jordan, *Spectra of adjacency matrices of random geometric graphs*. Unpublished, 2007.

[76] R. L. Graham, D. E. Knuth, O. Patashnik, and S. Liu, "Concrete mathematics: a foundation for computer science," *Computers in Physics*, vol. 3, no. 5, pp. 106–107, 1989.

[77] S. Rai, "The spectrum of a random geometric graph is concentrated," *Journal of Theoretical Probability*, vol. 20, no. 2, pp. 119–132, 2007.

[78] K. Avrachenkov, B. Ribeiro, and D. Towsley, "Improving random walk estimation accuracy with uniform restarts," in *International Workshop on Algorithms and Models for the Web-Graph*. Springer, 2010, pp. 98–109.

[79] S. Bochner, "Diffusion equation and stochastic processes," *Proceedings of the National Academy of Sciences of the United States of America*, vol. 35, no. 7, p. 368, 1949.

[80] A. Barrat, M. Barthelemy, and A. Vespignani, *Dynamical processes on complex networks*. Cambridge University Press, 2008.

[81] H. Touchette and C. Beck, "Asymptotics of superstatistics," *Physical Review E*, vol. 71, no. 1, p. 016131, 2005.

[82] G. J. Rodgers and A. J. Bray, "Density of states of a sparse random matrix," *Physical Review B*, vol. 37, no. 7, p. 3557, 1988.

[83] J. H. Cooperman, "Scaling analyses of the spectral dimension in 3-dimensional causal dynamical triangulations," *Classical and Quantum Gravity*, vol. 35, no. 10, p. 105004, 2018.

[84] S. Alexander and R. Orbach, "Density of states on fractals: "fractons"," *Journal de Physique Lettres*, vol. 43, no. 17, pp. 625–631, 1982.

[85] B. Durhuus, T. Jonsson, and J. F. Wheater, "Random walks on combs," *Journal of Physics A: Mathematical and General*, vol. 39, no. 5, p. 1009, 2006.

[86] P. W. Shor and J. E. Yukich, "Minimax grid matching and empirical measures," *The Annals of Probability*, pp. 1338–1348, 1991.

[87] F. T. Leighton and P. Shor, "Tight bounds for minimax grid matching, with applications to the average case analysis of algorithms," in *Proc. 18th Annual ACM Symposium on Theory of Computing*, 1986, pp. 91–103.

[88] A. Goel, S. Rai, and B. Krishnamachari, "Sharp thresholds for monotone properties in random geometric graphs," in *Proc. 36th Annual ACM Symposium on Theory of Somputing*, 2004, pp. 580–586.

[89] T. Müller, "Two-point concentration in random geometric graphs," *Combinatorica*, vol. 28, no. 5, p. 529, 2008.

[90] D. Ben-Avraham and S. Havlin, *Diffusion and reactions in fractals and disordered systems*. Cambridge University Press, 2000.

[91] R. Pastor-Satorras and A. Vespignani, "Epidemic dynamics and endemic states in complex networks," *Physical Review E*, vol. 63, no. 6, p. 066117, 2001.

[92] A. Guille, H. Hacid, C. Favre, and D. A. Zighed, "Information diffusion in online social networks: A survey," *ACM Sigmod Record*, vol. 42, no. 2, pp. 17–28, 2013.

[93] T. Jonsson and J. F. Wheater, "The spectral dimension of the branched polymer phase of two-dimensional quantum gravity," *Nuclear Physics B*, vol. 515, no. 3, pp. 549–574, 1998.

[94] V. Pestov, "An axiomatic approach to intrinsic dimension of a dataset," *Neural Networks*, vol. 21, no. 2-3, pp. 204–213, 2008.

[95] C. M. Bishop, *Pattern recognition and machine learning*. Springer, 2006.

[96] A. Nica and R. Speicher, *Lectures on the combinatorics of free probability*. Cambridge University Press, 2006, vol. 13.

[97] D. Krioukov, F. Papadopoulos, M. Kitsak, A. Vahdat, and M. Boguná, "Hyperbolic geometry of complex networks," *Physical Review E*, vol. 82, no. 3, p. 036106, 2010.

[98] K. Rohe, S. Chatterjee, B. Yu *et al.*, "Spectral clustering and the high-dimensional stochastic blockmodel," *The Annals of Statistics*, vol. 39, no. 4, pp. 1878–1915, 2011.

[99] S. Galhotra, A. Mazumdar, S. Pal, and B. Saha, "The geometric block model," in *Thirty-Second AAAI Conference on Artificial Intelligence*, 2018.

[100] ——, "Connectivity in random annulus graphs and the geometric block model," *arXiv preprint arXiv:1804.05013*, 2018.